Theses and Dissertations--Chemistry   Chemistry

2022

SUCCINYLATED POLYETHYLENIMINE GENE DELIVERY AGENTS FOR ENHANCED TRANSFECTION EFFICACY

Md. Nasir Uddin
University of Kentucky, nasiru.ns@gmail.com
Author ORCID Identifier:
https://orcid.org/0000-0002-1330-7381
Digital Object Identifier: https://doi.org/10.13023/etd.2022.016

Right click to open a feedback form in a new tab to let us know how this document benefits you.

SUCCINYLATED POLYETHYLENIMINE GENE DELIVERY AGENTS FOR
ENHANCED TRANSFECTION EFFICACY

_____

DISSERTATION

_____

A dissertation submitted in partial fulfillment of the
requirements for the degree of Doctor of Philosophy in the
the College of Arts and Sciences
at the University of Kentucky

By
Md. Nasir Uddin
Lexington, Kentucky
Director: Dr. Jason DeRouchey, Professor of Chemistry
Lexington, Kentucky
2021

ABSTRACT OF DISSERTATION

SUCCINYLATED POLYETHYLENIMINE GENE DELIVERY AGENTS FOR
ENHANCED TRANSFECTION EFFICACY

Gene therapy aims to treat patients by altering or controlling gene expression. Today, most clinical approaches are viral-based due to their inherent gene delivery activity. However, there is still a significant interest in nonviral alternatives for gene delivery, particularly synthetic lipids and polymers, that do not suffer the immunogenicity, high cost, or mutagenesis concerns of viral vectors. Polymeric vectors are of particular interest due to the ability to further tune the polymer properties through the incorporation of additional functional units such as targeting ligands or shielding domains. Polyethylenimine (PEI), a highly cationic polymer, is often considered a benchmark for polymer-based gene delivery and thus serves as an excellent model for investigating gene delivery mechanisms. One reason PEI, especially branched PEI, is thought to outperform many other cationic polymers is due to the presence of secondary and tertiary amines. These amines are thought to help facilitate escape from endocytic vesicles via a 'proton-sponge' mechanism. Despite its successful use for in vitro gene delivery, PEI was initially developed for use in common processes such as water purification. As such, the properties of PEI should not be expected to be optimal for gene delivery. In this dissertation, my research efforts focused on the incorporation of negatively charged succinyl groups to the PEI backbone to create succinylated zwitterion-like PEI (zPEIs). Specifically, we focused on the synthesis and characterization of zPEIs as well as the impact of zPEI on DNA condensation and gene expression.

This dissertation will discuss the results of three projects. In project (1), we studied the suitability of minimally modified zPEIs for gene expression. In this work, we reveal that modification of PEI as low as 2% amines was sufficient to provide significant improvements in gene delivery particularly in the presence of serum proteins. In project (2), we investigate the self-assembly of DNA induced by modified and unmodified branched PEIs using small-angle X-ray scattering (SAXS). Modified PEIs included both succinylated zPEI and acetylated PEIs (acPEI) both modified from 0-40%. We demonstrate that changing the degree of modification significantly alters the packing density of the resulting polyplexes. While acPEI shows a continuous decrease in DNA

packaging efficiency with increasing degree of modification, zPEI shows a crossover behavior where DNA-DNA interhelical spacings increase at low succinylation but decrease at higher degrees of succinylation. Studies on the pH dependence on the inter-DNA spacing also show that lowering the pH leads to tighter DNA packaging for all PEIs studied. These findings shed light on the complex correlation between DNA packaging density and gene expression ability of PEI and modified PEI mediated gene delivery systems. In project (3), we studied the efficacy of zPEI polyplexes at varying protein concentrations ranging from 0-10 mg/mL of bovine serum albumin (BSA). These high protein concentrations are comparable to in vivo protein concentrations. We show that while PEI/DNA transgene expression decreases with higher protein concentrations, the zPEI studied stayed approximately constant over the protein range studied. To test if these conditions may lead to the formation of a protein corona on the nanoparticles, which was recently shown to enhance serum-free transfection in unmodified bPEI/DNA, we also measured the transgene expression of polyplexes pre-treated to form a protein corona on the polyplexes.

KEYWORDS: Succinylated PEI, Gene delivery, Small-angle X-ray scattering, Packaging density of dsDNA in polyplex, Proton sponge effect, Protein corona

Md. Nasir Uddin

(Name of Student)

11/07/2021

Date

SUCCINYLATED POLYETHYLENIMINE GENE DELIVERY AGENTS FOR
ENHANCED TRANSFECTION EFFICACY

By
Md. Nasir Uddin

Dr. Jason DeRouchey
_____
Director of Dissertation

Dr. Yinan Wei
_____
Director of Graduate Studies

11/07/2021
_____
Date

DEDICATED

To *my Parents and my Family*

ACKNOWLEDGMENTS

First, I would like to express my sincere gratitude to Dr. Jason DeRouchey, who exemplifies the high-quality scholarship I aspire. In addition, Dr. DeRouchey provided timely and instructive comments and evaluations at every stage of the dissertation process, without whom this work would not have been possible. Thank you so much for your immense support, patience, and guidance throughout my Ph.D. program. Your insightful feedback & critical assessment pushed me to sharpen my thinking and brought my work to a higher level. It's genuinely a rewarding experience working with you.

I want to thank my advisory committee members Dr. Daniel Pack, Dr. Chad Risko, Dr. Stephen Testa, for their support throughout the process. I'm grateful for spending your precious time on my committee meetings, reading my dissertation, and giving valuable feedback. I'm also extremely thankful to Dr. Charles Lutz for serving as my external committee member.

I want to acknowledge Dr. Daniel Kirchhoff and Dr. Logan Warriner for training me small-angle X-ray scattering & in vitro gene expression techniques, respectively, and being very supportive colleagues. I also want to recognize Dr. Kanthi Nuti for being such a good friend, Ehighbai Oikeh, Richard Mitchell, Md Abu Monsur Dinar, for all your support, encouragement, all the memorable discussions about philosophy, food, religion, and culture. Thank you all for making this journey a memorable one.

Finally, I would like to extend my deepest gratitude to my wife Maria Kiptia Eve for her continuous support, encouragement, patience, and belief in me. My dearest

TABLE OF CONTENTS

LIST OF TABLES

LIST OF FIGURES

CHAPTER 1. RECENT ADVANCES AND CHALLENGES WITH NONVIRAL GENE
DELIVERY SYSTEMS

1.1   INTRODUCTION

Gene therapy is emerging as a promising treatment option for certain genetic diseases with the potential to transform therapeutic treatments for patients living with currently untreatable diseases. In its simplest form, gene therapy aims to regulate, repair, or replace genetic materials employing recombinant nucleic acid. In recent years, this genetic approach has treated diseases such as spinal muscular atrophy, Duchenne's muscular dystrophy, Beta-thalassemia, and cystic fibrosis and the list continues to grow. In addition, researchers are slowly uncovering the genetic basis of acquired neurodegenerative diseases such as Alzheimer's, cancer, type 2 diabetes, etc. providing new targets for future gene therapies. To date, there are 22 FDA-approved cellular and gene therapy products and over 500 ongoing studies on gene delivery listed on clinicaltrials.gov. Although most clinical trials worldwide address gene transfection using a virus as a vector, the history of virus-mediated gene therapy has not been smooth. Most current viral vector-based gene delivery uses retroviruses, lentiviruses, adenoviruses or adeno-associated viruses to transport a therapeutic gene for in vivo delivery. Viral vectors have the inherent advantage of higher delivery efficiency and an ability to target cells. However, viruses trigger immunogenic responses and mutagenicity, which could be fatal to a patient. The treatment induced cancer in some volunteers, and the tragic death of 18-year old Jesse Gelsinger, overshadowed initial success in gene therapy in the late 1990s, sparking a chain of events that nearly derailed the field.[1] This fear of massive immune response to viral vectors urged researchers to seek new alternative strategies to viral gene delivery, thus developing various nonviral, synthetic vectors.

1.2   Literature review on gene delivery agents

Genes are sequences of nucleotides embedded into deoxyribonucleic acid (DNA) that provide the blueprints for protein synthesis critical for the proper functioning of cells and organisms. Small changes to genes, either through random process mutation or inherited, can alter the expression of proteins, impacting the body's ability to function properly. In gene therapy, the goal is to deliver genetic materials, in the form of DNA or ribonucleic acid (RNA), that have the instructions to repair protein synthesis, thus producing a therapeutic response. To be successful, however, these nucleic acids need to be targeted for delivery to the cells or tissues identified to contain faulty genes. Naked nucleic acids alone cannot serve this purpose due to many complex biological systems posing barriers as depicted in **Figure 1.1**. First, these materials should avoid the reticuloendothelial systems (RES) and macrophage systems, which poses the first barrier after intravenous injection. Serum nuclease is another major hurdle for gene delivery. Next, therapeutic nucleic acids must overcome the challenge of endocytosis at the cell membrane level, which is a requirement for cell entry. Depending on the type of therapy, the payload must reach specific points in the cell. For example, upon entering a cell, noncoding RNA (such as micro-RNA and siRNA) must be delivered in the cytosol while DNA needs to reach the cell nucleus for transcription to occur. These multiple barriers are why a protecting vector is required to package the genetic payload and traffic them to the desired target site. Currently, vectors for gene therapy are broadly classified as viral, nonviral, and hybrid vectors. The following section will explore the advancement and challenges associated with these vectors.
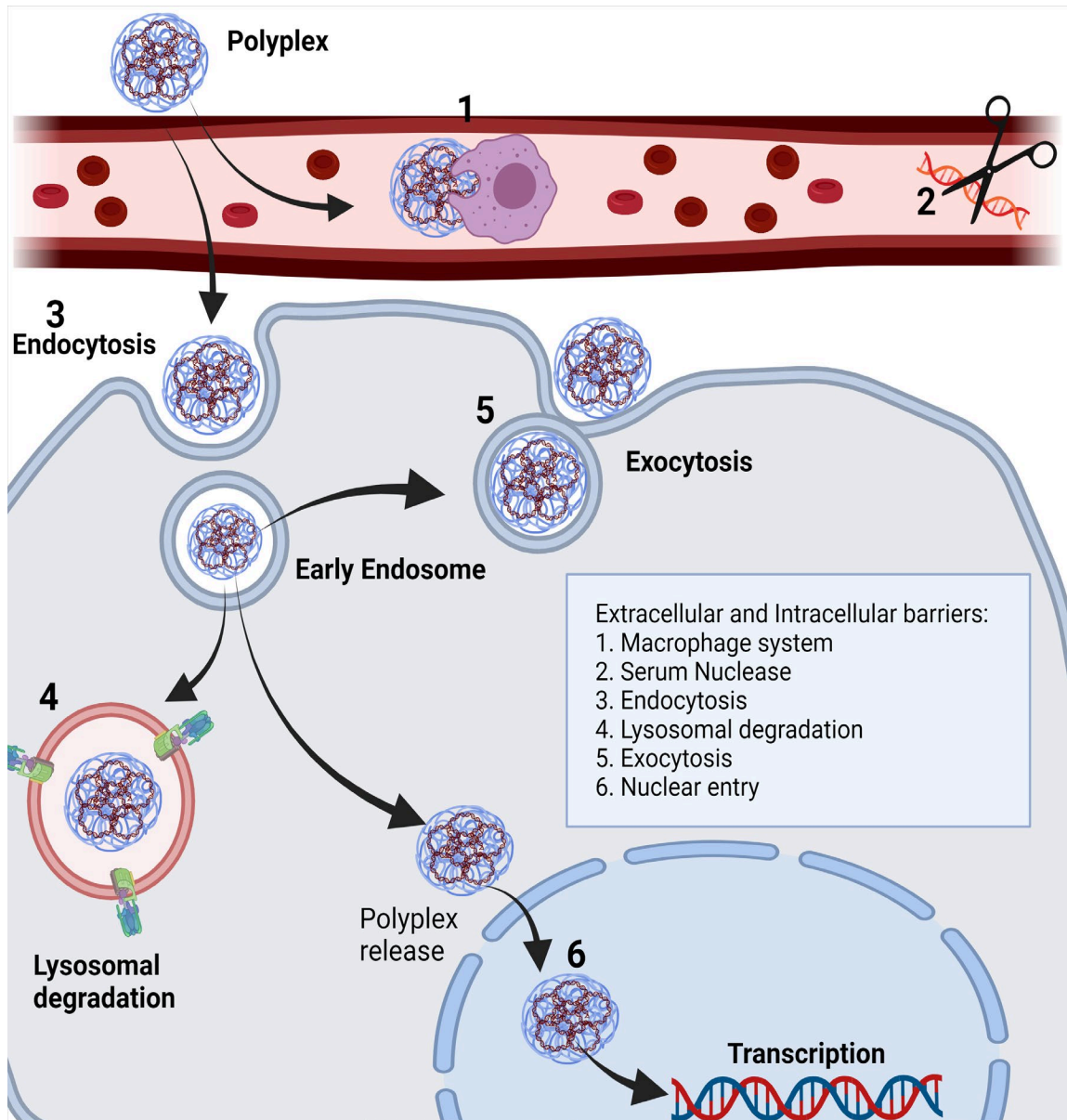
Figure 1.1. Barriers to viral and non-viral vectors. For simplicity, only nonviral model (polyplex) was used to describe all the challenges associated with gene delivery. A successful gene delivery agent must evade all these barriers to successfully express the transgene.

1.2.1   Viral vectors

Viruses have been evolved by nature to overcome most of the biological barriers depicted in **Figure 1.1**. The primary advantages of viral gene delivery lie with the innate ability of viruses to deliver genes in a highly specific manner to targeted cells as well as their capacity for efficient gene transduction. Due to these advantages, viral vectors currently have taken the leading role in gene therapy research. More than 70% of clinical gene therapy trials worldwide utilize viruses, primarily adenovirus, adeno associated virus (AAV), retroviruses, and lentiviruses.[2-4]

Adenoviruses are a non-integrating virus that transiently expresses their genes in the cytoplasm of cells. Adenovirus vectors have three main advantages: (1) they can transduce a variety of dividing and non-dividing cells (2) they can achieve a high level of gene expression and (3) certain common strains are easily purified and well-characterized.[5] Due to its nonpathogenic nature and broad tropism, adeno-associated virus (AAV) have also shown strong potential for in vivo gene therapy.[6] AAV is a non-enveloped virus that can be engineered to deliver nucleic acids (NAs) to target cells. The ability to generate recombinant AAV particles lacking any viral genes with DNA sequences of interest for therapeutic applications has proven to be one of the safest strategies for gene therapies.[7] However, AAVs are small in size (20-24 nm) limiting the size of genes it can deliver, so strategies involving the use of split AAV vectors and the reassembly of AAV genome fragments have been used to address AAV packaging capacity.[8] These modified AAV vectors have enhanced the success of AAV therapies which continue to grow at a fast pace in recent years. Retroviruses are enveloped RNA viruses that carry virally encoded elements that reverse transcribe their RNA payload into

double-stranded DNA (dsDNA). This dsDNA is then transported to the cell nucleus and stably integrated into the host genome employing a virally encoded integrase.[4, 9] While designing a recombinant virus, the retroviral genes (gag, pol, and env) are deleted and replaced with the therapeutic gene(s) of interest.[4] Murine leukemia virus are among the simplest retroviruses and named after their ability to cause cancer in mice. Moloney murine leukemia virus (MMLV) have been optimized for stable chromosomal integration and gene expression. With a transduction efficiency of more than 90% in dividing cells, MMLVs are one of the most studied retroviral vectors.[10] Lentiviral vectors (LV) have been extensively investigated and optimized over the past two decades.[11] First-generation LVs used significant portions of the HIV genome but in later generations various changes were made to create safer vectors. For example, self-inactivating LVs are used to introduce genes into hematopoietic stem cells to correct primary immunodeficiencies and hemoglobinopathies.[12] More recently, non-human lentiviruses have become attractive alternatives to conventional HIV-1-based LVs.[13] In 2017, the FDA approved its first gene therapy drug, named Kymriah, that uses lentiviruses as the transfecting agent.[14] With increasing interest in gene therapy, ongoing research is also recruiting other viral vectors such as vaccinia virus, herpes simplex virus, and poxvirus, comprising 4.9%, 3.6%, and 2.7% of all clinical trials, respectively.[5, 15]

1.2.1.1 Recent advances and challenges with viral vectors

Although gene therapy trials are on the rise, understanding the long-term risks associated with this type of treatment is necessary. According to an editorial published in 'Nature Medicine,' Bluebird Bio suspended phase 1/2 and phase 3 clinical trials of its

LentiGlobin gene therapy for sickle-cell disease very recently after two patients were diagnosed with cancer, five years after receiving treatment.[16] Earlier, in late 2018, another participant from the same trial had been diagnosed with myelodysplastic syndrome.[16] Although further review indicates that the lentiviral vector used in the studies is unlikely to cause cancer, this news highlights growing concerns about the late adverse effects of gene therapy.[16] In January 2020, the FDA updated guidelines on designing long-term follow-up studies using integrating vectors, genome-editing products, and AAV, hoping to better evaluate the long-term effects of gene therapy products on patients.

The major challenge with viral vectors is safety. As recently as this past year, deaths occurred in children with X-linked myotubular myopathy (MTM) being treated by AAV gene therapy serving as a reminder how difficult it is to predict outcomes in first-in-human studies. [17] Some hypotheses to explain this event have focused on the role of antibodies to AAV that either preexist or rapidly accumulate following vector infusion.[17] One major issue during the manufacturing and production of AAV vectors is the presence of empty capsids lacking the encapsidated vector genome. These empty capsids can elicit additional immune responses during in vivo gene therapies if not removed prior to treatment.[18] Another significant issue is the viral vector heterogeneity during lot-to-lot production. One approach to prevent the viral serotype variability is the post-translational modification of the capsid. For example, capsid deamidation to impact the transduction efficiency is a promising strategy to improve performance.[19] However, there needs to be a balance between vector performance and stabilized variants in a more complex functional context to succeed with such an approach. The application of machine learning

algorithms to accurately predict capsid viability across diverse variants might unlock vast areas of functional sequence space, with potential applications for the generation of improved, safer viral vectors.[20]

1.2.2 Nonviral delivery systems

While viral gene delivery is currently dominating current clinical trials, viruses have many drawbacks including concerns regarding their safety (such as immunogenicity and oncogenicity), limited genetic payloads, and difficulties in scaling up production of viruses to meet commercial demands. Therefore, much work has been done to find alternatives to virus for gene delivery. Synthetic, or nonviral formulations typically utilize cationic polymers or lipids as the delivery vehicle for nucleic acids. Unlike the logistic challenges with viral vectors, synthetic vectors are easy to scale up, readily formulated, and made available off the shelf, have the capacity to deliver larger payloads, and have reduced immunogenicity.[21] The possibilities for these nonviral vectors has recently been shown by the success of lipid formulations, originally developed for nonviral gene delivery, in the formulation of mRNA-based vaccines for COVID-19.[22-23] The delivery of mRNA suffers from all the challenges of delivery any nucleic acid for gene therapy. Lipid nanoparticles are used to protect mRNA during the production and transport of the vaccine as well as enhance their stability in vivo once the vaccine is administered. One clear drawback of the lipid formulations was the requirement that they must be refrigerated during transport and storage. Worldwide distribution of these lipid-nucleic acid complexes, and affordability in developing countries with infrastructural deficiencies in the cold chain therefore pose a significant challenge.[24] Due to these

challenges, both clinicians and biotechnologists widely acknowledge the need for synthetic delivery methods which will be safe and affordable by the mass community.[25-26] The success of the two lipid-based mRNA vaccines for COVID-19, distributed to hundreds of millions of people in the US alone, has triggered a renewed research interest in non-viral gene delivery platforms.

Cationic lipids, cationic peptides, chemically stabilized DNA/RNA, and cationic polymers have all been used as nonviral gene delivery agents in various laboratory studies and pre-clinical trials. Each synthetic gene delivery modalities have their own advantages and limitations. For example, cationic lipids, usually in the form of liposomes, are capable of condensing nucleic acids but their effectiveness depends on their hydrophobic tails. Cationic polymers are known to have stronger DNA binding ability compared to the liposomes and have been shown to result in higher transfection efficiency in vitro.[27] Polymers are also more amenable to the incorporation of additional functional units, such as targeting ligands or shielding domains to facilitate multifunctional delivery systems. Through electrostatic interactions, cationic polymers condense DNA into nanometer-sized complexes called polyplexes. Upon condensation, polyplexes protect nucleic acids from enzymatic degradation and facilitate cargo delivery to cells. Upon reaching the cells, polyplexes can bind cell membranes that can trigger intracellular uptake of the particles. Ultimately the polycation must release the nucleic acids for successful gene delivery creating a need to optimize the polymer-NA interactions to optimally balance the protection and release of the payload. Some examples of commonly used polymers are shown in **Figure 1.2**. The following sections

will briefly highlight critical advances in designing synthetic polymeric vectors and the different materials that comprise these carriers.
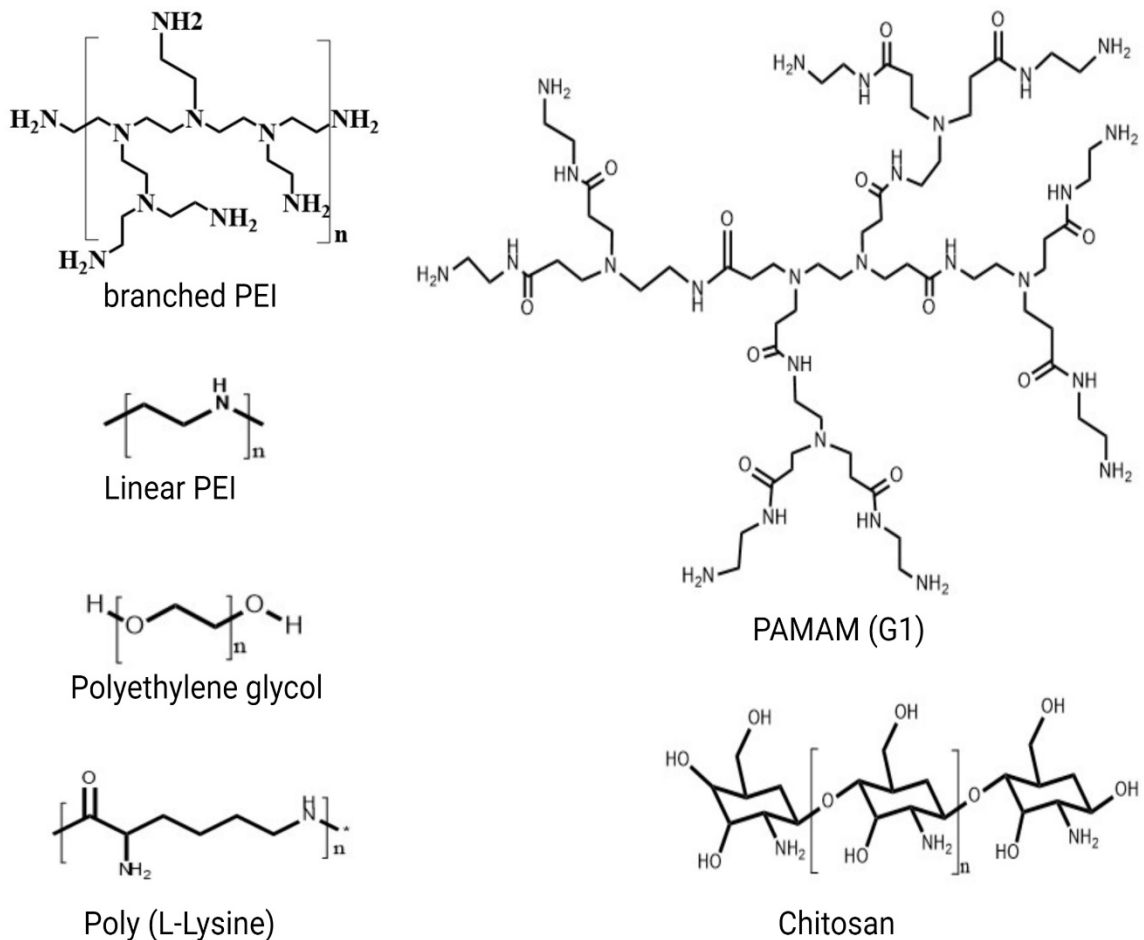
Figure 1.2. Examples of common polymers used in gene delivery.

1.2.2.1 Cationic polymer design with tunable motifs

Typically, cationic polymers consist of nitrogen-based moieties that can be integrated via direct polymerization or post-polymerization modification to noncationic polymers. Polycations with ammonium, imidazolium, and guanidinium moieties are commonly found in the literature as potential polyplex vectors. Along with balancing condensation and release, another significant barrier for nonviral delivery is the escape of the polyplexes from the endosome. While viruses have fusion peptides that allow them to

escape endosomes from membrane fusion and lipoplexes can enter cells through fusion with the cell membrane, polycations are not fusogenic. It is thought that one possible way to aid endosomal escape is by using cationic polymers with a pKa near physiological pH to act as a "proton-sponge". For example, the imidazolium group can obtain a pKa close to 7 thus resulting in a low charge at neutral pH that becomes charged during acidification thus thought to change the internalization pathway and improve gene transfection.[28] Another reason for a low pKa polycation is that higher pKa polymers are known to cause cytotoxicity. To date, a limited number of non-nitrogenous polycations containing phosphorous and sulfur atoms have also been reported in the literature. However, the scarce use of these atoms in gene delivery is predominantly due to fewer synthetic pathways and the concern of chemical instability in biological environments.[29]

Introducing hydrophobic moieties is another strategy utilized to fine-tune polymeric vectors to improve gene delivery efficacy. Incorporating hydrophobic groups into a polymeric vector induce hydrophobic−hydrophobic interactions with nucleic acids. These additional hydrophobic interactions have been shown to improve complex stability, enhance cellular uptake, and prolongs circulation time in vivo by slowing sown renal clearance.[30-31] Hydrophobic moieties, such as linear alkyl, cyclic alkyl, lipidic, aryl, and cholesteryl groups have been incorporated into cationic polymers to enhance gene transfection.[32] Low molecular weight polyethylenimines (LMW-PEI) are one of the prime candidates for introducing hydrophobicity to improve their gene delivery efficiency.[33-34] LMW-PEI (typically ~5-12 kDa PEI) shows higher cell viability but lower transfection efficacy when compared to higher molecular weight PEIs such as 25kDa PEI. Incorporating hydrophobic moieties on LMW-PEI has been shown to enhance gene

delivery.[35-36] The introduction of hydrophobic moieties has also been explored in other polycationic systems. In 2010, Piest et al. showed that incorporating hydrophobicity into a bio-reducible poly(amido amine) resulted in enhanced transfection efficiencies through reduced cytotoxic effects, increase polyplex stability, and improved endosomolytic properties.[37] Polycationic micelles formed from triblock copolymers containing a non-ionic hydrophilic block in addition to a cationic and a hydrophobic block have also been used as components for micelleplex formulations.[21] The use of these micelleplexes has been reported to co-deliver plasmid DNA and small molecule drugs for cancer therapy by taking advantage of the hydrophobic interactions between the drug and the hydrophobic block of the polymer micelle.[38]

Because polyplexes encounter different physiological conditions, such as varying pH, while trafficking the nucleic acid payloads into cell nuclei the incorporation of stimuli responsive moieties has also been a common strategy for enhanced gene delivery. For example, the use of an acid cleavable block copolymer of polyethylene glycol (PEG) and a modified poly(aminoethyl methacrylate) (PAEMA) was recently shown to deliver pDNA into tumor cells effectively.[39] The cleaving of PEG was shown to result in a change in the polyplex surface charge upon acidification that enables the complexes to better circumvent high blood clearance and minimize cytotoxicity.[39] Addition of photo responsive and redox-responsive moieties to a polymer are other strategies commonly employed to enhance gene delivery. In more recent years, research has focused on using multi-stimuli-responsive polymers to co-deliver drugs and nucleic acids to hard-to-transfect cells or drug-resistant cancers.

Most polyplexes result in the formation of DNA nanoparticles with a positive surface charge which can lead to stability issues in vivo such as polyplex aggregation with proteins and tissue damage. Serum-protein binding and colloidal instability often lead these polymer vehicles to be cleared out of in vivo circulation via reticuloendothelial systems. Polyethylene glycol (PEG) is a hydrophilic, uncharged flexible polymer. Incorporating PEG into polyplex formulations is a common means to shield the polyplex surface charge and reduce nonspecific interactions of the polyplex with surrounding molecules.[40] Although PEG has been shown to aid in tackling in vivo challenges, it markedly reduces cellular internalization, thus hampering gene expression. To improve transfection with PEGylated polyplexes, more recent studies have focused on optimizing PEG grafting density and PEG molecular weights for different polyplexes.[41-42] Recent studies have also examined the immunogenic and allergic response associated with PEGylated polymer mediated gene delivery.[43] Recently, it was shown that some people produce anti-PEG antibodies that may limit the activity of PEGylated particles.[44-45] Researchers are therefore also exploiting alternatives to PEG such as incorporating carbohydrate or zwitterionic moieties as hydrophilic agents that mitigate nonspecific interactions of molecules with the polyplexes.[46-47].

1.2.3   Polyethylenimine (PEI) at the forefront of gene delivery research

Polyethylenimine (PEI) is one of the most studied polycationic polymers in nonviral gene delivery and often considered a benchmark for polyplex gene delivery vectors. PEIs have a high cationic charge density and significant buffering capacity over a wide range of pHs. Branched PEI (bPEI), containing a mixture of primary, secondary,

and tertiary amino groups with different pKa values, results in the protonation state of PEI being pH dependent. At neutral pH, it is estimated bPEI has ~20-25% of its amines protonated but this can increase to ~45% protonated at pH 5.[48] From the PubMed database, more than two thousand articles using PEI for gene delivery have been published since 2000, revealing their significance in the field. However, due to the very high positive charge density of the polymer, PEI generally is cytotoxic, often posing a threat to cell viability. To circumvent this cytotoxicity, more recent research has focused on decreasing PEI charge density via post polymerization modification to enhance cell survival.

The recent development on the design and synthesis of PEI-based nanocarriers broadly focuses on i) PEI-based polymeric nanoparticle system; ii) PEI-based polymeric micelles systems; iii) PEI/silica nanoparticle systems, and iv) PEI/metal nanoparticle systems.[49] Commonly used functionalities for these modifications include but are not limited to polyethylene glycol (PEG), polysaccharides, poly (ε-caprolactone), small molecules & peptides, proteins, and poly (l-lactide) (PLLA).[50] PEI-based co-delivery strategies are also being explored as a new method for treating diseases by combining chemotherapy and gene therapy.[51] Some examples of co-delivery strategies include blocking NF-kB activation in inflammatory tissue,[51] improving antitumor efficacy and systemic toxicity,[52] and reversing multidrug resistance (MDR) in cancer to more effectively kill MDR cancer cells.[53]

1.3   CONCLUDING REMARKS

The list of nonviral-based gene therapy vectors is continuously expanding due to continuing interest in gene therapy. Surprisingly, the progress in nonviral agents with polymeric scaffolds has not yet achieved clinical relevance. Many barriers to nonviral gene delivery have not been fully understood yet. Therefore, we must understand how polymer synthesis and modification affect the body's gene delivery mechanism and vector interactions.

CHAPTER 2. ENHANCED GENE DELIVERY AND CRISPR/CAS9 HOMOLOGY-DIRECTED REPAIR IN SERUM BY MINIMALLY SUCCINYLATED POLYETHYLENE IMINE

This chapter is reprinted with permission from [Uddin, N., Warriner, L. W., Pack, D. W., and DeRouchey, J. E. (2021) Enhanced Gene Delivery and CRISPR/Cas9 Homology-Directed Repair in Serum by Minimally Succinylated Polyethylenimine. *Molecular Pharmaceutics,* 18 (9), 3452-3463. https://doi.org/10.1021/ acs.molpharmaceut.1c00368] Copyright © 2021 American Chemical Society.

All polymer synthesis and characterization, DNA binding assays, dextran sulfate displacement, DLS and ζ-potential measurements were completed by the author. Protein interaction, transfection, and CRISPR/Cas9 experiments were done by the co-first author Dr. Logan Warriner and performed in the laboratory of Dr. Daniel Pack.

2.1   INTRODUCTION

Therapeutic nucleic acids (NAs) are proving to be powerful tools capable of altering or controlling gene expression with the potential to treat intractable acquired and inherited diseases including cancer, neurodegenerative diseases, and genetic defects.[54] To date, more than a dozen different gene therapy drugs for treating immune and neuronal disorders, blindness, and cancer, as well as vaccines protecting against SARS-CoV-2, have been approved world-wide.[55] Promising clinical trials for sickle cell, hemophilia, neuromuscular diseases, and vaccines will also likely lead to additional approvals in the near future. The efficacy and clinical success of these therapies have been hindered to date primarily by the requirement for effective delivery of nucleic acids into specific intracellular locations and organelles within targeted tissues.[56-57] Recombinant virus-based delivery vehicles have accounted for the vast majority (~70%) of clinical trials due to their inherent gene delivery activity.[58] However, viruses have drawbacks including difficulty in producing commercially relevant quantities[59-60], high costs, limited genetic

payloads[61], and potential for insertional mutagenesis[62], immunogenicity[63] and oncogenecity.[64]

Nonviral or synthetic gene vectors have several advantages that give them the potential to overcome the inherent limitations of viral vectors.[65-67] Nonviral vectors typically condense negatively charged nucleic acids (NA) with cationic polymers or lipids to form nanoscale complexes known, respectively, as polyplexes or lipoplexes. Synthetic vectors allow for lower cost, ease of large-scale production, and improved safety potential while also the capacity to accommodate various kinds of NA payloads. For example, non-viral vectors may deliver plasmid DNA or mRNA to introduce a therapeutic gene product; siRNA or miRNA for silencing or regulation of specific genes; or CRISPR/Cas9 components for editing the target cell genome to permanently knock-in a therapeutic gene, knock-out an undesirable gene, or introduce specific point mutations to correct an aberrant gene. In addition, nonviral vectors hold advantages over recombinant viruses when short-term expression of the transgene is desired, as in the expression of Cas9 in CRISPR-based therapies.[68] The use of polymer vectors also facilitates multifunctional delivery systems through the incorporation of additional functional units such as targeting ligands, shielding domains, and endosomolytic units to improve efficacy.[69-70] To date, however, synthetic polyplexes suffer from lower delivery efficiency relative to viral vectors due to complications including the creation of poorly defined formulations, the need to balance NA protection and release, lack of serum stability, rapid clearance, and inefficient targeting.[71-72] There is still a need for a better fundamental understanding of the complex correlations of physicochemistry and biology

of synthetic delivery systems to improve efficacy in vivo and move nonviral gene therapy into clinical use.

The size, stability, shape, and surface properties of these polyplex nanoparticles are known to play a critical role in cellular uptake processes and in-vivo biodistribution.[73-74] Therefore, the chemical structure of the polymer used for polyplex formulations is known to be a key determinant for polyplex efficacy and toxicity. Polyethylenimine (PEI) is often considered a benchmark for polymeric, nonviral gene delivery vectors thus serving as an excellent model for investigating gene delivery mechanisms.[75-77] PEI is a highly cationic polymer that readily condenses NAs through electrostatic interactions to create suitable particles for effective gene delivery. Complete complexation of NAs with PEI results in polyplexes with a net positive surface charge, which has been shown to promote interactions with the negatively charged components of the cell membrane.[78] In addition, the substantial quantity of secondary and tertiary amines in branched PEI results in a large buffering capacity, thought to facilitate escape from endocytic vesicles, a crucial bottleneck in the transfection process, via the 'proton-sponge' mechanism.[79] However, PEI was originally developed nearly 50 years ago as a chelator for use in the water purification and mining industries.[80] As such, the properties of PEI should not be expected to be optimal for gene delivery.[81] The excess positive charge typical of PEI/DNA polyplexes induces nonspecific binding to negatively charged serum proteins, which leads to polyplex aggregation and, ultimately, clearance by the reticuloendothelial system.[82-83] The high charge density can also contribute to cytotoxicity, causing changes in cellular morphology, damage to the cell membrane,

decreased metabolism, and lysis.[84] Finally, the strong electrostatic interactions between PEI and DNA can hinder vector unpackaging, which is required for transcription.[85-86]

Due to high cytotoxicity, endosomal degradation, and aggregation on cell surfaces encountered with native PEIs, chemical modification of PEI has been a common strategy to enhance performance.[75, 87] Many of these modifications have focused on means to reduce a net cationic charge of the resulting polyplexes. For example, acetylation of primary and secondary amines on PEI (acPEI) resulted in polymers exhibiting enhanced gene delivery, demonstrating the relative importance of buffering capacity and polymer/DNA binding strength in PEI-mediated gene delivery.[88-89] Acetylation was shown to weaken polymer/DNA interactions and dissociate more readily within cells leading to enhanced transgene expression in vitro. Transfections of acetylated PEI in the presence of serum however resulted in lower activity suggesting acPEI still suffered from serum instability due to aggregation. To decrease aggregation in serum and increase retention in the bloodstream, incorporation of shielding domains, such as polyethylene glycol (PEG), has been a commonly employed strategy.[82, 90] PEGylation has been found to possibly induce immune responses,[91] leading to studies of alternative shielding domains for PEI including polyethers,[92] poly(N-(2-hydroxypropyl)methacrylamide),[93] and dextran[94]. Polyplex shielding has been shown to improve blood circulation times and increase accumulation within tumors compared to unmodified PEI. Polyplexes comprising such modified PEI, however, suffer from a reduced cellular uptake and decreased transfection efficiency.

Less commonly studied has been the incorporation of negatively charged groups to polycations to generate polyampholytic vectors suitable for polyplex formation. Early

work focused on charge-shifting polymers which under physiological acidification converted neutral esters to anionic carboxylates.[95-96] These materials were shown to modify polymer-DNA interactions and enhance gene delivery of linear PEI. More recently, work on succinylated PEIs showed a significant increase in effectiveness for the delivery of siRNA compared to unmodified PEI,[97] typically a poor siRNA carrier, with the targeted gene expression reduced to nearly 10% of the relative control. In 2017, Khalvati et al. showed modest improvement of DNA delivery under serum-free conditions by succinylated PEIs modified at 10−40% of their amines.[98] We recently synthesized a series of succinylated PEIs with modification of 9-55% of amines on the polymer to create zwitterion-like PEI (zPEIs) and examined the gene delivery efficiency in vitro in the absence and presence of serum.[99] Lower modifications (9-25%) were found to be most effective for gene delivery. While these succinylated PEIs also showed only modestly improved transfection efficiencies (~5 to 10-fold) in the absence of serum, the most surprising aspect of the zPEIs was the highly effective in-serum transfection. For unmodified PEI, the presence of serum during transfection is well known to result in a significant decrease in the transfection efficiency. For example, we previously observed a decrease in gene expression of 10- to 20-fold for HeLa and MDA cells and over 100-fold in MC3T3 cells for PEI/DNA transfected in-serum when compared to serum-free conditions.[99] In contrast, a 9% modified zPEI mediated transgene expression in the presence of serum that was comparable to, or even surpassed (up to 51-fold), that of unmodified PEI/DNA in the absence of serum in all three cell lines. We further showed that high degrees of succinylation decreased polymer/DNA interactions while reducing aggregation in the presence of anionic proteins and lowering cytotoxicity.

In this work, we focused on examining two critical questions: (i) what the minimum amount and optimal range of succinylation is required to observe improvement in gene expression in the presence of serum, and (ii) does zPEI also enhance CRISPR/Cas9 gene knock-in modifications in the presence of serum. To address these questions, a series of minimally modified zPEIs (2-11.5%) were synthesized and characterized by FT-IR and ^{1}H-NMR. These sparsely modified zPEIs remarkably all show similarly enhanced transfection efficacy in the presence of serum, as previously observed.[99] Most surprisingly, modification levels as low as 2%, corresponding to ~12 of 581 amines in 25kDa PEI, were sufficient to enhance transfection, including remarkably increased efficiency of CRISPR/Cas9-mediated knock-in, in the presence of serum. We previously hypothesized that a hydration barrier around the mixed-charge zPEI/DNA polyplex may account for the increased protection from serum-protein binding and aggregation. The minimally functionalized zPEIs were, therefore, directly compared to a commercial PEI-PEG$_{2k}$ to assess relative biocompatibility and cytotoxicity. We show that while PEGylation more effectively shields the resulting polyplexes against protein aggregation, the minimally modified zPEIs still significantly outperform the PEGylated particles in the presence of serum in both HEK293 and HeLa cells.

2.2   MATERIALS AND METHODS

2.2.1   Materials

25-kDa branched polyethylenimine (bPEI), succinic anhydride, and dextran sulfate (9-20 kDa from Luconostoc spp) were purchased from Sigma Aldrich (St. Louis, MO). D$_2$O was purchased from Cambridge Isotope Laboratories (Andover, MA).

Plasmid DNA pUC19 (1 mg/mL) was purchased from New England Biolabs (Ipswich, MA). Solid agarose I and 0.2 µm syringe filter units were purchased from VWR Life Science (Randor, PA). Bromophenol blue was purchased from Eastman Kodak (Rochester, NY). PEGylated, branched polyethylenimine (10% amines modified with 2 kDa PEG) was purchased from Nanosoft Polymers (Winston-Salem, NC). All other materials and chemicals were purchased from Thermo Fisher Scientific (Waltham, MA) and used without further purification.

2.2.2 Synthesis and characterization of zPEI

Succinylated, or zwitterion-like PEI (zPEI) was synthesized as follows. 0.5 gram of branched polyethylenimine (bPEI, 25kDa) was dissolved in 3 mL of sodium bicarbonate buffer (HCO_3, pH 9) and reacted with the desired mole ratio of succinic anhydride. The succinylation reaction proceeded for 4 hours at 60 ºC and the final product, zPEI, was purified by dialysis (membrane molecular weight cutoff = 3.5 kDa) against double distilled water for 24 hours with the water replaced every 4 hours. After dialysis, the solution was filtered through a molecular-weight cutoff filter (EZFlow Syringe Filter with Foxx Hydrophilic PVDF membrane, 0.22 µm). Upon re-dissolving, the zPEI solutions were often observed to have some cloudiness which was not removed with filtering. To improve the solubility of the zPEIs, all polymers were subsequently buffered to pH 7 by addition of HCl (0.1M) clarifying the solutions. After acidification, the product was frozen overnight and lyophilized for 24 hours. The dried product was placed in a -80 ºC freezer for storage. Successful reaction and percent succinylation were determined by FT-IR and ^{1}H NMR in D_2O, respectively. For NMR analysis, 6.5 mg of lyophilized polymer was dissolved in 0.65 mL D_2O and ^{1}H-NMR spectra were recorded

using a 400 MHz Bruker Avance NEO spectrometer equipped with a smart probe. A series of low percent modified zPEIs ranging from 2-11.5% modification of the total PEI amines was used in this study.

bPEI25k: ^{1}H-NMR δ_H (400 MHz, D$_2$O, ppm). 2.6–3.3 (broad multiplet, PEI)

zPEI: [1]**H-NMR δ_H (400 MHz, D$_2$O, ppm)**. 2.4-2.5 (broad singlet, 4H,–C$_2$H$_4$–COOH), 2.6–3.3 (broad multiplet, PEI), 3.3–3.6 (broad multiplet, 2H, PEI–CH$_2$–NH–CO-C$_2$H$_4$–).

FT-IR ν (ATR, cm^{-1}). 1635 (C=O; amide I), 1563 (N-H; amide II).

2.2.3 Evaluation of DNA binding by Electrophoretic mobility shift (EMSA) and Ethidium Bromide (EtBr) Exclusion Assays

EMSA was utilized to assess DNA binding efficiency for the zPEIs used in this study. 0.8 w/v % agarose gels were prepared by dissolving agarose in a 0.2 μm filtered TAE buffer (40 mM Tris base, 20 mM acetic acid, 1 mM EDTA). 200 ng pUC19 plasmid DNA (1 mg/mL) was used per well. Polyplexes were formed in 10 mM Tris (pH 7.5) by addition of the appropriate amount of each zPEI polymer to achieve the desired polymer/DNA weight ratio and diluted to a total volume of 12 μL. After mixing, polyplexes were incubated for 45 mins at room temperature. Before gel loading, 2 μL of 6X loading dye was then added to each sample, mixed, then the samples were loaded onto the gel. Electrophoresis was performed at 100V for 90 minutes. PEI-PEG$_{2k}$ samples were prepared and loaded in a similar fashion. For visualization, gels were stained with

ethidium bromide (0.5 μg/mL) after electrophoresis, and a BioRad ChemiDoc MP Imaging system was used to image each gel using Image Lab software.

For EtBr exclusion assay experiments, stock solutions of calf thymus DNA (ctDNA, 0.24 μg/μL) and EtBr (0.024 μg/μL) were prepared in 10 mM Tris-HCl (pH 7.5) buffer. From the stock, 50 μL EtBr (1.2 μg) was mixed and incubated to 50 μL ctDNA (12 μg), and then the volume was adjusted to 500 μL with 10 mM Tris-HCl. After equilibrating at room temperature for 10 minutes, the required volume (and concentration) of polycation equivalent to the desired polymer/ ctDNA weight ratio was mixed to this solution and incubated for another 30 minutes before placing the sample into a semi-micro quartz cell. The fluorescence emission decay was recorded on a Thermo Lumina Spectrophotometer at λ_{ex} = 520 nm and λ_{em} = 610 nm. The reduction in fluorescence was recorded in terms of the relative fluorescence (%) = $[(F-F_0)/(F_{Max}-F_0)]$ *100, where F is the emission intensity of sample, F_0 is the emission intensity of ethidium bromide and F_{Max} is the emission intensity of DNA intercalated with ethidium bromide.

2.2.4   Dextran Sulfate Displacement Assay

zPEI polyplex stability was checked by dextran sulfate displacement. 200 ng pUC19 samples were complexed with a fixed zPEI/DNA weight ratio of 2.0 at a total volume of 5 μL in 10 mM Tris buffer at pH 7.5. This polycation/DNA weight ratio was observed to be sufficient for complete DNA complexation for all zPEIs used in this study. For PEI-PEG$_{2k}$ /DNA, a weight ratio of 5.0 was required for complete complexation of the DNA. Polyplexes were well mixed and incubated for 45 min at room temperature to ensure complete DNA complexation. Dextran sulfate (DS) was then added at various

weight ratios relative to the DNA and the final solution volume was brought up to 12 μL by addition of buffer. Samples were subsequently incubated for an additional 30 minutes to allow plasmid DNA release from the polyplexes. 2 μL loading dye was then added to each sample followed by sample loading onto a 0.8% agarose gel and electrophoresed as described above. PEI-PEG$_{2k}$ samples were prepared and loaded similarly. DNA was visualized by post-run staining with ethidium bromide (0.5 μg/mL) and imaged using the BioRad ChemiDoc MP Imaging System.

2.2.5   Particle size and ζ-potential analysis

The particle sizes for bPEI/DNA, zPEI/DNA and PEI-PEG$_{2k}$/DNA polyplexes was measured by nanoparticle tracking analysis (NTA) using a Nanosight NS300. Polyplexes were prepared with 0.1 μg pUC19 plasmid DNA at the desired polymer/DNA weight ratio in 200 μL of double distilled water (ddH$_2$O) resulting in a 0.5 μg DNA/mL solution. All samples were further diluted 1:5 with ddH$_2$O and subjected to NTA analysis. A 180s movie containing the Brownian motion tracking of the polyplex nanoparticles was recording using the NTA image analysis software (Version 3.4). Each polyplex sample was repeated three times with freshly injected samples and the resulting particle diameters are reported as the arithmetic mean ± standard deviation.

Zeta potential measurements of polyplexes were performed on a Malvern Instruments Zetasizer (Nano-ZS90) at a 15° scattering detector angle. Polyplexes were formed using 2 μg pUC19 DNA (0.1 mg/mL) and mixed at the desired weight ratio with condensing polymer. Samples were diluted to 1mL total for a final DNA concentration of

2 ng/µl before zeta analysis. Zeta potentials were recorded 3 times each and are reported as mean ± standard deviation.

2.2.6 Polyplex Transfection

HeLa and HEK293 cell lines were cultured in DMEM supplemented with 10% FBS according to ATCC recommendations. Cell lines were seeded in 24-well plates at 7.5 x 10^4 cells/well 24 h prior to transfection. Polymer/DNA complexes were formed by diluting 20 µL of 0.1 µg/µL DNA solution with 80 µL of phosphate-buffered saline (PBS) in a 1.5 mL microcentrifuge tube. Polymer solutions (100 µL) at various concentrations were added dropwise to the DNA solution under constant agitation to achieve the desired polymer/DNA weight ratio. Particles were allowed to incubate at room temperature for 30 min. Immediately before transfection, 200 µL polyplex solution was deposited into 2.8 mL of serum-present medium. Regular growth medium was aspirated from cells and replaced with 750 µL of polyplex/growth medium solution (0.5 µg DNA/well). After 4 h, the transfection medium was replaced with normal growth medium. Transfection efficiency was quantified via luciferase expression 24 h post initial transfection. A Promega luciferase assay kit (Madison, WI) was used to measure protein activity in relative light units (RLU) using a Synergy 2 plate-reader (BioTek, Winooski, VT). Results were normalized to total cell protein using a bicinchoninic acid (BCA) assay from G-Biosciences (St. Louis, MO).

2.2.7 CRISPR/Cas9 Knock-In

Knock-In efficiency of zPEI 2 was evaluated by utilizing a dual plasmid transfection system from Origene (Rockville, MD). The first plasmid, pCas-Guide-AAVS1, encodes the Cas9 enzyme and a guide RNA that targets the AAVS1 region on the genome, while the second plasmid, pAAVS1-Puro-GFP-DNR, encodes for the donor DNA that carries an expressible GFP region. The donor DNA targets the AAVS1 region using 500 base pair left and right homology arms. HEK293 cells were seeded in 6-well plates at 3.0×10^5 cells/well 24 h prior to transfection. Polymer/DNA complexes were formed by diluting 160 μL of 0.1 μg/μL DNA solution containing of 1:1 ratio of the Cas9 and donor DNA plasmids with 500 μL of PBS in a 1.5 mL microcentrifuge tube. Lipofectamine 2000 solution was prepared according to manufacturer protocol. zPEI 2 and bPEI solutions were prepared using the optimum weight ratios determined by luciferase transfection described previously. Equi-volume polymer or Lipofectamine solutions were added dropwise to the DNA solution under constant agitation to achieve the desired carrier/DNA weight ratio. Particles were allowed to incubate at room temperature for 30 min. Immediately before transfection, 1.32 mL polyplex solution was added to 10.68 mL of DMEM with or without 10% FBS. Growth medium was aspirated from cells and replaced with 3 mL of polyplex/growth medium solution (4 μg DNA/well). Transfection was allowed to proceed overnight. The following morning, transfection media was aspirated and replaced by regular growth media. Cells were allowed to grow for 48 h undisturbed, before being seeded in T75 flasks. Cells were then passaged twice over the course of two weeks to eliminate any transient expression. Cells

were analyzed for GFP expression via FACS on a LSR II flow cytometer (BD Biosciences, Franklin Lakes, NJ).

2.2.8 Fluorescent Imaging of GFP

In order to visualize GFP production, transfected cells were subjected to fluorescent microscopy via a Cytation 7 Cell Imaging Multi-Mode Reader (BioTek,Winooski, VT). Cells were transfected as previously described and allowed to passage twice before being seeded into an eight-chamber Lab-Tek II slide at 3.0×10^4 cells/well. Cells were allowed to grow for 24 h before being live stained with Hoechst 33342 nucleus stain (Invitrogen, Carlsbad, CA) according to the manufacturer's protocol. Immediately after staining, cells were imaged live using a widefield integrated microscope with a 10x objective. Hoechst 33342 and GFP were visualized using filter cubes with an excitation/emission of 377/447 and 469/525, respectively.

2.2.9 Protein Interaction Study

The affinity for nonspecific protein binding interactions was assessed by mixing 0.5 mL of bovine serum albumin (BSA) standard (2 mg/mL) with 0.5 mL of each polymer (1 mg/mL). Each mixture was incubated at 37 °C for 1 h. The mixtures were then centrifuged, and samples of the resulting supernatants were collected. The protein concentrations of the samples were determined through the use of a BCA assay and a standard BSA calibration curve. The protein interaction value, A, was defined as:

$$A = 1 - \frac{C_s V_s}{C_i V_i}$$

where C_i is the initial BSA concentration (2 mg/mL); C_s is the BSA concentration in the supernatant determined by BCA; V_i is the initial volume of the BSA solution (0.5 mL); V_s is the total volume of the BSA after adsorption measurement (1 mL). The interaction value A, as it has been described, is essentially a measure of how much protein has been removed from the initial solution via aggregation with polymer, and thus, ranges between 0 (no removal of protein) and 1 (complete removal of protein).

2.3   RESULTS AND DISCUSSION

2.3.1   Synthesis and characterization of minimally succinylated PEIs (zPEIs)

As the objective of this study was to investigate the gene delivery efficacy of sparsely modified bPEI via conjugation to succinic anhydride and subsequently compare the 'shielding abilities' with commercial PEI-PEG$_{2k}$, a series of minimally functionalized zwitterion-like PEI (zPEI) was synthesized. Strategies for the modification of branched, 25-kDa PEI were adapted from our previous work (**Figure 2.1a**).[99] By varying the feed mole percentages of succinic anhydride with respect to the total amine content of PEI, we controlled the percent modification of total amines of the zPEIs to the range of 2-11.5% as determined by ^{1}H-NMR and confirmed by FT-IR. Some cloudiness was observed in the zPEI product solutions due, presumably, to aggregation of the polymer product under the basic conditions used to synthesize the zPEIs. To improve solubility, the zPEIs were clarified by addition of small amounts of 0.1 M HCl to near neutral pH (pH ~7). All NMR and FT-IR spectra are shown in the supporting information (**Figure 2.8-2.9**). Upon succinylation, two characteristic new peaks at 1635 cm^{-1} and 1563 cm^{-1} are
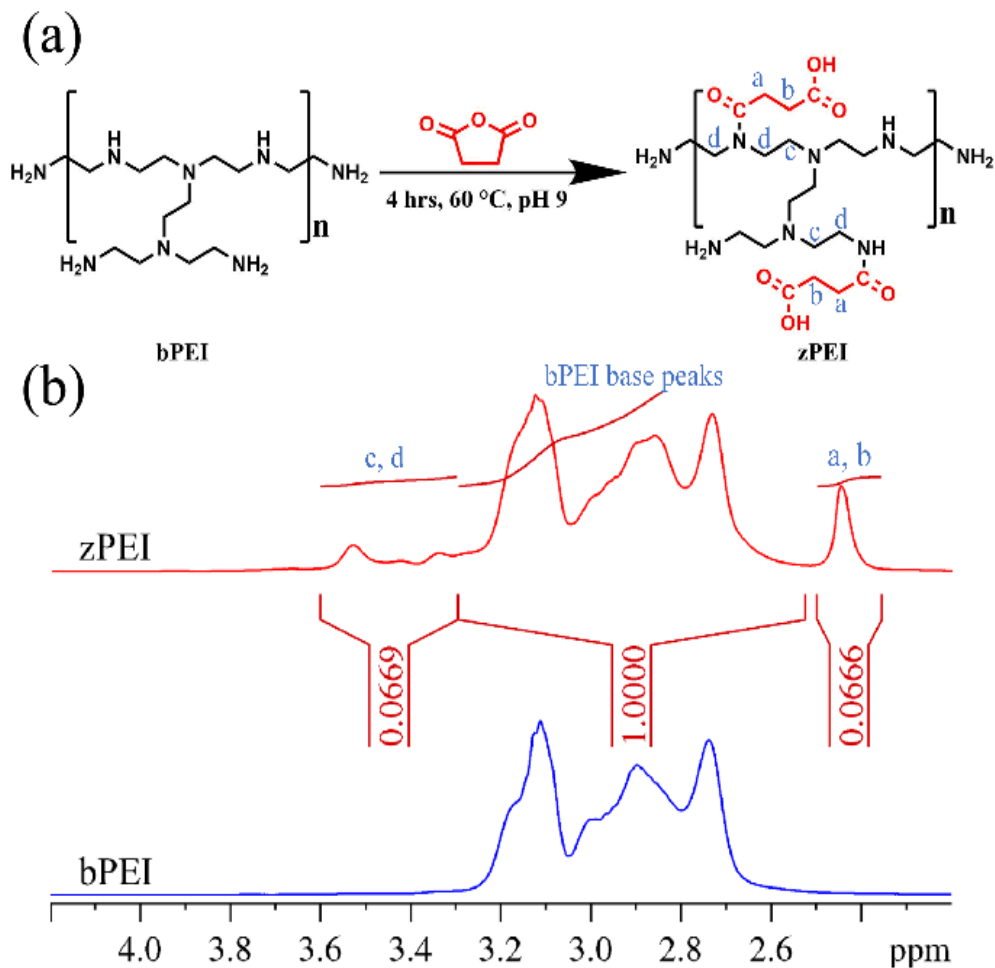
Figure 2.1. (a) Synthesis scheme for zwitterionic-like PEIs (zPEIs) via succinylation of primary and secondary amines of a 25-kDa branched PEI polymer. (b) representative 1H-NMR spectra of bPEI and zPEI after neutralization to pH 7. Shown are 6.5% functionalized zPEI (zPEI-6.5, top) and unmodified bPEI (bottom).

observed by FT-IR for all zPEIs due to the carbonyl stretch and N-H bend, respectively, of the amide moiety of the succinyl group grafted to the PEI polymer. While all of the PEIs have a characteristic set of methylene proton base peaks at 2.6 to 3.3 ppm by ^{1}H-NMR, upon succinylation two sets of new peaks are also observed as described above in Methods and Materials. The degree of modification was subsequently analyzed and

quantified by ^{1}H-NMR from the ratio between methylene of PEI (δ 2.6-3.3 ppm) and methylene of the succinyl group (δ 2.4-2.5 ppm). In **Figure 2.1b**, we show the ^{1}H-NMR spectra of unmodified bPEI (lower) compared to 6.5% modified zPEI (zPEI 6.5, upper) where the degree of modification was expressed as the percentage of the total amines in bPEI that were succinylated.

2.3.2   zPEI complexation of DNA

A prerequisite for effective gene delivery is the ability to assemble stable polyplexes. The complexation of DNA by polycations occurs by entropically driven electrostatic interactions.[100] The ability of the minimally modified zPEIs to condense plasmid DNA was assessed using both electrophoretic mobility shift assay (EMSA) (**Figure 2.2a**) and EtBr exclusion assays (**Figure 2.2b**). Compared to bPEI, nearly all succinylated zPEIs ($\geq$ 3% modified) required higher polymer:DNA weight ratios to fully retard DNA migration in agarose gel electrophoresis (**Figure 2.2a**). The required polymer:DNA weight ratio increased with the percent modification of the PEI, presumably due to the reduction of the positive charge density upon conjugation to the succinyl group. Higher degrees of modification resulted in more zPEI being required to fully bind the DNA. For example, unmodified PEI required a bPEI/DNA ratio 0.375 (wt/wt) in good agreement with prior literature[101]. In contrast, to fully condense the DNA, zPEI 3, 6.5, 9, and 11.5 required polymer/DNA ratios of 0.625, 0.625, 0.75, and 1.125 (wt:wt), respectively. No significant difference in DNA binding between PEI and zPEI 2 was observed.

The influence of succinylation on the ability of zPEI to condense DNA was further investigated by ethidium bromide exclusion assay (**Figure 2.2b**). Upon intercalation between DNA base pairs, the fluorescence intensity of EtBr increases significantly. Condensation of DNA by the binding of polycations prohibits binding of EtBr, leading to a corresponding drop in the fluorescence intensity. All the polycations displayed similar sigmoidal condensation curves. zPEIs were able to fully condense calf thymus DNA to the same extent as unmodified bPEI, as evidenced by the same residual relative fluorescence, at sufficiently high polymer/DNA ratios. The EtBr exclusion assay curves shifted to higher polymer/DNA ratios with increasing degree of succinylation. All zPEIs studied (2-11.5% modified) achieved condensation by polymer/DNA ratio 1 (wt/wt). These polymer/DNA ratios required for full condensation by EtBr exclusion assays were often found to be slightly higher than those observed by EMSA, suggesting an effect of the applied electric field on the migration of the plasmid DNAs in the agarose gels.
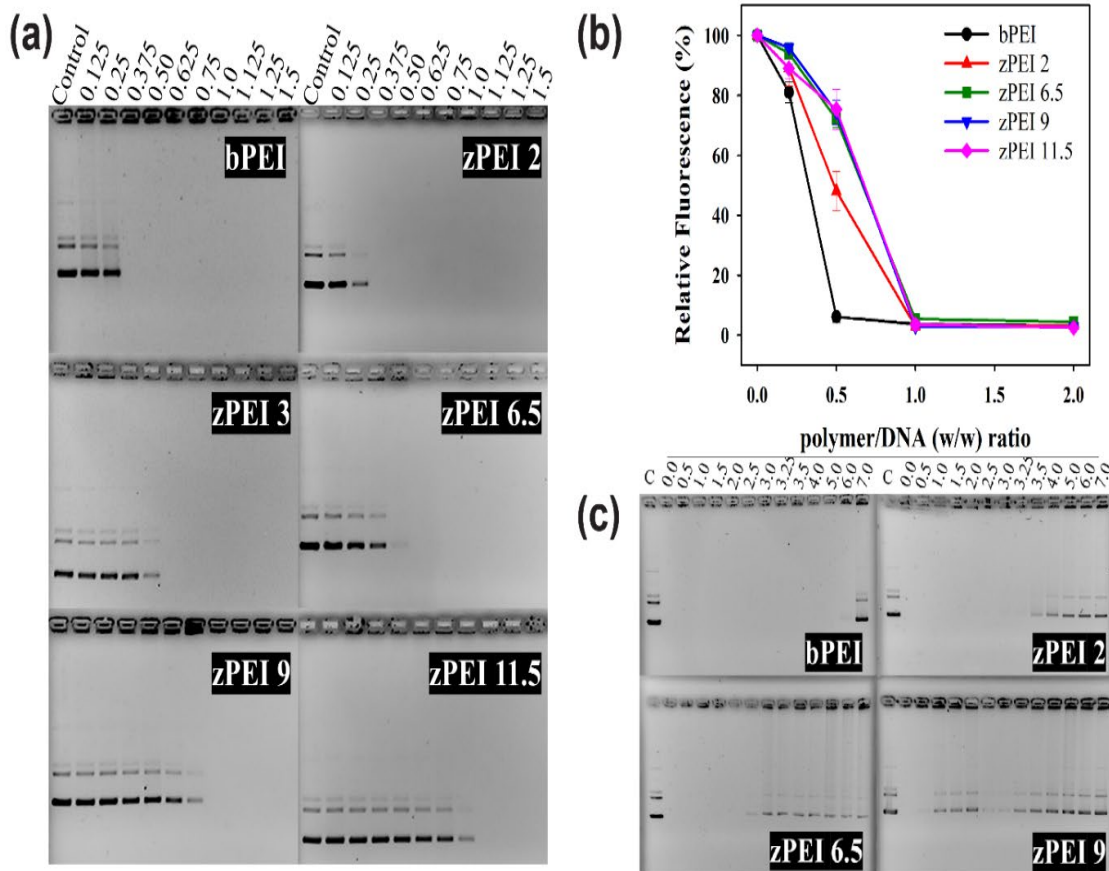
Figure 2.2. Polyplex complexation and stability assessment. (a) Evaluation of pUC19 plasmid DNA complexation with unmodified bPEI and zPEI (2-11.5%) by electrophoretic mobility shift assay (EMSA). Complete retardation for all polycations was achieved by polymer/DNA weight ratio of 1.0. The number above each lane signified the polymer/DNA wt/wt ratio used to form each corresponding polyplex. Uncomplexed DNA control is also shown. (b) DNA condensation by unmodified bPEI and zPEI (2-11.5%) as determined by an ethidium bromide exclusion assay measured at λ_{ex} = 520 nm and λ_{em} = 610 nm. Calf thymus DNA (ctDNA) was used for all polyplexes. The fluorescence intensity was expressed as a percentage relative to the initial fluorescence. Data are presented as mean +/- SD (n = 3). (c) Dextran sulfate (DS) displacement assay of bPEI and zPEI complexes formed at polymer/DNA weight ratio 2:1 analyzed by agarose gel electrophoresis. As percent modification increases, the binding strength of zPEI decreases requiring less DS to displace the DNA from the polyplexes. Shown are pUC19 plasmid DNA complexed with unmodified PEI (bPEI) and zPEI 2, zPEI 6.5, and zPEI 9. The first lane is a control (C, free DNA) while the numbers above each lane represent DS:DNA weight ratio.

2.3.3   Dextran sulfate displacement assay

For transcription to occur, polyplexes must be able to dissociate into free DNA and polymer upon entering the cell. This creates a well-known bottleneck for polyplexes requiring balancing of the polymer-DNA interactions to create particles that are sufficiently stable to reach cells but not too stable as to prevent dissociation inside the cell. To investigate how these low degrees of succinylation alter complex stability in our zPEI polyplexes, we evaluated the stability of our particles to a competing polyanion, the sulfated polysaccharide dextran sulfate (DS, 9-20 kDa). DS mimics sulfated extracellular glycosaminoglycans (GAGs), such as heparan sulfate, that are well known to competitively displace DNA from cationic polymers in polyplexes in vivo.[102] The relative strength of polymer-DNA interactions can be quantified by determining the ability of DS to displace polycation from DNA. Unmodified bPEI and zPEI polyplexes were prepared at polymer/DNA ratio 2 (wt/wt) sufficient to completely condense DNA for all zPEIs studied, and subsequently incubated with DS at various concentrations. Polyplex dissociation was followed by agarose gel electrophoresis (**Figure 2.2c**). With increasing succinylation, we observed a systematic decrease in the amount of DS required to release DNA in the zPEI series. Unmodified bPEI required 7 μg DS/μg DNA to completely displace DNA from its polyplex, while 3.4, 3.0 and 1.0 μg DS/μg DNA were required for the onset of DNA release with zPEI 2, 6.5 and 9, respectively. For minimally modified zPEI, the release of DNA was not always complete on the gel. This incomplete release was not observed for unmodified bPEI or previously studied highly modified zPEIs. This suggests the sparsely modified zPEIs are maintaining some weak interaction with the polyplex DNA even in the presence of excess polyanion competitor. However, the

amount of DS required for onset of DNA release still decreased in a systematic way with increasing degree of modification, consistent with a weakening of the polymer-DNA interactions with increasing amounts of grafted anionic succinate groups to the PEI backbone.

2.3.4 Characterization of PEI-PEG Polyplex complexation and stability

In our previous study with high percent modified zPEIs (9-55%), we observed that succinylation led to a substantial decrease in nonspecific protein binding. We proposed this reduced affinity for protein interactions may result from the formation of a tightly bound hydration layer due to the assumed zwitterionic nature of the polyplex surface. This tightly bound water layer thus acts in a fashion similar to more commonly used strategies to incorporate shielding domains, such as PEG, to polyplex formulations. We were therefore interested in directly comparing our minimally functionalized zPEI series to PEGylated PEI. To investigate the effects of PEGylation on PEI condensation of DNA, we compared unmodified 25-kDa bPEI to PEI-PEG$_{2k}$ copolymer by a mobility shift assay (**Figure 2.3a**). Here, the PEI-PEG$_{2k}$ is a graft copolymer of 25-kDa, branched PEI modified with 2-kDa PEG at a 10% substitution ratio of primary amines. Unmodified bPEI is observed to fully condense DNA at a polymer/DNA weight ratio 0.5. Assuming the theoretical 25:50:25 ratio of primary, secondary, and tertiary amines for bPEI, we can estimate the 10% substitution on PEI results in ~15 PEG chains per PEI molecule resulting in a total polymer MW for PEI-PEG$_{2k}$ of ~55 kDa. Some experiments have shown commercial bPEI may have closer to a 33:33:33 ratio of primary, secondary, and
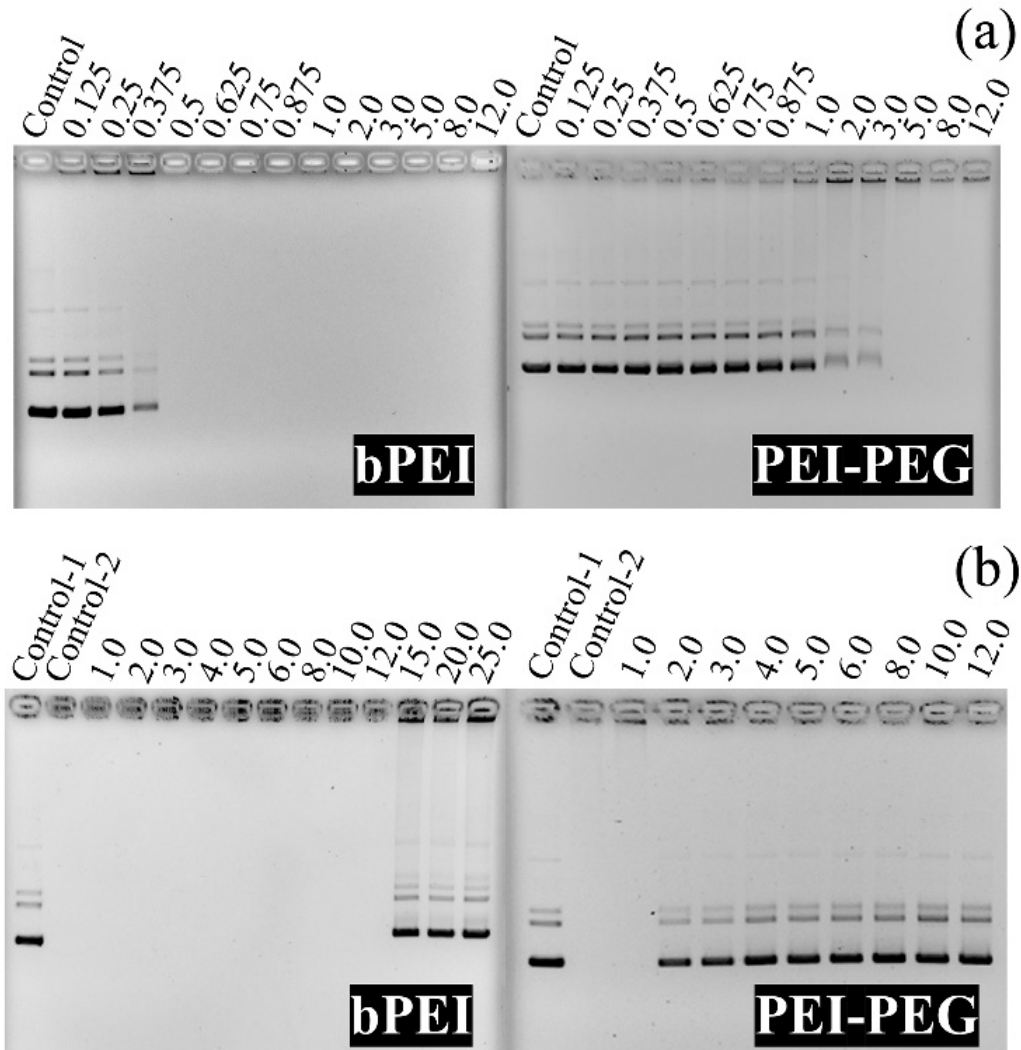
Figure 2.3. (a) Electrophoretic mobility shift assay (EMSA) of 200 ng pUC19 plasmid complexed with bPEI and PEI-PEG$_{2k}$. Numbers above the lanes signify the polymer/DNA weight ratio used to form each corresponding polyplex. The leftmost lane is uncomplexed pUC19 DNA as control. (b) dextran sulfate (DS) displacement assay for bPEI and PEI-PEG$_{2k}$ complexes formed at polymer/DNA weight ratio 5. Control-1 is pUC19 with no polycation present, while control-2 is polymer/DNA complex with no DS present. Numbers above the lanes designate the DS:DNA weight ratio.

tertiary amines.[103] This ratio at 10% substitution would result in ~19 PEG chains per PEI resulting in a total MW for PEI- PEG_{2k} of ~63kDa. If we only consider the PEI part of the copolymer, and assume the PEG is not altering the PEI:DNA interactions, we would expect full condensation of PEI-PEG_{2k} by polymer/DNA weight ratio of 1.1-1.25. Instead, we observe the PEI-g-PEG_{2k} does not achieve full complexation until polymer/DNA weight ratios > 3. This suggests the PEG is sterically hindering the polycation interactions with DNA, altering the polymer-DNA interactions in the polyplexes. This is consistent with prior reports that suggest a complex relationship between PEGylation and transfection efficacy that can depend on PEG MW and percent substitution.[104] We also examined the effect of PEGylation to alter the complex stability in PEI- PEG_{2k} polyplexes when compared to unmodified bPEI/DNA using the dextran sulfate displacement assay (**Figure 2.3b**).

As the PEGylated PEI required more polymer to achieve full condensation, the displacement assay was done at the higher polymer/DNA weight ratio of 5 for both bPEI and PEI-PEG_{2k}. At this higher polymer/DNA ratio, unmodified bPEI released DNA from its complex at 15 μg DS/μg DNA, while PEI-PEG_{2k} required only ~2 μg DS/μg DNA for significant release of its DNA. This release occurred at DS/DNA ratios significantly lower than expected even if we only consider the PEI component of the copolymer, again consistent with the PEG greatly reducing the PEI-DNA interaction strength, thus reducing the polyplex stability.

2.3.5   Particle size and zeta potential measurement

Polyplex size and zeta potential are known to be key parameters that dictate transfection performance. To better understand how bPEI, zPEI and PEI-PEG$_{2k}$ polyplex particles differ, we measured their size by nanoparticle tracking analysis (NTA) at polymer/DNA weight ratios sufficient for complete DNA condensation. Results are given in **Table 2.1**. As shown, bPEI/DNA (wt/wt 0.5) results in nanoparticles exhibiting a mean size of 97.5 ± 10 nm and a zeta potential of +12.3 mV indicating compact polyplex formation with a positive surface charge. In general, the minimally modified zPEI polymers at weight ratio 1, all produce polyplexes with nearly the same mean size with a small increase observed for the highest modified zPEI studied. The zeta potential of the low percent modified zPEI polyplexes decreased slightly compared to unmodified bPEI/DNA. 2-11.5% modified zPEI resulted in nanoparticles with zeta potential of ~10-11 mV compared to 12.3 for unmodified bPEI/DNA and no clear trend with increasing percent modification. Since the addition of the succinyl group to zPEI is expected to both neutralize

Table 2.1. NTA analysis and ζ-potential of polyplexes. Data presented as mean ± SD (n = 3)

	Polymer: DNA (wt:wt)	Polyplex Diameter (nm)	ζ-potential (mV)
PEI	0.5:1	97.5 ± 10	12.3 ± 0.9
zPEI 2	1:1	101.5 ± 17	11 ± 2
zPEI 6.5	1:1	102.7 ± 25	11 ± 1.43
zPEI 9	1:1	103.7 ± 3	10.4 ± 1.4
zPEI 11.5	1:1	112.6 ± 4.7	11.2 ± 1.0
PEI-PEG$_{2k}$	5:1	118 ± 5.3	4.81 ± 1.6

a positive charge while simultaneously adding a negative charge, this minimal impact on the zPEI polyplex surface charge is surprising but consistent with our prior study.[99] One possible explanation for this is that the addition of a succinyl group onto a PEI amine may increase the pKas of neighboring amines resulting in a net charge on the zPEIs comparable to bPEI. Previously, we showed that only at very high percent modification (>40%) did we observe significant decrease in zPEI polyplex zeta potential. PEGylation of polyplexes is well known to typically result in a decrease in the particle zeta potential due to PEG shielding the positive surface charge of PEI. Here, we determine the mean particle size and zeta potential for our PEI-PEG$_{2k}$/DNA particles at weight ratios sufficient for complete DNA condensation (wt:wt 5). We observe slightly larger polyplexes (mean diameter ~118 +/- 5 nm) but a significant decrease in the particle zeta potential (z = 4.81mV) when compared to bPEI or zPEI polyplexes.

2.3.6 In-Vitro Transfection Efficiency

In previous studies, we and others showed that succinylation of PEI results in modest improvement of transfection of DNA in the absence of serum.[98-99] In contrast, we see significant improvement in transfection efficacy in the presence of serum for zPEI/DNA polyplexes. This improvement is such that zPEI efficacy in the presence of serum was observed to meet or exceed transfection of unmodified bPEI in the absence of serum. In our previous study of more highly modified zPEIs,[99] we found the lowest percent modifications studied (9-25%) were the most effective for gene delivery to HeLa, MC3T3-E1 and MDA-MB-231 cells. To further study the effectiveness of zPEIs, we study here a series of sparsely modified zPEIs (2-11.5%) to determine both a minimum

modification needed for enhanced transfection as well as the range of modifications resulting in maximum gene delivery improvement. For this study, two cell lines (HEK 293 and HeLa) were transfected with polyplexes of unmodified PEI, minimally functionalized zPEIs, and PEI-PEG$_{2k}$ to determine gene expression in the presence of serum at various polymer/DNA ratios (**Figure 2.4**). Unmodified PEI exhibited a nearly constant level of gene expression under the polymer/DNA weight ratio range of 1:1 to 6:1 for both cell lines. The minimally modified zPEIs (2-11.5%) generally all show significantly improved transgene expression at nearly all weight ratios in both cell lines. Remarkably, even PEI succinylated at levels as low as 2% still show this significant enhancement of the transgene expression in both cell lines upon transfection in the presence of serum. Here, maximum gene expression for zPEI was observed at polymer/DNA weight ratio 2:1 and 4:1 for HEK293 and HeLa cells, respectively. Comparing these maximum transfection efficiencies, zPEI 2 exhibited 477-fold higher gene expression in HEK293 cells (**Figure 2.4a**) and 262-fold in HeLa cells (**Figure 2.4b**) as compared to unmodified PEI. While an optimal modification percent was not clear, we see a broad range of 2-10% modification results in the maximal gene expression in the presence of serum for zPEIs. In nearly all transfections, zPEI efficacy is observed to decrease at modifications higher than 10%. Yet even the highest modification studied in this manuscript (zPEI 11.5) at polymer/DNA weight ratio 2:1 exhibited 85- and 143-fold higher gene expression as compared to maximum gene expression of unmodified bPEI in HEK293 and HeLa cell lines, respectively.

Lastly, we compared zPEI to a commercially available PEI-PEG$_{2K}$ to directly compare in-serum transfection efficiencies. PEGylation is known to decrease interaction
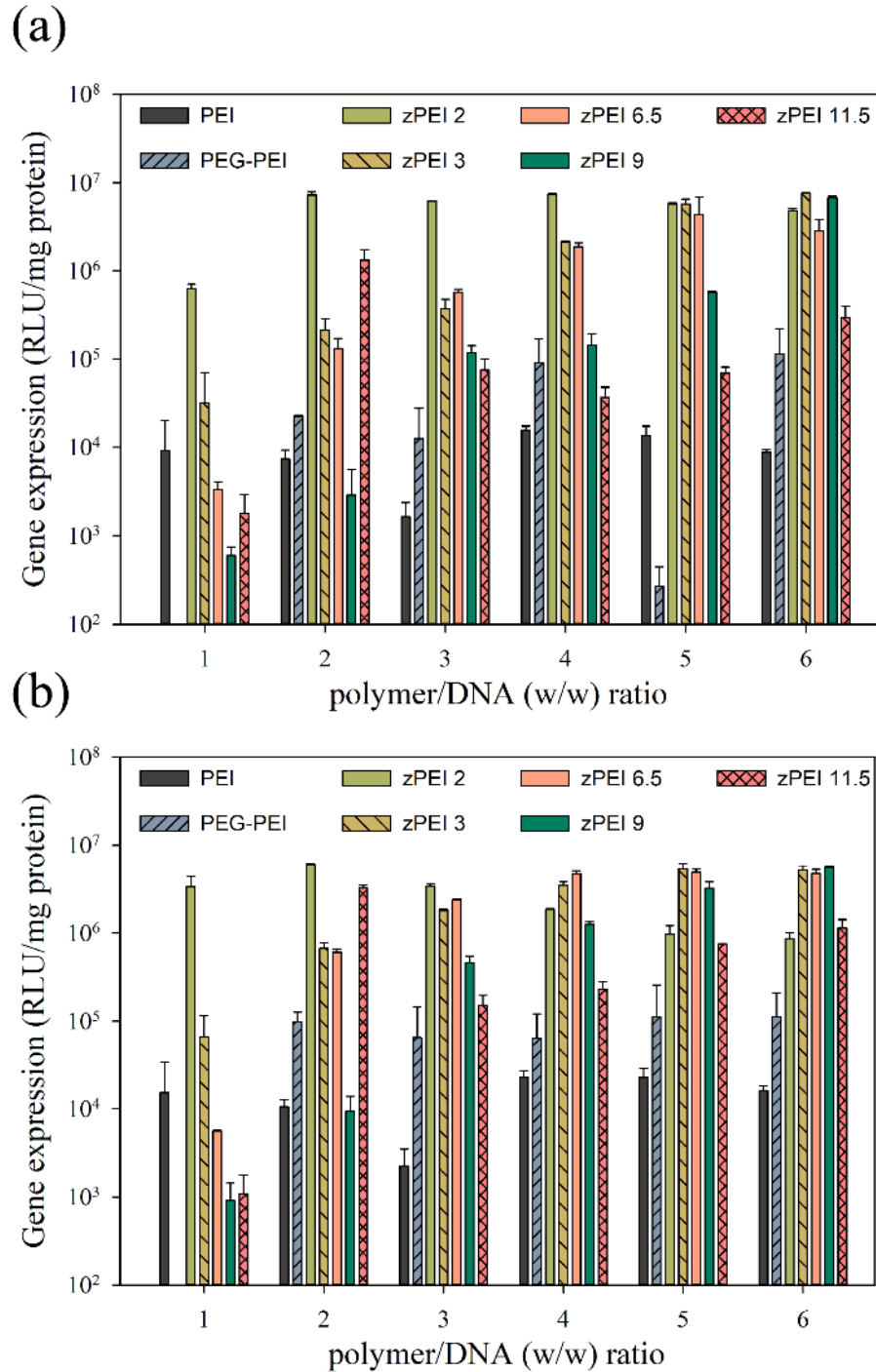
Figure 2.4. In vitro transfection efficiency of polyplexes of plasmid DNA (pGL3) with unmodified, PEGylated, and succinylated PEI in (a) HEK293 and (b) HeLa cells in the presence of 10% FBS. Luciferase activity in the cell lysates is reported as relative light units (RLU) normalized by the mass of total protein in the lysate. (n = 3; error bars represent standard deviation.)

of the polymers with serum proteins, often resulting in decreased toxicity and improved biodistribution compared to unmodified PEI.[104] We previously showed higher degrees of succinylation of PEI also results in decreased toxicity and reduced interactions with proteins.[99] For transfections in-serum, the maximum gene expression of PEI-PEG$_{2k}$ was found to occur at polymer/DNA weight ratio 5:1 for both HEK293 and HeLa cell lines (**Figure 2.4**). When compared to unmodified PEI, the transgene expression is found to be only 5- to 7-fold higher. In comparison to PEI-PEG$_{2k}$, zPEI 2 exhibited 65- and 53-fold higher transgene expression in HEK 293 and HeLa cells, respectively, at polymer/DNA weight ratio 2:1. PEI-PEG$_{2k}$ at polymer/DNA weight ratio of 1 was not used in this study as the previous binding assays (**Figure 2.3**) showed PEI-PEG$_{2k}$ did not sufficiently bind DNA to form polyplexes at this weight ratio.

2.3.7   CRISPR/Cas9 Knock-In Efficiency

CRISPR/Cas9-mediated knock-in of genes by homology-directed recombination typically requires simultaneous expression of Cas9, transcription of a single guide RNA (sgRNA), and delivery of a "donor" plasmid containing the gene sequence to be introduced. The efficiency of knock-in is often very poor (less than 1%), especially in primary cells or in vivo.[105] Knock-in in such cases may be more efficient, and cell viability may be better preserved, if efficient transfection of the CRISPR/Cas9 components could be achieved in the presence of serum. Thus, we investigated knock-in efficiency in HEK293 cells using zPEI 2 to co-deliver a plasmid that encodes Cas9 and a sgRNA targeting the AAVS1 locus, and a donor plasmid that encodes GFP, both in the absence and presence of serum, in comparison to bPEI and Lipofectamine 2000 (L2k).

Transfections with zPEI 2 resulted in significantly higher percentages of GFP-expressing cells than PEI and L2k in both the presence and absence of serum (**Figure 2.5**). Knock-in efficiency, quantified as the percentage of GFP-positive cells determined by flow cytometry (**Figure 2.6**), was two- and 1.6-fold greater upon transfection in the absence of serum with zPEI 2 compared L2k and bPEI, respectively. In the presence of serum, however, knock-in efficiency with zPEI 2 increased slightly. Transfection with L2k and bPEI, in contrast, decreased significantly in the presence of serum. As a result, zPEI 2 provided a remarkable 16-fold increase in the knock-in efficiency compared to both controls. The increased knock-in efficiency with zPEI 2 in the presence of serum than in its absence may be attributed to deleterious effects upon incubation of the cells in the absence of serum overnight, which may be expected to decrease cell viability. In many protocols, the decrease in viability (and, thus knock-in efficiency) due to the absence of serum is outweighed by the severe decrease in transfection efficiency observed with many conventional transfection reagents in the presence of serum. Using zPEI 2, however, we achieved efficient transfection while maintaining cell viability (**Figure 2.10**).
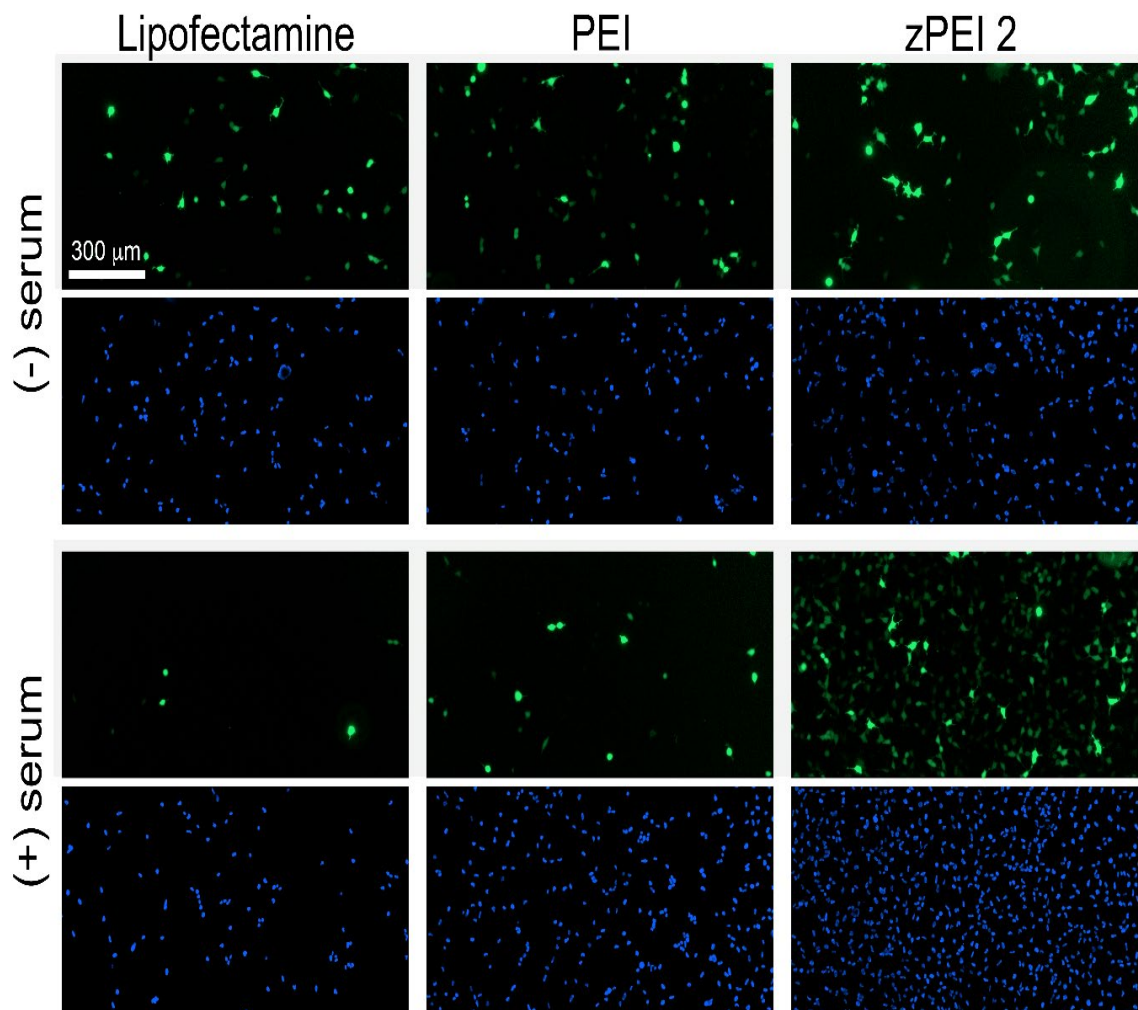
Figure 2.5. Confocal fluorescence micrographs of HEK293 cells transfected with a dual-plasmid CRISPR/Cas9 system to knock in GFP, mediated by Lipofectamine 2000, bPEI, or zPEI 2, in the absence and presence of serum. Cell nuclei were stained with Hoechst 33342(blue). Scale bar = 300 µm.
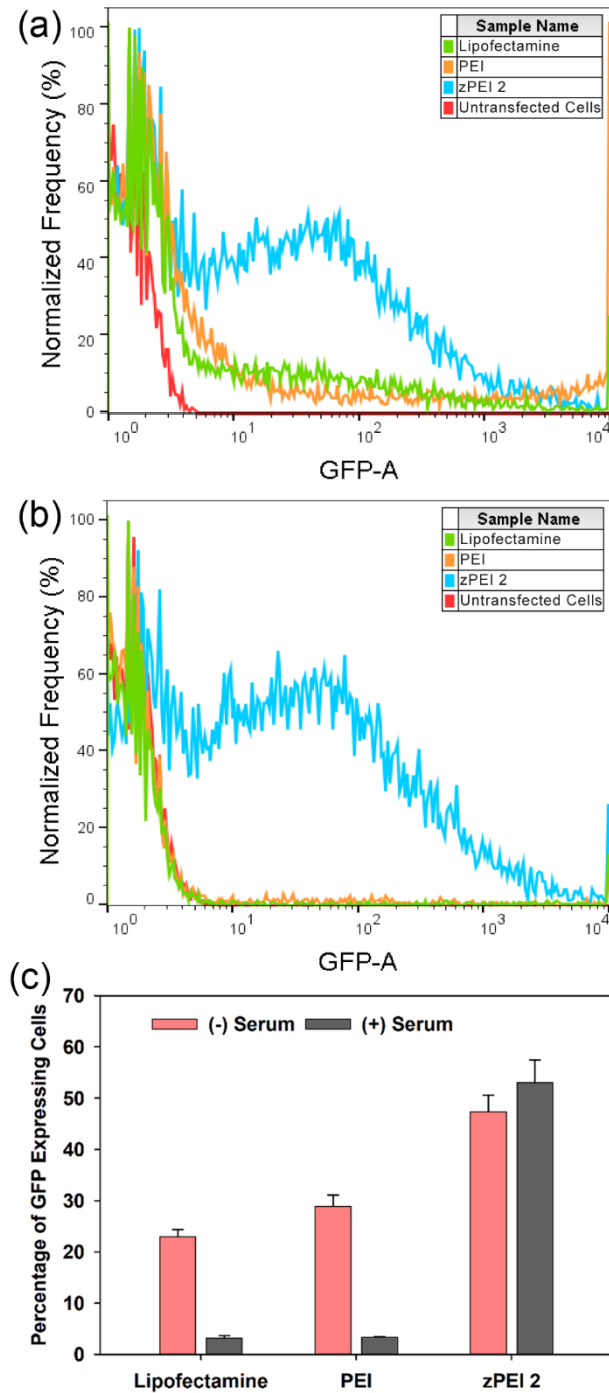
Figure 2.6. Flow cytometry of HEK293 cells following CRISPR/Cas9-mediated knock-in of GFP upon transfection using L2k, bPEI, and zPEI 2 in (a) the absence and (b) the presence of serum. (c) Knock-in efficiency as determined by the percentage of GFP-expressing cells. Cells were allowed to grow normally for two passages to eliminate any transient GFP expression. (n=3; error bars represent standard deviation).

2.3.8 Interaction of Polymers with Serum Proteins

To further evaluate the relative stabilities of our different polymer systems in the presence of serum proteins, we quantified the ability of bPEI, zPEI and PEGylated PEI to aggregate bovine serum albumin (**Figure 2.7**). At physiological pH, most serum proteins are anionic. Due to the low isoelectric point of bovine serum albumin (BSA, pI = 4.7), it remains anionic under physiological conditions and thus serves as a model serum protein.[106] All polymers were incubated with 2 mg/mL BSA for 1 h. This protein
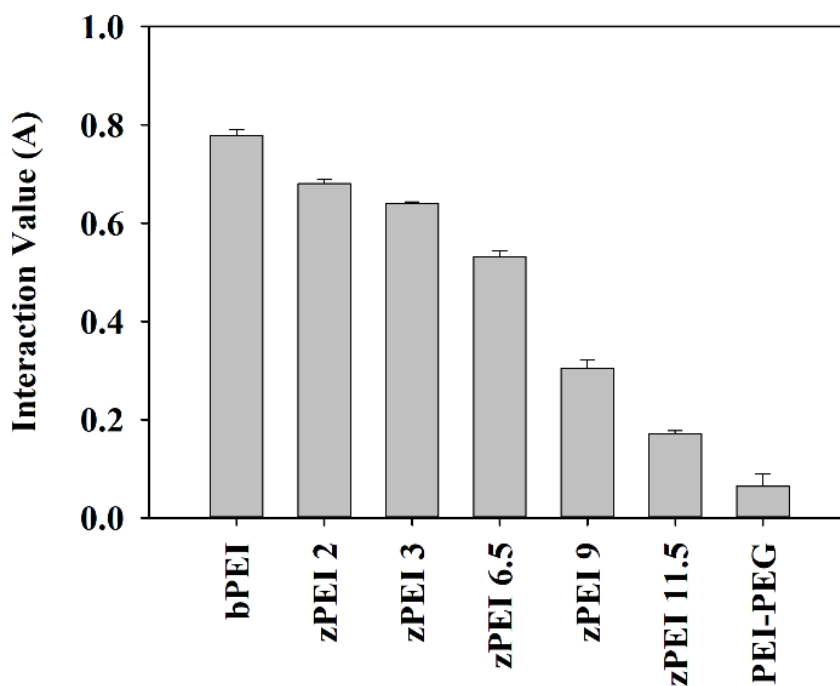
Figure 2.7. Protein interaction values of free polymers incubated with BSA standard for 1 h. Interaction values were expressed as the percentage of protein adsorbed per weight of polymer determined through the difference in protein concentration before and after incubation. (n = 3; error bars represent standard deviation).

concentration is comparable to the anionic protein concentration in growth media containing 10% serum. Unmodified PEI interacts most strongly with BSA, resulting in the highest observed interaction values. PEI-PEG$_{2k}$ shows a strong decrease in the protein interaction due, presumably, to the reduced net charge and steric hindrance of the grafted PEG chains. For our minimally modified zPEIs, we only see a significant decrease at succinylation levels $\geq$ 9%. Zwitterionic materials, with equimolar amounts of positive and negative charges on the same chain, have been extensively studied for nonfouling applications. These systems are thought to resist nonspecific protein binding due to a tightly bound water layer with the zwitterionic surface that forms a physical and energetic barrier to adsorption of proteins.[107-108] The very low degree of succinylation for the zPEIs studied here would suggest the resulting polyplexes are unlikely to have sufficient positive and negative surface charges to form such a tight water layer. The high efficacy of sparsely modified zPEIs such as zPEI 2, in which only ~12/581 PEI amines have been functionalized, is thus highly surprising. From binding and competition assays, zPEI 2 seems to bind and release DNA in a similar fashion to unmodified PEI. Previously, we observed in HeLa, MDA-MB-231 and MC3T3-E1 cell lines that higher levels of succinylation (>14%) were required to significantly decrease cytotoxicity of the zPEIs.[99]

In addition, the cellular uptake for the best performing zPEIs (9-25%) in that study were not significantly higher than unmodified bPEI. From **Figure 2.7**, we also see zPEI 2 gene expression in serum is not correlated to reduced nonspecific protein interactions. Recently Zhu et al.[109] showed that proteins such as BSA can adsorb onto PEI polyplexes to form a protein corona, significantly altering the gene delivery activity of the complexes. Similarly, the low-percent-modified zPEIs may alter the adsorption of

serum proteins onto the zPEI complexes relative to unmodified PEI polyplexes, which may explain the significant enhancement of zPEIs in the presence of serum. Another possible explanation is the succinylation of zPEI may trigger a response from the succinate ligand-receptor on the cell surface, possibly leading to uptake by macropinocytosis or another internalization pathway leading to increased transgene expression.[110-111] Further investigations into uptake pathways for zPEI are currently underway.

2.4 CONCLUSION

We have synthesized a series of minimally succinylated polyethylenimines to determine their transfection efficacy and biocompatibility in the presence of 10% serum. The introduction of negatively charged succinate group neutralizes a small fraction of amines resulting in decreased polymer/DNA binding ability but retaining transfection efficiency. Overall, the key finding from this study is that succinylation of PEI on as few as 2% of amines provides significant improvements in gene delivery. Maximum transfection efficacy was observed at ~2-10% modification with a significant decrease in transfection efficiency for zPEI with succinylation higher than 10%. These minimally (<10%) modified zPEIs, all exhibited 220-fold to 490-fold improvement in transgene expression in the presence of serum as compared to that of unmodified bPEI and more than 50-fold higher efficacy than commercial PEI-PEG$_{2k}$ polyplexes in both HEK293 and HeLa cell lines. Furthermore, zPEI 2 allowed highly efficient knock-in of a marker gene in the presence of serum, which may provide a significant advantage in CRISPR-

mediated genome editing in difficult-to-transfect cells. Tuning positive charge density of a polymer vector is thought to be crucial to optimize serum stability and electrostatic interaction with proteins on the cell membrane to initiate endocytosis. However, the protein interaction for our minimally modified zPEIs does not correlate with the transfection efficacy, suggesting that reduced adsorption of serum proteins on polyplexes is not the critical factor for a successful transgene polyplex carrier.

2.5 Supplementary Information

2.5.1 Synthesis of polymers

zPEIs were synthesized using the protocol from our previous work by Warriner et.al. (2018). Half a gram of branched PEI (bPEI, 25kDa) was dissolved in 3 ml bicarbonate buffer (0.1 M, pH 9) and reacted with succinic anhydride at different mole ratios for 4 hours at 60 °C. The reaction mixture was then dialyzed with snakeskin dialysis tubing (3.5 kDa MWCO) in double distilled water for 24 hours changing the water every 4 hours. After dialysis, the products were filtered with 0.22 μm PVDF membrane filter, then frozen overnight and lyophilized for another 24 h. Upon re-dissolving, the zPEI solutions were often observed to have some cloudiness that was not removed with filtering. To improve solubility, the zPEI polymers were subsequently buffered to pH 7 by addition of HCl (0.1M) clarifying the solution. After acidification, the product was frozen overnight and lyophilized again for 24 hours. The dried product was placed in a -80 °C freezer for storage. Successful reaction and percent succinylation were subsequently determined by FT-IR and ^{1}H NMR, respectively.

2.5.2 Fourier transform infrared (FTIR)

FTIR analysis of bPEI and all zPEIs were collected to confirm the polymer modification using an iS50 FT-IR equipped with a diamond ATR within the range 400-4000 cm^{-1} equipped with OMNIC software. Upon successful coupling reaction of the bPEI with succinyl anhydride to form zPEI, characteristic peaks at 1563 cm^{-1} and 1635

cm^{-1} are seen corresponding to the carbonyl stretch and N-H bend of the amide, respectively. FTIR spectra are given in **Figure 2.8**.
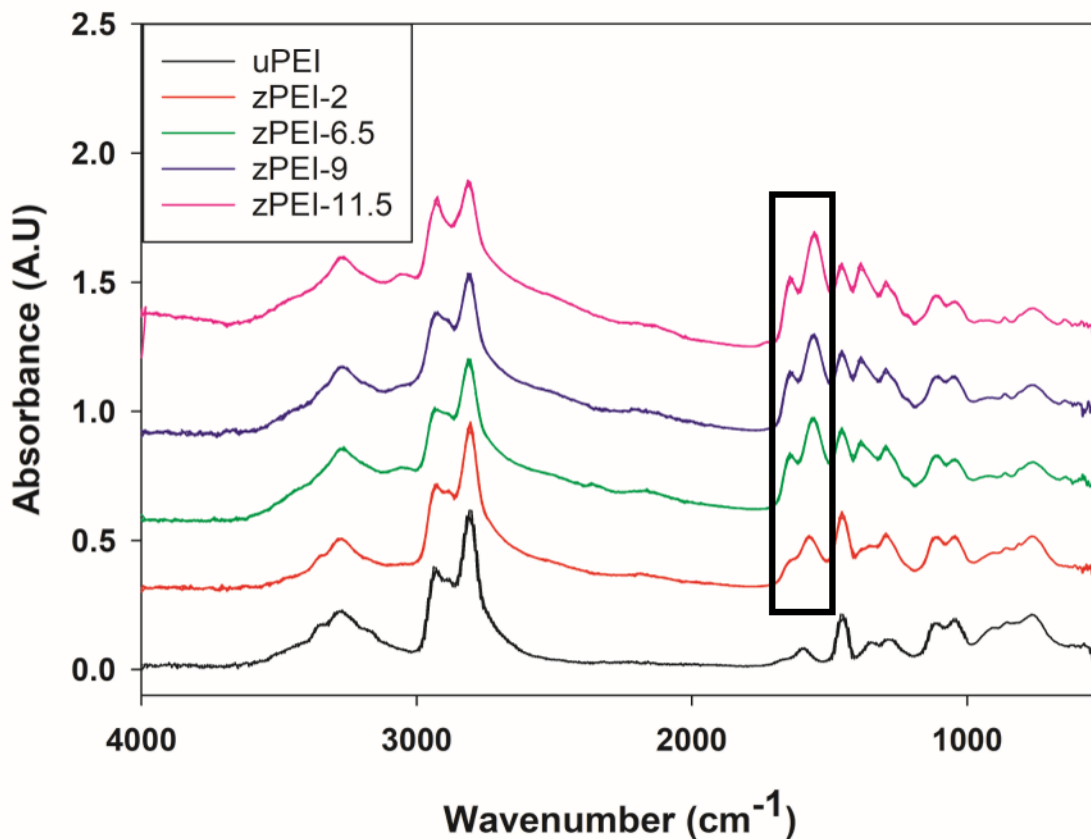
Figure 2.8. The FTIR spectra of unmodified bPEI and zPEI (2-11.5% modified) polymers.

2.5.3 NMR characterization of bPEI and zPEI

To quantify the degree of modification of the polymers, ^{1}H-NMR characterization was conducted on a 400 MHz Bruker Avance NEO spectrometer equipped with a smart probe. For NMR analysis, 6.5 mg of lyophilized polymer was dissolved in 0.65 mL D$_2$O and data was analyzed with Topspin 4.0.3 data analysis software. NMR spectra are given in **Figure 2.9**. The relative area of succinate methylene peaks (δ 2.4-2.5 ppm) was

compared to the peaks of branched PEI methylene protons (δ 2.6-3.3 ppm) to determine the degree of modification of zPEIs.
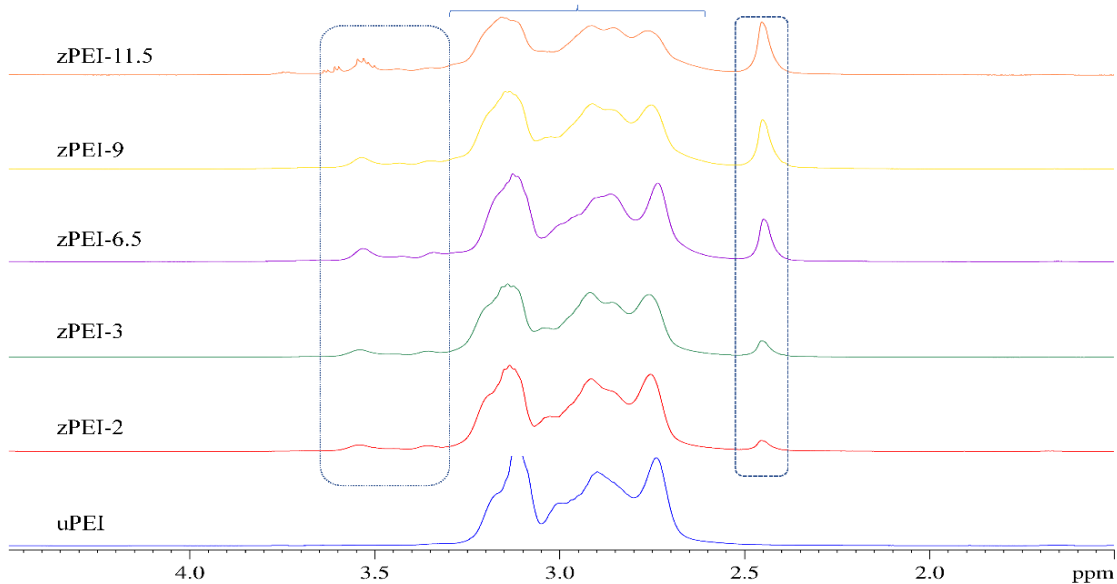
Figure 2.9. ^{1}H NMR of unmodified bPEI and zPEI (2-11.5% modified).

2.5.4 Toxicity of Serum Deprivation

HEK293 cells were seeded in 24-well plates at 7.5 x 10^4 cells/well 24 h prior to transfection. Polymer/DNA complexes were formed by diluting 20 μL of 0.1 μg/μL DNA solution containing of 1:1 ratio of the Cas9 and donor DNA plasmids with 80 μL of PBS in a 1.5 mL microcentrifuge tube. Lipofectamine 2000 solution was prepared according to manufacturer protocol. zPEI 2 and bPEI solutions were prepared using the optimum weight ratios determined by luciferase transfection described previously. Equi-volume polymer or Lipofectamine solutions were added dropwise to the DNA solution under constant agitation to achieve the desired carrier/DNA weight ratio. Particles were allowed to incubate at room temperature for 30 min. Immediately before transfection, 200 mL

polyplex solution was added to 2.8 mL of DMEM with or without 10% FBS. Growth medium was aspirated from cells and replaced with 0.75 mL of polyplex/growth medium solution (0.5 µg DNA/well). Transfection was allowed to proceed overnight. The following morning, transfection media was aspirated and replaced by regular growth media containing CellTiter-Blue metabolic dye. Cells were allowed to incubate for 4 h at 37 °C and 5% CO_2. Then, cells were immediately excited with a 560-nm laser and the fluorescence was read at 590 nm using a Synergy 2 plate-reader (BioTek, Winooski, VT). Fluorescence was normalized to non-transfected cells under normal growth conditions.
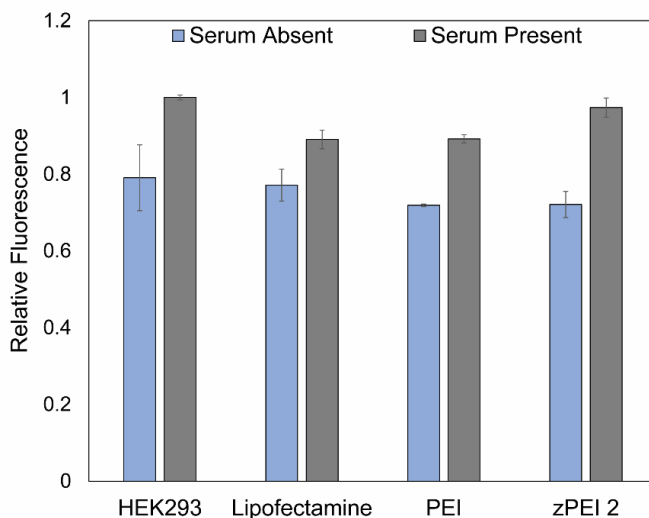
Figure 2.10. Cytotoxic effects of extended serum deprivation on HEK293 cells during transfection. Metabolic activity was assessed 16 h post introduction of polyplexes or lipoplexes and normalized to the activity of untreated cells (n = 3, error bars represent standard deviation).

2.5.5   CRISPR/Cas9 Knock-In

Knock-In of GFP into AAVS1 using zPEI 2 was verified by transfecting HEK293 cells with pAAVS1-Puro-GFP-DNR and pAAVS1-Puro-GFP-DNR in tandem with pCas-AAVS1-Guide. The first plasmid, pAAVS1-Puro-GFP-DNR, encodes for the donor DNA

that carries an expressible GFP region, while the second plasmid, pCas-Guide-AAVS1, encodes the Cas9 enzyme and a guide RNA that targets the AAVS1 region on the genome. The donor DNA targets the AAVS1 region using 500 base pair left and right homology arms. Insertion into AAVS1 should only occur when the guide cassette is present. HEK293 cells were seeded in 6-well plates at 3.0 x 10^5 cells/well 24 h prior to transfection. Polymer/DNA complexes were formed by diluting 160 µL of 0.1 µg/µL DNA solution containing either entirely the donor plasmid or a 1:1 ratio of the Cas9 and donor DNA plasmids with 500 µL of PBS in a 1.5 mL microcentrifuge tube. The equi-volume polymer solution was added dropwise to the DNA solution under constant agitation to achieve the desired carrier/DNA weight ratio. Particles were allowed to incubate at room temperature for 30 min. Immediately before transfection, 1.32 mL polyplex solution was added to 10.68 mL of DMEM with 10% FBS. Growth medium was aspirated from cells and replaced with 3 mL of polyplex/growth medium solution (4 µg DNA/well). Transfection was allowed to proceed overnight. The following morning, transfection media was aspirated and replaced by regular growth media. Cells were allowed to grow for 48 h undisturbed, before being seeded in T75 flasks. Cells were then passaged twice over the course of two weeks to eliminate any transient expression. After two weeks the cells were analyzed for GFP expression via FACS on a Symphony A3 flow cytometer (BD Biosciences, Franklin Lakes, NJ). Data is plotted in **Figure 2.11**.
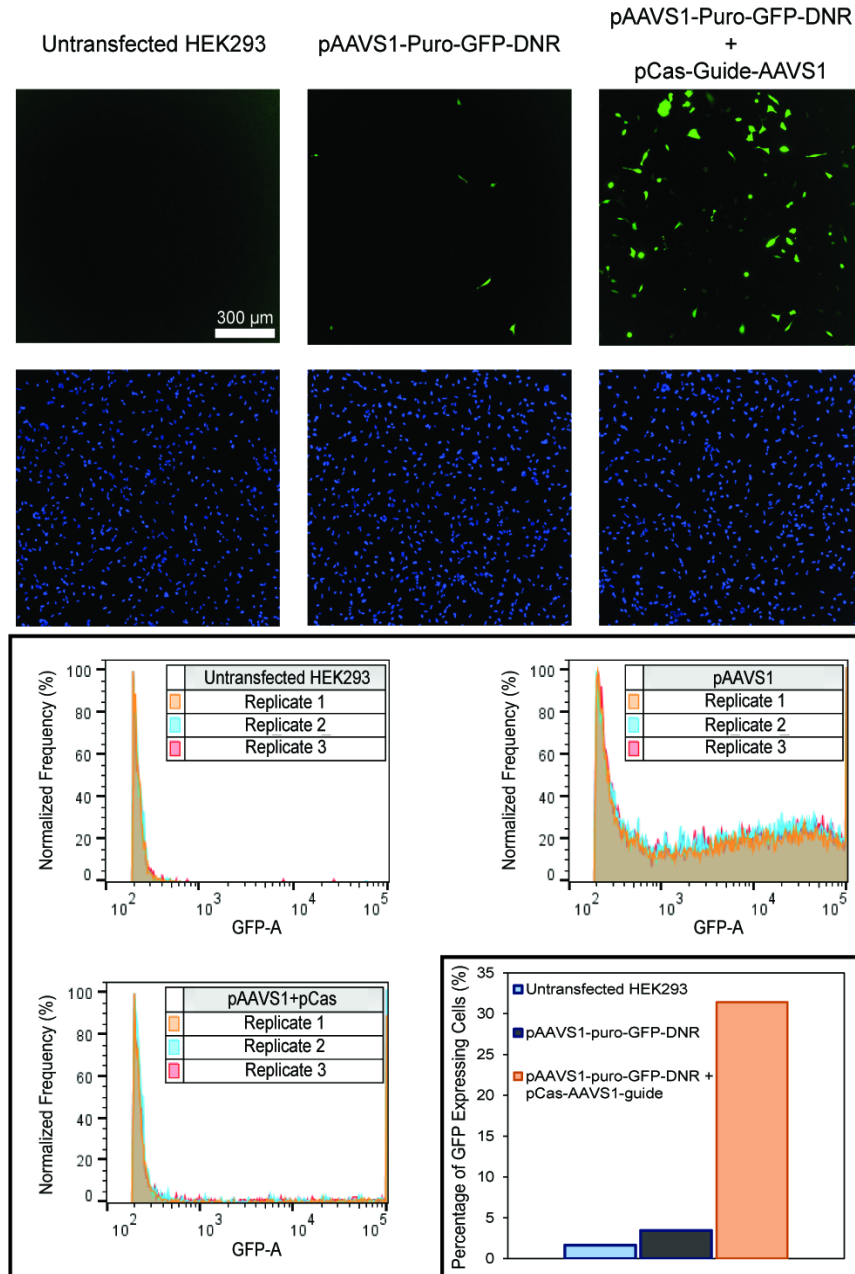
Figure 2.10. (Top) Cell micrographs displaying the GFP expression of untransfected HEK293 and HEK293 that have been transfected with either the GFP donor plasmid (pAAVS1-Puro-GFP-DNR) or the donor plasmid and cas9 guide cassette (pCas-Guide-AAVS1) using zPEI 2 in the presence of serum. (Bottom) Histograms of FACS analysis and the corresponding percentage of cells producing GFP displayed in a bar graph. Cells were passaged twice over the course of two weeks after the initial transfection to eliminate any transient expression. Cells were visualized and analyzed for GFP expression via a Cytation 7 multimode plate reader and a Symphony A3 flow cytometer, respectively.

CHAPTER 3. STRUCTURAL INVESTIGATIONS OF PEI AND MODIFIED PEI-DNA COMPLEXES CORRELATING TO TRANSFECTION EFFICACY

Preface: This work was performed in collaboration with the group of Dr. Daniel Pack of the Departments of Chemical & Materials Engineering and Pharmaceutical Sciences at the University of Kentucky. All polymer design, synthesis and characterization, DNA binding assays, dextran sulfate displacement, DLS, ζ-potential and SAXS measurements were completed by the author in the lab of Dr. Jason DeRouchey. Gene transfection experiments were performed by Levi Lampe in the laboratory of Dr. Daniel Pack.

3.1 INTRODUCTION

Gene therapy has gained significant attention in recent years as a potential treatment for genetically intractable diseases, infectious diseases, neurodegenerative diseases, and cancer owing to the advances in nucleic acid research both in biology and chemistry. To date, most of the gene therapy clinical trials worldwide (~70%) are conducted with recombinant viruses to deliver genetic materials due to their inherent capacity for high efficiency in cell targeting as well as their ability to enter cells efficiently.[58, 112] But viral gene delivery suffers from fundamental drawbacks such as immunogenicity, oncogenicity, toxicity, and high production costs that have driven the development of nonviral gene delivery alternatives.[69] Unlike viruses, nonviral gene delivery agents, such as cationic polymers, dendrimers, lipids, and peptides have several advantages compared to the inherent limitations of viral vectors including lower cost and flexibility in chemical modification. Although there is a lack of transferability compared to a virus, nonviral vectors offer a way to better understand the key limiting steps in the transfection process to create more efficient gene delivery agents.[113]

Among the first generations of nonviral alternatives, cationic polyethylenimine (PEI) is considered a benchmark for polymeric, nonviral gene delivery vectors. PEI is

highly cationic and readily condenses DNA to create positively charged nanoparticles capable of being taken up into cells for effecient gene delivery. In addition, branched PEI (bPEI) has a large number of primary, secondary and tertiary amines that can both buffer pH and provide sites for further chemical modification to potentially improve the physicochemical and biological properties of the resulting PEI-DNA complexes.[69, 114-116] Grafting functional domains to the PEI polymer backbone, such as shielding domains[117-119], targeting ligands[120], endosomolytic agents[121], or multifunctional groups[122-123] are common strategies to improve gene delivery efficacy. Many of these modifications ultimately reduce the net cationic charge of the PEI and have been shown to decrease the cytotoxicity of PEI. For example, acetylation of a 25kDa bPEI was shown to reduce the surface charge of the resulting polyplex particles and lower the buffering capacity resulting in enhanced gene delivery and reduced vector cell toxicity.[88-89] While modifications neutralizing the PEI amine charge are relatively common, less studied has been the incorporation of negatively charged moieties to generate polyampholytic polymers. In 2008, succinylated PEI was shown to be an effective delivery agent for siRNA.[97] More recently, we and others have shown that succinylated PEI also results in a modest improvement in serum-free transfections in vitro.[98-99] Surprisingly, we also found these succinylated, or zwitterionic-like, PEIs (zPEI) were especially beneficial for gene delivery done in the presence of serum proteins that more closely mimics in vivo gene delivery conditions.[99] PEI polyplexes transfected in the presence of serum proteins is well known to result in a significant decrease in transfection efficiency on the order of 10- to 100-fold. While high degrees of succinylation were not beneficial, we found that lower levels of succinylation resulted in significant enhancement of transgene expression in the

presence of serum that was comparable or even surpassed unmodified bPEI/DNA in the absence of serum.[99] More recently, we synthesized a series of minimally succinylated zPEIs (2-11.5% modification) and found that succinylation levels <10% enhanced transgene expression in the presence of serum proteins were beneficial in both HEK293 and HeLa cell lines,[124] also found in **Figure 2.5**. Surprisingly even succinylation of only 2%, corresponding to ~12 of the 581 amines in 25kDa bPEI, was sufficient to both enhance transfection as well as increase efficiency of CRISPR/Cas9-mediated knock-in in the presence of serum proteins. Succinylating only 2% of PEI amines (zPEI 2) was sufficient to enhance transgene expression 260-fold to 480-fold higher than unmodified PEI in serum for HEK293 and HeLa cells, respectively. We also showed this same zPEI 2 polymer also enhanced the efficiency of CRISPR/Cas9 gene knock-in in both serum and serum-free transfections. In the presence of serum, a 16-fold increase in CRISPR/Cas9 gene knock-in was observed for zPEI 2 when compared to unmodified PEI. Surprisingly, this minimal succinylation did not significantly decrease the PEI interactions with serum proteins nor the polymer-DNA interaction strength yet still was able to provide enhanced transgene expression and gene knock-in when serum proteins are present. The successful modification of PEI by both acetylation and succinylation are promising first steps but also highlight the need for more fundamental understanding of the complex correlations between polycation-DNA interactions and the resulting physiochemistry of the polyplexes and transgene expression observed in cells. A better understanding of the critical barriers to nonviral gene delivery are required to improve efficacy in vivo and ultimately move nonviral vectors into clinical applications.

In vitro experiments show that the condensation of DNA depends on the net charge of the polycation.[125] Due to the high charge, DNA helices in solution naturally repel each other. In the presence of cations with valence +3 or larger, these repulsions can be overcome and the polycation can effectively condense DNA.[126] Through this self-assembly process, the resulting condensate has a compacted structure with DNA being typically packaged in a columnar hexagonal lattice with well-defined equilibrium separation between DNA helices. The separation of the helices is a result of the balancing of short-range repulsions and long-range attractions in the system.[127-129] Depending on the polycation used, these DNA-DNA equilibrium spacings result in ~7-15 Å of water separating the surface of neighboring DNA helices.[129-130] To account for the attractions driving DNA condensation, most models require a correlation of charges or water structuring.[131-132] For example, the electrostatic zipper model proposes that cations bind in the major or minor grooves of DNA resulting in attractive interhelical correlations between the bound positive charge of the cation and the negatively charged phosphate of an apposing helix.[133-135] Most structural studies of DNA condensation to date have focused on metallic or linear polycations. There is experimental evidence suggesting these polycations do bind in DNA grooves.[136-138] Branched synthetic polymers, such as PEI, presumably would not be able to bind and correlate their charges in the same manner as linear polycations possibly requiring other binding modes, such as bridging, to induce condensation. Despite its importance in polymeric gene delivery not much work has been done to investigate how PEI and modifications of PEI alter the internal nanoscale structuring of DNA within polyplexes.

We have investigated the internal structure of polyplexes resulting from the condensation of DNA with unmodified and modified branched PEIs as well as determined their effectiveness as transfection agents in the presence of serum proteins. Two series of modified PEI were synthesized by modification of 25kDa bPEI by either acetylation (10-50%) or succinylation (2-40%). The acetylated PEI (acPEI) and succinylated PEI (zPEI) were characterized by FT-IR and 1D- and 2D-NMR. Nearly all modified PEIs were found to be capable of condensing DNA and inducing transgene expression in HeLa cell line. SAXS experiments were performed to determine the internal packaging of the resulting polyplexes. Both succinylation and acetylation modifications resulted in decreased polycation-DNA interactions, suggesting more loosely ordered structures. For acetylated PEI, SAXS experiments revealed that the inter-DNA spacings increase monotonically. zPEI however shows a crossover behavior where DNA-DNA spacings increase at low degrees of modification but decrease again at higher levels of succinylation. Time-course SAXS studies reveal small rearrangements in the PEI and modified PEI polyplexes over time. Lastly, we show that pH has strong effects on the resulting DNA packaging in all the PEI polyplexes. Specifically, condensing at low pH (pH 4) results in tighter DNA packaging within PEI and modified PEI polyplexes relative to polyplexes condensed at near neutral pH (pH 7.5). In addition, polyplexes initially formed at pH 7.5 and then acidified show significant structural rearrangements within one hour, resulting in a more highly packaged DNA. Polyplexes formed by both modified PEIs show larger pH induced changes in the nanoscopic structure when compared to the unmodified bPEI polyplexes.

3.2 METHODS AND MATERIALS

3.2.1 Materials

Branched polyethylenimine (PEI, 25kDa), acetic anhydride, succinic anhydride, dextran sulfate (9-20 kDa from Luconostoc spp), and highly polymerized calf-thymus (CT) DNA sodium salt (molecular weight ~10−15 million Da) were purchased from Sigma-Aldrich (St. Louis, MO). The presence of protein impurities with the CT DNA was checked by measuring the ratio of absorbance at 260 and 280 nm by UV/VIS. DNA solutions were found to be satisfactory with A260/A280 ≥ 1.8. Ethidium bromide was purchased from International Biotechnologies Inc. (Newhaven, CT), and D_2O was purchased from Cambridge Isotope Laboratories (Andover, MA). All other chemicals were purchased from Thermo Fisher Scientific (Waltham, MA) and used without further purification.

3.2.2 Synthesis and Characterization of succinylated and acetylated PEI

Succinylated (or zwitterion-like PEI, zPEI) and acetylated (acPEI) were synthesized from unmodified branched PEI (bPEI) as follows. Half a gram of bPEI was dissolved in 3 mL of 0.5 M sodium bicarbonate buffer (pH 9) and reacted the desired mole ratio of either succinic or acetic anhydride. Succinic anhydride was added directly as a dry powder, while acetic anhydride was added dropwise to the PEI solution. These reactions then proceeded at 60 ºC for 4 hours and the crude product was filtered using a 0.22 μm PVDF syringe filter. Final modified PEI products were subsequently purified by dialysis (membrane molecular weight cutoff = 3.5 kDa) against double distilled water for 48 hours with the water replaced every 4 hours. After dialysis, the products were frozen

overnight and lyophilized for 48 hours. The dried product was placed in a -80 ºC freezer for storage. A series of modified succinylated PEI (zPEI, 2-40%) and acetylated PEI (acPEI, 10-50%) were synthesized.

Final modified PEI products were characterized by FT-IR (ATR) and 1D-NMR and 2D-NMR (HSQC, HMBC). For NMR analysis, 6.5 mg of lyophilized polymer was dissolved in 0.65 mL D_2O and NMR spectra were recorded using a 400 MHz Bruker Avance NEO spectrometer equipped with a smart probe. The degree of modification was determined by ^{1}H-NMR from the ratio between the relative peak areas of methylene backbone of PEI (δ 2.45-3.6 ppm) and succinyl protons (δ 2.25-2.45 ppm) or methyl protons of acetate (δ 1.85-2.1 ppm). To enable an assignment of the modified PEI peaks, 2D-NMR (HSQC and HMBC) spectra were acquired. (Supplementary information, **Figure 3.10-3.26**).

bPEI25k: ^{1}H-NMR δ_H (400 MHz, D_2O, ppm). 2.45–2.85 (bm, PEI)

zPEI: ^{1}**H-NMR δ_H (400 MHz, D_2O, ppm).** 2.3-2.45 (bs, 4H, $-C_2\mathbf{H_4}-COOH$), 2.6–3.2 (bm, PEI), 3.3–3.6 (bm, 2H, $-C\mathbf{H_2}-NH-CO-C_2H_4$-).

2D-NMR δ_H (HMBC, 400 MHz, D_2O, ppm). 3°-amide (F1: 174.1 ppm, F2: 2.45 ppm), 2°-amide (F1: 181.4 ppm, F2: 2.45 ppm).

2D-NMR δ_H (HSQC, 400 MHz, D_2O, ppm). $-C_2\mathbf{H_4}-COOH$ (F2: 2.45 ppm, F1: 32.45ppm & 32.55 ppm).

acPEI: ^{1}H-NMR δ_H (400 MHz, D$_2$O, ppm). 1.85-2.1 (bs, 3H, NH-CO–CH$_3$), 2.4-3.15 (bm, PEI), 3.3–3.6 (bm, 2H, –CH$_2$–NH–CO–CH$_3$).

2D-NMR δ_H (HMBC, 400 MHz, D$_2$O, ppm). 2°-amide (F1: 181.3 ppm, F2: 1.86 ppm), 3°- trans amide (F1: 174.1 ppm, F2: 2.01 ppm), 3°- cis amide (F1: 174.1 ppm, F2: 2. 1 ppm)

2D-NMR δ_H (HSQC, 400 MHz, D$_2$O, ppm). -CO–CH$_3$ (2°-amide, F2: 1.86 ppm, F1: 23.40 ppm), -CO–CH$_3$ (3°- trans amide, F2: 2.01 ppm, F1: 22.03 ppm) & -CO–CH$_3$ (3°- cis amide, F2: 2.1 ppm, F1: 20.55 ppm).

FT-IR ν (ATR, cm^{-1}). 1635 (C=O; amide I), 1563 (N-H; amide II). [Common to both conjugation products]

3.2.3 Ethidium bromide (EtBr) exclusion assay

The formation of polycation-DNA complexes, or polyplexes, was followed by ethidium bromide displacement assay. Stock solutions of calf-thymus DNA and EtBr were prepared by dissolving in 10 mM Tris–HCl buffer (pH 7.5) overnight to a final concentration of 0.24 µg/µL and 0.024 µg/µL, respectively. 12 µg of ctDNA in Tris buffer (pH 7.5) was incubated with 1.2 µg EtBr at room temperature for 10 min. This corresponds to a labelling ratio of approximately 1 EtBr per 10 DNA base pairs. After incubation of the DNA with EtBr, the desired volume and concentration of polymer stock solutions were added to achieve the desired nitrogen-to-phosphate (N/P) charge ratio. The resulting polyplexes were incubated for another 30 min at room temperature. After incubation, the final volume was adjusted to 500 µL using 10 mM Tris buffer before

measurement by fluorescence spectroscopy. Measurements were performed with samples in a quartz cuvette. The fluorescence intensity of the polyplex solutions was recorded on a Thermo Lumina Fluorescence Spectrometer at $\lambda_{ex} = 520$ nm and $\lambda_{em} = 610$ nm. A sample containing only pDNA and EtBr was defined as maximum fluorescence (100 %). The percentage of EtBr displaced upon polyplex formation was calculated by determining the relative fluorescence (rf%) = $[(F-F_0)/(F_{Max}-F_0)]$ *100, where F, F_0, and F_{Max} are the emission intensity of the sample, the EtBr alone, and ctDNA/EtBr control, respectively.

3.2.4 Dextran sulfate displacement assay

The polyplex stability was checked by dextran sulfate displacement. 200 ng pUC19 samples were complexed with a fixed polymer/DNA weight ratio of 6.0 at a total volume of 5 μL in 10 mM Tris buffer at pH 7.5. This polymer/DNA weight ratio was sufficient for a complete complexation of DNA by all polymers used in this study. Polyplexes were mixed and brought to a total volume of 5μL by addition of 10 mM Tris. Polyplexes were then incubated at room temperature for 45 mins to ensure complete DNA complexation. Dextran sulfate (DS) was then added at various weight ratios relative to the DNA, and the final solution volume was brought up to 12 μL by addition of 10 mM tris buffer. Samples were subsequently incubated for another 30 minutes to allow plasmid DNA release from the polyplexes. 0.8 w/v % agarose gels were prepared by dissolving agarose in a 0.2 μm filtered TAE buffer (40 mM Tris base, 20 mM acetic acid, 1 mM EDTA). Before loading onto the agarose gel, 2 μL loading dye was added to each sample. Samples were electrophoresed for 30 minutes at 100 volts. DNA was visualized

by post-run staining with ethidium bromide (0.5 µg/mL) and imaged using the BioRad ChemiDoc MP Imaging System.

3.2.5 Transfection Efficiency

HeLa cells were cultured in DMEM supplemented with 10% FBS according to ATCC recommendations. Cells were seeded in 24-well plates at 7.5×10^4 cells/well 24 h prior to transfection. Polyplexes were formed by diluting 20 µL of 0.1 µg/µL pGL3 plasmid DNA solution with 80 µL of phosphate-buffered saline (PBS) in a 1.5 mL microcentrifuge tube. Polymer solution (100 µL) at various concentrations was added dropwise to the DNA solution under constant agitation to achieve the desired polymer/DNA weight ratio. Polyplex particles were allowed to incubate at room temperature for 30 min. Immediately before transfection, 200 µL polyplex solution was deposited into 2.8 mL serum-containing medium. Regular growth medium was aspirated from cells and replaced with 750 µL of polyplex/growth medium solution (0.5 µg DNA/well). After 4 h, the transfection medium was replaced with a standard growth medium. Transfection efficiency was then quantified via luciferase expression at 24 h post initial transfection. A Promega luciferase assay kit was used to measure protein activity in relative light units (RLU) using a Synergy 2 plate-reader. Results were normalized to total cell protein using a bicinchoninic acid (BCA) assay from G-Biosciences (St. Louis, MO).

3.2.6   Particle size and zeta potential measurements

Polyplex size and size distribution were measured using dynamic light scattering (DLS). Polymer/DNA complexes were formed in double distilled water at the optimum condensing weight ratio for each of the modified and unmodified polymers as determined by EtBr exclusion assay. Polyplexes were formed as described earlier and following a 30 min incubation at room temperature, the polyplexes were diluted to 2 ug of DNA/mL using water. The solution was then immediately read using a 90Plus/BI-MAS automatic particle sizer (Brookhaven Instruments, Holtsville, NY). DLS measurements were performed prior to zeta (ζ)-potential measurements. To assess polyplex particle charge, ζ-potential was measured using a BIC ZetaPALS (Brookhaven Instruments, Holtsville, NY) at a 15° scattering detector angle. Each measurement was taken in triplicate with 4 runs and 10 cycles acquisition per run. **Table 3.1** provides representative particle size distributions as measured by DLS for each polyplex and reported as mean ± standard deviation (S.D.).

3.2.7   Circular dichroism spectra

Circular dichroism (CD) spectra of the polyplexes were recorded at room temperature on a JASCO J-815 CD spectrometer (Jasco International Co. Ltd) using a 1 cm path length cuvette. Each spectrum is the average of three scans over the wavelength range 220–300 nm with an interval of 1 nm at a scan rate of 100 nm/min.

3.2.8 Sample preparation for X-ray scattering experiments

For x-ray experiments, fibrous polycation-DNA complexes were formed as follows. First, concentrated polymer stock solution (1 mg/mL) and stock calf thymus DNA solutions (2 mg/mL) were prepared in buffer and equilibrated for at least overnight. The condensing polycations were added to ~200 μg of DNA to achieve the desired N/P charge ratio where all DNA was shown to be complexed as determined by EtBr exclusion assay. The resulting fibrous polycation−DNA samples were then incubated at room temperature for 30 min and centrifuged (14500 g/5 min) to collect the condensate. The condensate was then moved to a bathing solution of fresh buffer to equilibrate for 1 hour before X-ray analysis. To mimic transfection-like conditions, two buffers were used either a 10 mM Tris buffer (pH 7.5) or a 10 mM acetate buffer (pH 4) similar to the low pH observed in late endosomes. DNA double helix structure is known to be stable over this pH range. For pH studies, both DNA and polymer were prepared in the same Tris or acetate buffer and after condensation the condensate were moved to fresh buffer of the same pH. This maintains the DNA, polycation and polyplex at the same pH throughout the experiment and therefore labeled as pH 7.5 or pH 4 samples. To look at polyplex response to acidification a third set of samples were made where the DNA, polycation and polyplex were formed in 10 mM Tris (pH 7.5) and equilibrated for half an hour. After equilibration, these samples were then moved to a fresh 10 mM acetate buffer solution (pH 4) and equilibrated for 1 hr or 1 day before x-ray experiments. These samples are labeled pH 7.5-4 to indicate the pH change after polyplex formation. For time course studies, samples were also monitored by X-ray over a month to observe changes in DNA packaging with time.

3.2.9   X-ray scattering

Small-angle X-ray scattering experiments (SAXS) were performed using a graded-multilayer-focused Cu Kα (λ = 1.54 Å) radiation from a Nonius FR-591 rotating anode fine-focus X-ray generator operating at 45 kV and 20 mA. Samples were sealed in a cell with a bath of equilibrating buffer solution and mounted in a sample holder at room temperature. The flight path from the sample to detector was filled with helium gas to minimize air scatter. The primary beam was collimated by a fine aperture beam tunnel. Diffraction patterns were recorded with a Platinum 135 CCD detector with phosphor optimized for Cu Kα radiation, and the images were analyzed with Fit2D and Origin Pro 2019 software. The sample to detector distance for the SAXS was determined using silver behenate and found to be 22.7 cm. Bragg scattering peaks were used to determine interaxial DNA-DNA spacings. Bragg spacings are calculated as $D_{Bragg} = 2\pi/q_{Br}$, where q_{Br} is the scattering vector q (defined as $q = (4\pi/\lambda) \sin\theta$, where 2θ is the scattering angle) and corresponds to the maximum in the scattering. For a hexagonal lattice, the relationship between the Bragg spacing and the actual interaxial distance between DNA helices (D_{int}) is calculated as $D_{int} = (2/\sqrt{3}) D_{Bragg}$. For samples equilibrated under the same buffer conditions, D values were reproducible to within ~0.1 Å. There was no significant sample degradation due to X-ray exposure or pH buffer conditions. Typical exposure times were 2 minutes.

3.3 RESULTS

3.3.1 Synthesis and characterization

To assess the relationship between PEI modifications and the structure of the resulting DNA complexes, we first synthesized a series of succinylated PEI (zPEI, 2-40%) and acetylated PEI (acPEI, 10-50%) by modification of 25kDa branched PEI (bPEI) through reaction with succinic or acetic anhydride. Strategies for the modification of bPEI were adapted from our previous work (**Figure 3.1a**) with both zPEI and acPEI shown to enhance transfection efficiency when compared to unmodified bPEI.[88, 99] By varying the feed molar percentages of succinic or acetic anhydride with respect to the total amine content of PEI, we controlled the percent modification of total amines in the resulting zPEI and acPEI polymers. Polymer names reflect molar percentage of anhydride in the feed, so acPEI 10 represents enough acetic anhydride was added to modify 10% of the total PEI amines. Successful reaction was determined by FT-IR spectroscopy. Upon modification with either anhydride, two characteristic new peaks at 1635 cm^{-1} and 1563 cm^{-1} are observed by FT-IR for both acPEI and zPEI characteristic of the carbonyl stretch and N−H bend, respectively, of the amide moiety of the modified group after reaction of the anhydrides with bPEI. The degree of modification was analyzed and quantified by ^{1}H-NMR from the relative proton peak area ratio between methylene of PEI (2.45-3.6 ppm) and methylene of the succinyl protons (2.3-2.45 ppm) or methyl protons of the acetyl group (1.85-2.1 ppm). Results are given in supplementary information (**Table 3.2)**. For most polymers, nearly complete quantitative PEI modification was observed with the lowest yields obtained for the highest monomer
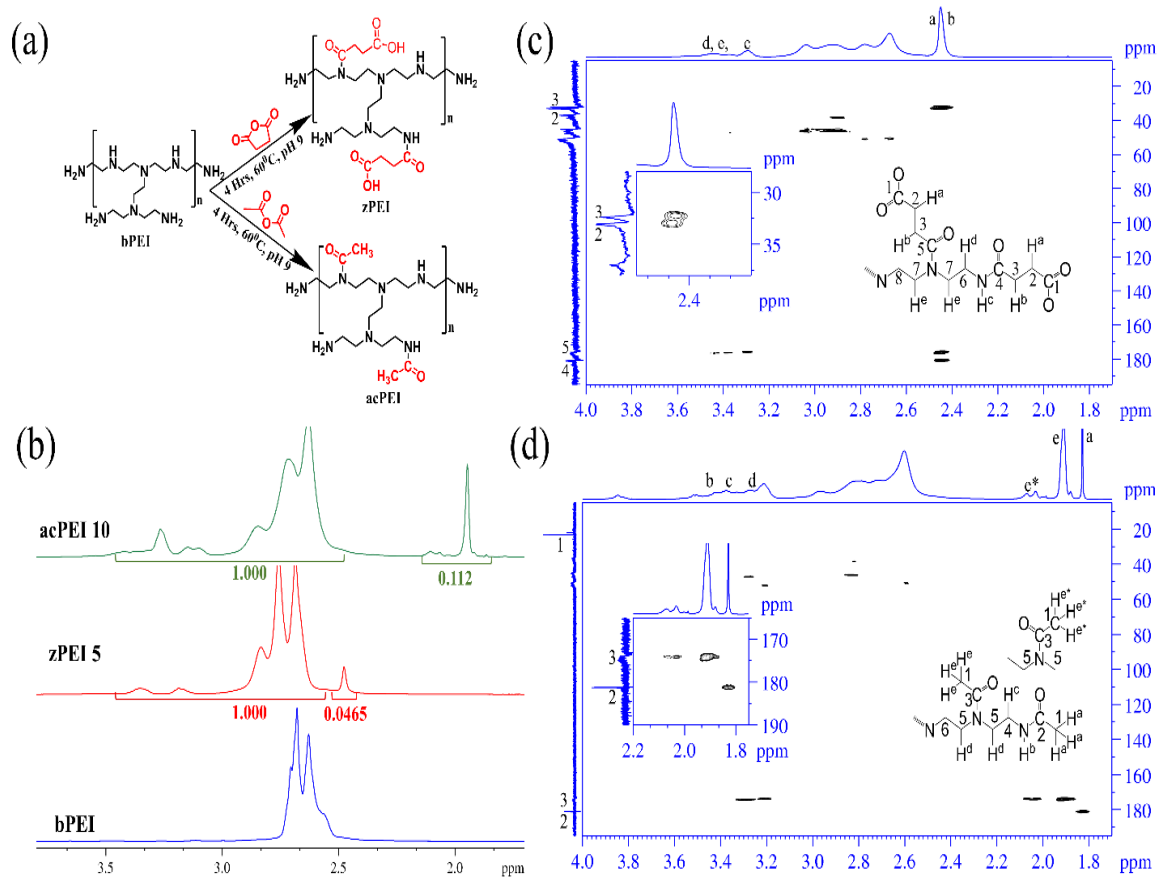
Figure 3.1. Synthesis scheme and characterization of zPEI and acPEI. **a)** Synthesis from bPEI using succinic anhydride and acetic anhydride, respectively maintaining the same reaction condition. **b)** Representative ^{1}H-NMR characterization of unmodified and modified PEIs. Degree of modification reported as amine/reagent feed ratio. **c)** & **d)** 2D-HMBC spectra of zPEI 20 and acPEI 40, respectively. Inset (spectra) showing the most important peaks characteristic of these two polymers. Both spectra confirm the formation of tertiary amides higher than secondary amides from secondary and primary amines, respectively.

feeds of succinyl anhydride (zPEI 30/40). The degree of modification is reported as the % of total amines modified but, for simplicity, we described the polymers by the PEI amine/reagent feed ratio. The % modification presented here agrees with the literature reports from other research groups.[97] In **Figure 3.1b**, we show representative ^{1}H-NMR spectra of the unmodified bPEI (bottom) compared to zPEI 5 (middle), and acPEI 10 (top).

The bPEI polymer structure has primary, secondary and tertiary amines. It has been proposed previously that PEI modifications, similar to ours, would primarily occur at primary amines due to less steric restrictions. To determine where zPEI and acPEI modifications occurred under our reaction conditions, we performed 2D-NMR (HMBC) spectroscopy (**Figure 3.1c /d**). We observe reactions with succinyl, and acetic anhydride occur more at secondary amines of PEI compared to primary amines. F-1 axis (C-13, y-axis) of the spectra shown in **Figure 3.1c, d** has two distinct peaks corresponding to tertiary amides (174.1 ppm) and secondary amides (181.4), respectively. acPEI spectra differ from zPEI by the chemical environment of -CH$_3$ groups (F-2 axis, 1.86, 1.94, 2.1 ppm) compared to -C$_2$H$_4$- groups (F-2 axis, 2.45 ppm). The methylene protons at 2.45 ppm of zPEI are correlated to 32.45 ppm and 32.55 ppm (**Figure 3.1c**, inset), respectively, revealing a similar chemical environment due to carboxyl and amide group on two opposing sides. This similarity in chemical environment indicates the carboxyl groups of zPEIs form intramolecular H-bond with the neighboring amines that retain a negligible deshielding ability on -CH$_2$- near the -COO$^-$ functional group. The 2D-NMR data show the relative reaction preference between primary and secondary amines of bPEI. Accordingly, conjugation starts on secondary amines forming tertiary amides until

a significant percent modification is achieved. Only at high modification is there significant reaction of the anhydrides with primary amines to form secondary amides on both of the modified PEIs in this study. All NMR and FT-IR spectroscopy data are provided in the supporting information (supplementary information, **Figure 3.8-3.26**).

3.3.2   Complexation of DNA by bPEI and modified PEIs

A necessary requirement for successful gene delivery is the ability for the polycation to self-assemble with DNA to form stable polyplex particles**.** Modification of PEI is known to alter the ability of the polymer to condense DNA. The ability of bPEI, acPEI, and zPEI polymers to condense DNA was assessed using ethidium bromide (EtBr) exclusion assay. Intercalation of EtBr into double stranded DNA results in a significant increase in the observed fluorescence intensity. Upon complexation of DNA by polycations, some of the intercalator is displaced resulting in a reduction in the relative fluorescence intensity. All the polycations, except the highest modified PEIs, display similar sigmoidal condensation curves due to condensation with the modified PEIs (**Figure 3.2a**). bPEI/DNA is fully condensed by polymer/DNA weight ratios of 0.5. zPEI 2-10% and acPEI 10-20% are also able to fully condense calf thymus DNA (ctDNA) to the same extent as the unmodified bPEI by polymer/DNA weight ratios of 0.5 to 1.0. acPEI 40, acPEI 50, and zPEI 20 also maintain a sigmodal shape but do not reduce the relative fluorescence to <5% like lower modified acPEI/zPEI and unmodified bPEI. For zPEI 20, the EtBr exclusion assay curves shifted to higher polymer/DNA ratios of 3 before plateauing at ~20% normalized fluorescence. For zPEI 30
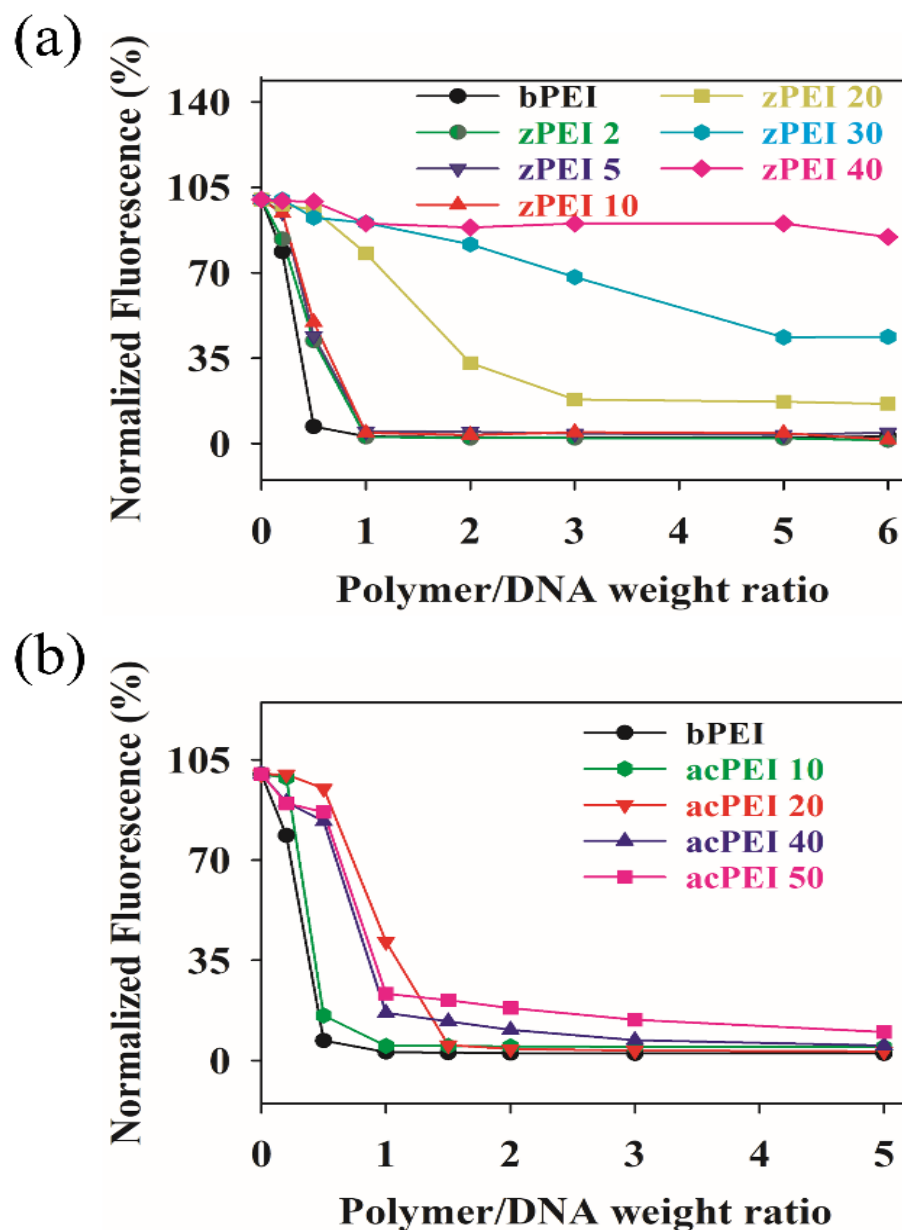
Figure 3.2. DNA condensation ability determined with ethidium bromide (EtBr) exclusion assay. Demonstrated here is the DNA condensation ability of both zPEI and acPEI, decreasing with increasing % modification. Here, the succinylated PEI has a relatively lesser DNA condensing power than acetylated PEI. This variability is probably due to anionic moieties that add up repulsive force between DNA phosphates and succinyl groups.

and zPEI 40, we observed a significant change in the shape of the curves suggesting that zPEI 30 is only partially complexing DNA (normalized fluorescence = 60%) while 40% modification is unable to condense DNA even at polymer/DNA weight ratios as high as 6. Likely, these differences between zPEI and acPEI are due to the nature of the modification. Acetylation reduces the net charge of the PEI by replacing a secondary or primary amine with an acyl group. Acetylation places an acetyl protecting group on secondary or primary amines of PEI neutralizing the potential positive charge of the reacted amine. Succinylation of the PEI amines results in grafted succinate groups to the PEI backbone both potentially neutralizing the charge of the original amine but also introducing a negatively charged group. Succinylation of PEI clearly has a larger impact on DNA condensation compared to PEI acetylation.

3.3.3   Dextran sulfate displacement assay

Another well-known bottleneck of polymeric gene delivery is that for gene transcription to occur the polycation must be able to dissociate from the DNA once inside the cell. This requires balancing polycation-DNA interactions to create particles stable enough to reach cells but not too stable to prevent dissociation in cells. One way to tune these polymer-DNA interactions is through post-polymerization modifications. To investigate how succinylation and acetylation alter PEI polyplex stabilities, we performed a dextran sulfate (DS) displacement assay. Here, the sulfated polysaccharide (DS) acts as a competing polyanion and serves as a mimic of sulfonated extracellular glycosaminoglycans, such as heparan sulfate, found in vivo that are known to competitively displace DNA from polyplexes. The relative strength of polymer−DNA

interactions can be assessed by determining the ability of DS to displace polycations from DNA at various DS/DNA weight ratios. Here, unmodified and modified PEI polyplexes were prepared at polymer/DNA ratio of 6 (wt/wt) which was previously determined sufficient to achieve complete or maximum DNA condensation for all polymers in this study. These polyplexes were then subsequently incubated with DS at various concentrations and DNA dissociation was followed by agarose gel electrophoresis. Results are shown in **Figure 3.3**. As expected, grafting succinyl or acetyl groups to the PEI weakens polymer-DNA interactions resulting in a systematic decrease in the amount of DS required to release DNA from the polyplexes. Unmodified bPEI-DNA (wt/wt 6) polyplexes requires a DS/DNA weight ratio of 20 for the onset of DNA displacement to be observed. zPEI 5, 20 and 30 require DS/DNA weight ratios of 15, 2, and 1, respectively, for significant DNA release to be observed. Acetylation of PEI has a weaker effect on polyplex stability. acPEI 10, 20, 40 and 50 resulted in DNA displacement starting at DS/DNA weight ratios of 15, 15, 8, and 8, respectively. These results are consistent with the weakening of polymer-DNA interactions with increasing amount of modification of the PEI backbone. The significant differences between zPEI and acPEI at high modification is again consistent with the acetylation reaction having a weaker effect on PEI-DNA interactions as compared to the presence of anionic succinyl groups. In section 3.3.5, these polyplexes are evaluated for their gene transfection efficiency in the presence of serum proteins. We also examined each complex by DS displacement assay at the optimum polymer/DNA (wt/wt) ratio based on EtBr exclusion assay (supplementary information, **Figure 3.28**) where all polymers were found to fully condense the DNA.
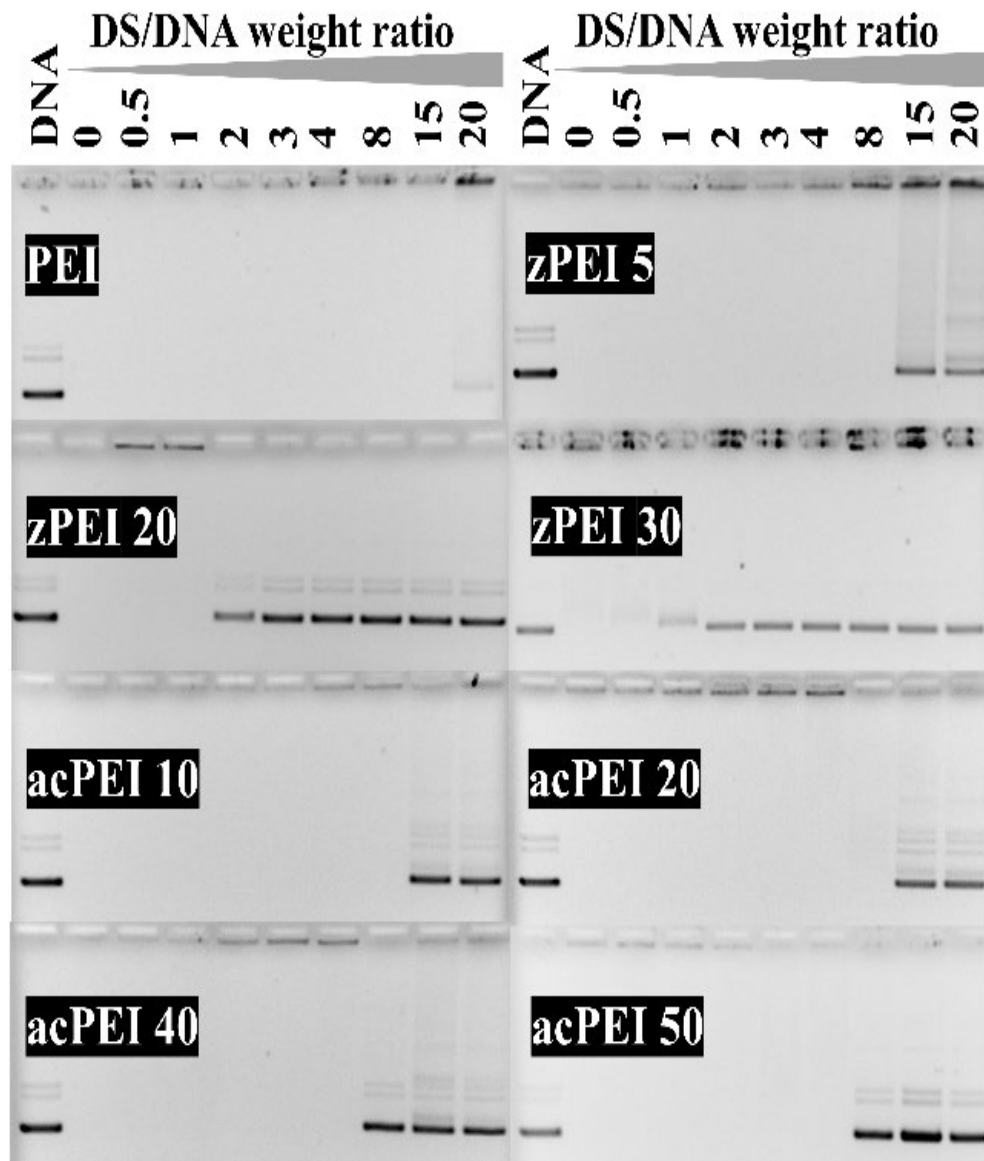
Figure 3.3. Dextran sulfate (DS) displacement assay. The numbers above each lane represent the DS/DNA weight ratio. Polymers were condensed at polymer/DNA weight ratio 6:1 that shows full DNA condensation achieved by all the modified polymers. Among the polymers, unmodified PEI retains the most potent DNA binding capability, reducing with higher modification. Acetylation of PEI retains moderate DNA binding strength even up to 50%. However, with higher % succinylation displays minimal DNA binding strength.

3.3.4 Particle size and ζ-potential measurements

The size and charge of polyplexes are known to be important parameters affecting transfection efficacy. To compare how bPEI, acPEI and zPEI differ in their ability to make nanometer-sized polyplex particles, we measured their size by dynamic light scattering (DLS). Here we focused on polymer/DNA weight ratios sufficient for complete DNA condensation as determined by EtBr displacement assay. Results are shown in **Table 3.1** with their corresponding polyplex particle diameters (nm) as determined by DLS. Plasmid DNA size does not affect the physicochemical properties of polyplexes,[139] so for these studies, plasmid pUC19 DNA was used to correlate to polyplexes used in transfection studies. All PEI/DNAs were measured at polymer/DNA weight ratio of 3, except for zPEI 30 which required wt/wt 6 for full condensation. We hypothesized that PEI modification would result in larger sized nanoparticles compared to unmodified bPEI. As shown bPEI/DNA results in nanoparticles exhibiting a mean diameter of 83.8 ± 5 nm. Succinylation in the zPEI series all resulted in larger polyplex particles that increased in size with higher degrees of polymer modification from zPEI 2 resulting in 98 nm particles to zPEI 20 resulting in 181 nm particles at wt/wt 3. zPEI 30 at wt/wt 6 resulted in even larger (>200 nm) particles. We have reported similar zPEI/DNA particle sizes in previous studies at similar wt/wt ratios.[99] Likely this increase in colloidal size is a result of having more DNA present in the highly succinylated polyplex particles.

As discussed earlier, polymer chemistry plays a crucial role in the formation of polyplexes. While succinylation introduces a negative moiety to the PEI polymer, acetylation increases hydrophobicity. Because of an additional hydrophobic moiety in PEI structure, polyplexes formed with acPEI possibly complexed with less plasmid DNA.

Thus, the smaller particle size obtained with acPEI/DNA polyplexes ranging between 87.4-97.1 nm in diameter with increasing % modification. Our results show that acetylated PEI, even as high as 50% modified, still gives polyplex diameters (87.4-97.1 nm) similar to unmodified bPEI-DNA (83.8 nm).

Next, we determined the resulting zeta potential of the various polyplexes. Unmodified bPEI/DNA (wt:wt 3:1), resulted in particles with a zeta potential of $+21 \pm 1.8$ mV, consistent with compact polyplex particles with a highly positive surface charge. As expected, acetylation of PEI amines resulted in a decrease of the polyplex surface charge which decreased further with increasing percent modification. For example, acPEI 10 decreased the polyplex surface charge to 18.9 mV while acPEI to 50% further reduced the surface charge to 13.2 mV. The zeta potential of the zPEI series did not significantly reduce the particle zeta potentials except at the highest % modification studied (30%) succinylating 2-5% of the PEI amines only reduces the zeta potential to 20 mV. Increasing succinylation to 20% (zPEI 20) decreased the particle surface charge further to $+14.5$ mV. Only at 30% succinylation (zPEI 30, wt:wt 6:1), was a significant change in the zeta potential observed with particles exhibiting a net negative surface charge (-7.8 mV). These results are somewhat surprising but consistent with our previous studies on zPEI.[99] The negative surface charge upon condensation by zPEI 30 would suggest that zPEI 30 polyplexes would not be able to have favorable electrostatic interactions with the negatively charged cell membrane which should be unfavorable for endocytosis.

Table 3.1. Particle size and ζ-potential

	Polymer: DNA (wt:wt)	Particle Diameter (nm)	ζ-potential (mV)
PEI	3:1	83.8±5	21±1.8
zPEI 2	3:1	98.3±6	20.1±2.35
zPEI 5	3:1	100.5±7.7	20.02±2.9
zPEI 10	3:1	115.3±5.4	17.04±1.3
zPEI 20	3:1	181.1±5.8	14.54±1.02
zPEI 30	6:1	206.3±19.3	-7.81±0.5
acPEI 10	3:1	87.4±4.1	18.9±0.5
acPEI 20	3:1	86.9±4.5	17.8±1.8
acPEI 40	3:1	87.9±2.7	15.2±1.7
acPEI 50	3:1	94.1±2	13.2±0.8

*Polyplexes formed at the polymer/DNA weight ratio required to obtain full DNA condensation. The ζ-potential measurement was conducted using the PALS software and Smoluchowki limit, and the hydrodynamic diameter was determined by applying the Stokes-Einstein equation from the experimentally determined translational diffusion coefficient. Data presented as mean±SD (n =3)

3.3.5 Gene transfection efficiency in the presence of serum

Previously reported an improved transfection efficacy for acPEI and zPEI (both in and out of serum) likely due to decreased charge density of the modified PEIs compared to bPEI.[88, 98-99, 124] Indeed, the enhancement of transgene expression of zPEI in the presence of serum proteins was shown to meet or exceed expression of bPEI/DNA in the absence of serum proteins. To further study the effectiveness of these PEI modifications for gene delivery in the presence of serum, we studied our zPEI and acPEI polymer series for their effectiveness in transgene expression. Here, HeLa cells were transfected with polyplexes of the unmodified PEI, zPEI series or acPEI series (**Figure 3.4**). The unmodified PEI exhibited the highest levels of transgene expression in the presence of serum at low

polymer/DNA (wt/wt) ratios of 2 or below. The gene expression of bPEI polyplexes decreased ~10-fold more at higher wt/wt ratios of 3 or above compared to wt/wt ratio 1. Minimally succinylated zPEIs (<10%) show the best transgene expression (**Figure 3.4a**), consistent with our previous studies reporting an increase with higher polymer/DNA (wt/wt) ratios by over 100-fold for zPEI 5. Here, maximum gene expression was observed at polymer/DNA weight ratio 4:1 and 5:1 for zPEI 5 and zPEI 10, respectively. Compared to unmodified PEI, gene expression by zPEI 5 and zPEI 10 showed 73-fold and 12-fold higher transgene expression, respectively. Higher succinylation modifications (>10%) resulted in poor transgene expression for all wt/wt ratios. Prior work with acPEI showed improvement in transgene expression ability in serum-free conditions.[88] In contrast to serum-free transfections, acetylated PEIs (**Figure 3.4b**) did not enhance gene expression in the presence of serum proteins and performed similarly or worse than unmodified bPEI at all polymer/DNA weight ratios. Improved efficacy shown by acPEI 20 and acPEI 40 at polymer/DNA wt ratios of 6 and 5 that do not agree with general trend of the acPEI series. Even if we consider these results as not due to random error, the maximum transgene expression observed was only 1.2- and 0.5-fold higher than bPEI.
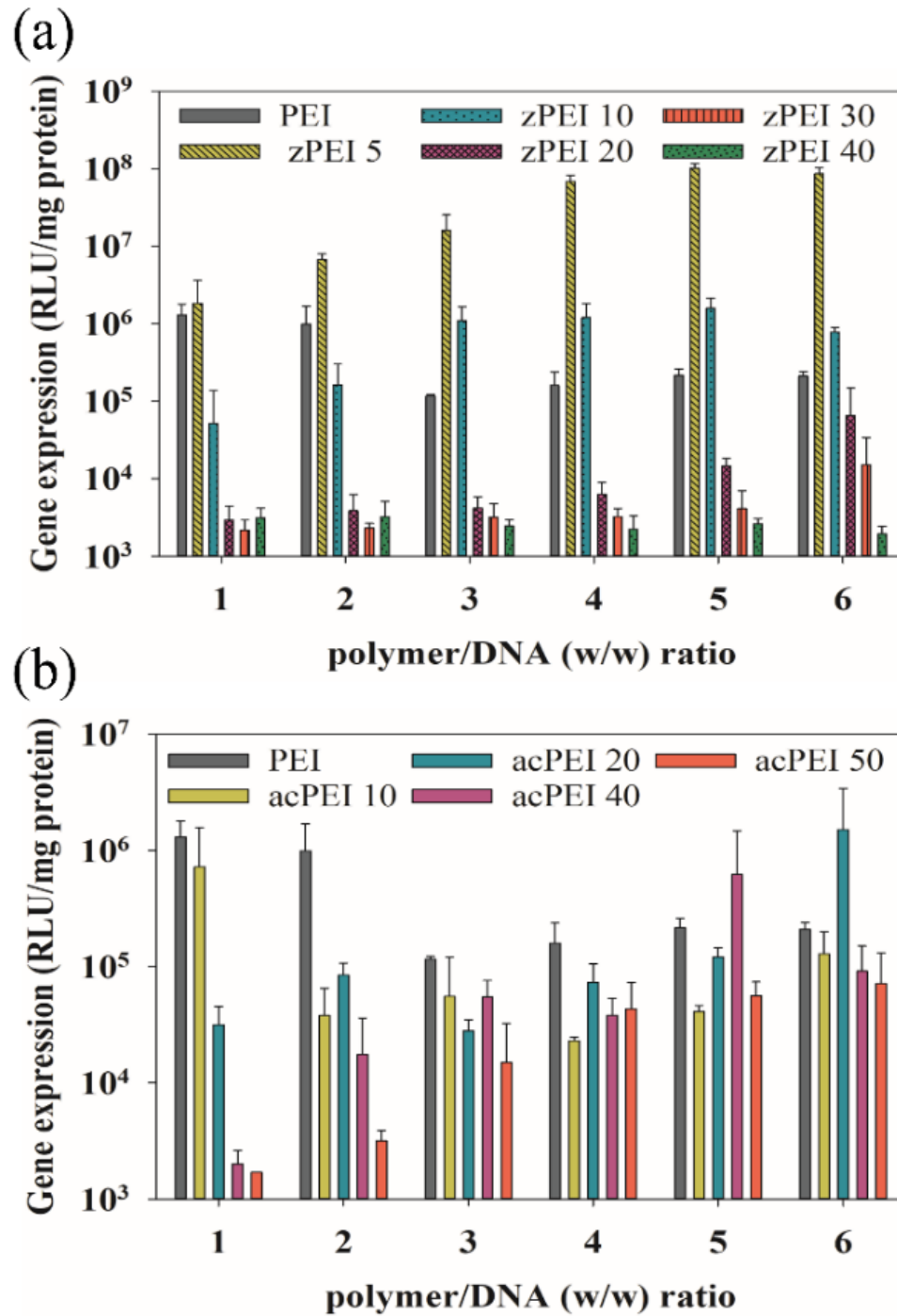
Figure 3.4. In vitro gene transfection efficiency in HeLa cells in the presence of serum. Luciferase activity in the cell lysates was measured 24 h post-transfection and reported as relative light units (RLU) normalized by the total protein's mass in the lysate. (n =3, error bars represent standard deviation)

3.3.6 Small-Angle X-Ray Scattering

We performed small-angle x-ray scattering (SAXS) experiments to investigate the nanoscopic structure of unmodified and modified PEI complexes with DNA. Specifically, we want to assess the relationship between PEI modifications and the resulting DNA packaging inside the polyplexes. Here, calf thymus DNA were used to form fibrous polyplex samples as described in the methods. Previous work has shown the DNA packaging in these fibrous DNA samples is comparable to that achieved in polyplex nanoparticles.[140] In the presence of linear polycations of charge +3 or higher, DNA is typically self-assembled into a columnar hexagonal arrangement. SAXS experiments allow for the measurement of the inter-DNA spacings inside the DNA condensate. Depending on the chemistry of the cation used for condensation, DNA-DNA separations typically vary from ~27-32 Å with DNA helices separated by water between the DNA surfaces. Representative normalized scattering intensity profiles from unmodified and modified PEI-DNA complexes are shown in **Figure 3.5**. Here, all samples were condensed in 10 mM Tris (pH 7.5) and allowed to incubate for one hour before SAXS measurements. bPEI-DNA (0% modified) has a characteristic Bragg peak observed at Q = 2.533 nm^{-1} corresponding to a D_{Bragg} spacing of 24.7 Å. bPEI-DNA is known to form a hexagonal lattice so this Bragg spacing corresponds to an interaxial DNA-DNA spacing (D_{int}) of 28.6 Å. This is consistent with previous measurements of bPEI-DNA that showed close-packed DNA.[140]

We hypothesized that modifications of PEI, either through acetylation or succinylation, would likely decrease the attractions of the modified PEI relative to

unmodified PEI resulting in decreased DNA packaging densities (or larger DNA-DNA spacings). Typically, polycations of net charge +3 or higher are known to spontaneously condense DNA. 25kDa bPEI has approximately 581 amines and while there is some debate it is generally agreed that approximately 1/4 to 1/5 of these amines are charged at near-neutral pH. This corresponds to a net charge of bPEI of approximately +116 to +145 at pH 7. This high net charge of the PEI strongly suggests that even at the highest degrees of modification used in this study we can expect to be well above the +3 charge threshold typical for DNA condensation. We next examined the DNA packaging in acetylated PEI polyplexes with the degree of modification ranging from 0 to 50% (**Figure 3.5a, left**). A clear shift of the Bragg reflection to lower Q with increasing percent modification of the acPEI is observed. As DNA-DNA spacings are inversely proportional to the scatter vector, Q, diffraction peaks observed at lower Q correspond to larger DNA-DNA spacings. As Bragg spacings are independent of the array, we focus here on D_{Bragg}. The corresponding D_{Bragg} spacings are plotted in **Figure 3.5b (left)** ranging from 24.7 Å for 0% modified bPEI to 28.8 Å for acPEI 50. Surprisingly, increased succinylation of zPEI does not behave in this manner.
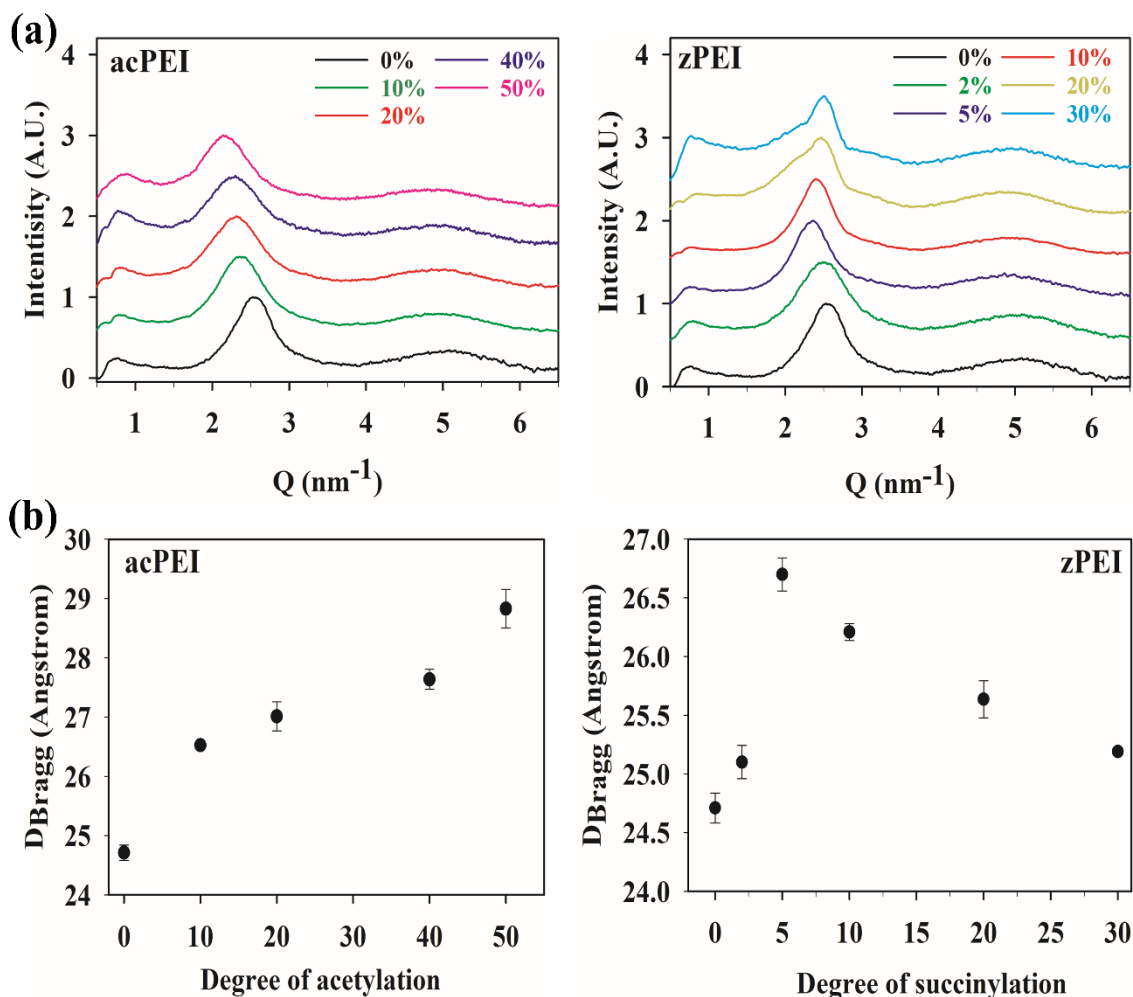
Figure 3.5. Representative scattering profiles for zPEI and acPEI-DNA under 'transfection-like' conditions. **a)** Intensity vs. Q plot obtained from samples prepared in fresh 10 mM tris buffer (pH 7.5) equilibrated for 1 hour. Scattering vector Q starts to decrease until 5% succinylation to PEI and then increases again with further % On the other hand, with increasing acetylation (acPEI 10-50), the Q value decreases. **b)** The average D_{Bragg} values derived from the maximum Bragg scattering plotted as a function of PEI modification. The Bragg spacing increases with increasing succinylation (zPEI 2-5), but the value drops with further modification (zPEI 10-30). As expected with acPEIs, the Bragg spacing increases with increasing modification. [Here, the condensates were formed at polymer/DNA weight ratio 0.5, 1.0, 1.0, 1.0, 3.0, 6.0 for bPEI, zPEI 2, zPEI 5, zPEI 10, zPEI 20 and zPEI 30 while 1.0, 1.5, 2.5 and 3.0 for acPEI 10, acPEI 20, acPEI 40 and acPEI 50 respectively. The results presented as mean±SD (n = 3)]

Instead, what we see at levels of modification $\leq$ 5% is a shift of the Bragg peak to lower Q. As shown in **Figure 3.5 b (right)**, these diffraction peaks correspond to D_{Bragg} values that increase from 24.7 Å at bPEI to a maximum D_{Bragg} of 26.7 Å from zPEI 5. With increasing succinylation, the Bragg peak is observed to shift to higher Q values corresponding to D_{Bragg} ranging from 26.7 to 25.2 Å as the degree of succinylation changes from 5% to 30% in zPEI-DNA complexes. This tighter DNA packaging in higher modified zPEI condensates does not correlate to more stable polyplexes, however, as we already showed that the amount of DS required to release the DNA decreases steadily with increasing degrees of succinylation, consistent with a weakening of the polymer-DNA interactions due to the increased amounts of succinyl groups to the PEI backbone. Using circular dichroism, we also verified that DNA within the polyplexes is still in B form, consistent with condensation having no effect on the configuration of the DNA helices (supplementary **Figure 3.27**). For zPEI 20 and zPEI 30 polyplexes, the Bragg reflection is significantly broader, suggesting a possible coexistence of two different phases in this highly succinylated polyplexes. zPEI 40 was not able to condense DNA, which is consistent with the low transgene expression observed in **Figure 3.4**. While the nature of this crossover behavior is not clear, this may suggest that higher levels of succinylation, while still reducing polymer-DNA interactions, also reduce the hydration layers between DNA helices allowing for the tighter packaging by zPEIs at high degrees of modification. Clearly, degree of modification in modified PEIs allows for the tuning of the polymer−DNA interactions and resulting packing densities in the polyplex condensates.

3.3.7 Time course studies by SAXS

Rearrangement within polyplexes is known to occur over time.[140] We next wanted to examine the evolution of our polyplex nanostructure as a function of time after condensation. **Figure 3.6** shows a plot of the measured Bragg reflection as a function of time for PEI, acPEI and zPEI polyplexes taken at 1 hr, 1 day, 7 days and 1 month after condensate formation. Here all samples were prepared at 10 mM Tris (pH 7.5). A modest (~2-3%) rearrangement of the polyplex structure was observed for all the unmodified and modified PEI polycations over this time period resulting in more tightly condensed structures over time. Most of the changes in the polyplexes occurred within the first 24 hours after formation. The smallest rearrangements occurred in the highest succinylated PEIs (zPEI 20/zPEI 30) possibly suggesting these highly succinylated polymers are more readily able to reach their equilibrium spacings.

3.3.8 Role of pH on DNA packaging in unmodified and modified PEI polyplexes

Altering the PEI through modifications like acetylation and succinylation are thought to influence gene transfection efficacy by changing the charge density of the PEI chains thus altering the ability of the modified PEI to condense/release DNA, and changing other factors including particle size and cytotoxicity.[141-142] Although debated, one of the leading hypotheses of the effectiveness of PEI for gene delivery is based on the idea of the "proton sponge" effect. This hypothesis is directly related to the large buffering capacity of PEI. It is suggested that PEI can absorb protons upon acidification of the endosome, increasing the osmotic pressure and aiding in the rupture and
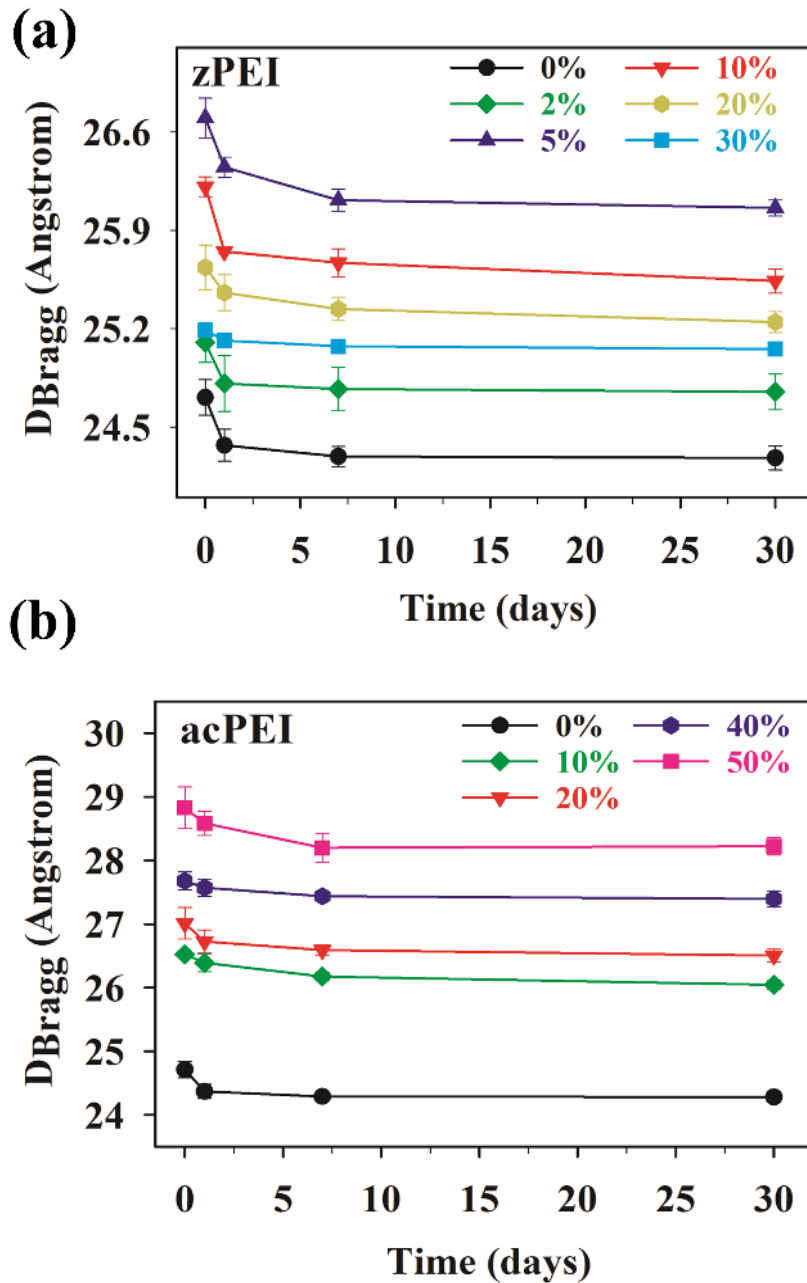
Figure 3.6. Interhelical spacings over time. Shown here is the Polymer/DNA internal packaging assembly of **a)** zPEI and **b)** acPEI. Data presented as the average Bragg spacing for maximum Bragg peaks plotted as a function of time. It requires at least a week to obtain complete equilibrium with these modified PEI polyplexes.

subsequent escape of the polyplexes from the endosomes. Release of polyplexes from endosomes is considered a significant barrier to effective gene delivery.[66, 143] Changes in the protonation of PEI during endosomal acidification has also been suggested to result in an "overcharging" of the polyplex resulting in a release of PEI and/or looser DNA packaging helping with the dissociation of the PEI.[79, 144-145] While cytoplasmic pH is near 7, endosomes are more acidic. Early endosomes maintain pH near 6.5 and during maturation become acidified to pH of ~4.5. DNA double helix structures are stable throughout this pH range, but the charge state of free PEI is known to increase at low pH. At neutral pH, PEI is thought to have approximately 20% of its amines charged, while at pH 4 this protonation increases to approximately 60%.[48] Since 25kDa PEI consists of roughly 581 amines per polymer chain, this results in PEI having a net charge of ~ +116 at neutral pH. Lowering the pH further increases the PEI charge due to protonation of additional amines. At pH 4, this results in a PEI molecule with an approximate net charge of +349. To examine the effect of pH on the observed DNA packaging in our PEI-based polyplexes during endosome acidification, we performed SAXS experiments on samples made at high pH (pH 7.5, Tris buffer) and low pH (pH 4, acetate buffer). Here, both DNA and PEI stock solutions were prepared in the same pH buffer and subsequently mixed to form the polyplex. Since low modified zPEI (< 10%) was observed to be most effective in transfection, we focused on polyplexes made with 10% modified zPEI and acPEI and compared them to unmodified bPEI. **Figure 3.7A** shows the representative normalized SAXS profile curves as a function of the pH at which condensation occurs for bPEI, acPEI 10 and zPEI 10. In this figure, samples were irradiated approximately one day after polyplex formation. For unmodified and both modified PEIs, lowering the pH results in a

shift of the Bragg peak to higher Q or equivalently smaller DNA-DNA spacings. For example, bPEI-DNA at pH 7.5 has a diffraction peak at $Q = 2.53$ nm^{-1} while at pH 4 a peak at $Q = 2.69$ nm^{-1} was observed. This corresponds to Bragg spacings ranging from 24.8 Å to 23.4 Å. acPEI 10 shows a larger decrease in D_{Bragg} from 26.5 Å at pH 7.5 to 24.0 Å at pH 4. Similarly, zPEI 10 has a larger decrease in spacings compared to bPEI with D_{Bragg} of 26.3 Å at pH 7 decreasing to 23.3 Å by pH 4. This shift in Bragg spacing corresponds to a ~5.6% change in spacing for bPEI compared to a ~9.4 to 11.4% change in the 10% modified PEIs when condensed at pH 4 compared to pH 7.5. Under most transfection conditions, polyplexes would be formed at near neutral pH and only be acidified after the formation of the complex. Therefore, we also created a third set of fibrous samples, pH 7.5-4, which were formed and equilibrated for 1 h in Tris buffer (pH 7.5), then transferred to acetate buffer (pH 4) and equilibrated again for 1 h before SAXS measurements. Blue curves (pH 7.5-4.0) in **Figure 3.7A** show SAXS scattering profiles for these samples. In all three systems, we see a shift to higher Q upon acidification that is intermediate compared to polyplexes condensed at pH 7.5 (black curves) and pH 4.0 (red curves). This is most likely due to bound PEIs in the polyplexes having different pK_as compared to unbound PEI free in solution. This different pK_as result in preformed polyplexes being less sensitive to changes in pH compared to complexes formed at different pHs.

Lastly, we also did a time course study for these different pH samples to check for rearrangements over time inside the polyplexes. **Figure 3.7B** shows a plot of D_{Bragg} as a function of time for bPEI, acPEI 10 and zPEI 10 for all three pH conditions (pH 4, 7.5 and
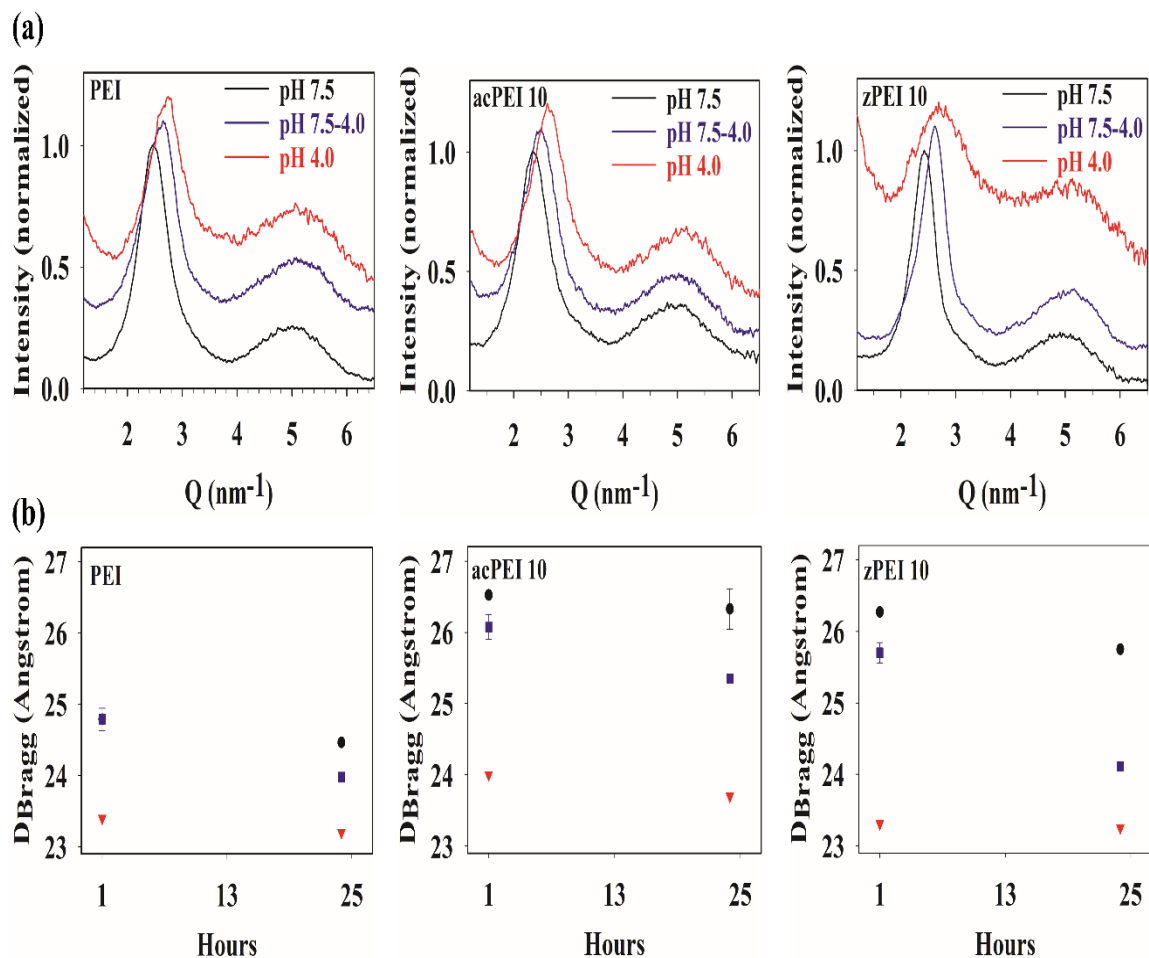
Figure 3.7. Modified PEI/DNA packaging density changes with pH. **a)** I vs. Q plotted as a function of scattering vector Q (data obtained after equilibrating the condensate for 1-day in designated pH). **b)** The pH effect on DNA interhelical spacing over time. [pH 7.5 (black): pellets formed in pH 7.5 buffer and transferred to fresh buffer to equilibrate for 1- hour & 24-hours, respectively. pH 7.5-4.0 (blue): pellets were formed in pH 7.5 buffer and then transferred to equilibrate in pH 4.0 acetate buffer (1-hour & 24-hours). pH 4.0 (red): pellets were formed with polymer & DNA solutions (pH 4.0 acetate buffer as solvent) and transferred the pellets to fresh pH 4.0 buffer.]

7.5-4). As polyplexes are not likely to stay complexed in vivo for long times, we focused on changes in DNA packaging within 24 hours. For all three polyplex systems, the observed D_{Bragg} decreased slightly (~2%) at 24 hours compared to 1 hour incubation. For pH 7.5-4 samples, additional incubation at pH 4 resulted in zPEI 10/DNA having fairly large structural rearrangements resulting in a D_{Bragg} closer to that observed for zPEI 10 polyplexes condensed at pH 4. pH 7.5-4 samples for bPEI and acPEI 10 polyplexes however still have D_{Bragg} peaks closer to those observed for polyplexes formed at pH 7.5. All the Q and D_{bragg} values for these plots are tabulated in supplementary **Table 3.4**. The larger structural rearrangements for zPEI 10 polyplexes may suggest that the pK_as of bound zPEI are closer in value to the pK_as of unbound zPEI.

3.4   DISCUSSION

A nonviral polymer gene therapy carrier faces several intra- and extracellular barriers before successful gene transfection.[72, 146-147] First, the polyplex must travel to targeted cell while avoiding degradation of its payload by nucleases or clearance by the reticuloendothelial system. Upon arriving at the target cell, the polyplexes must interact with the negatively charged cell walls and be taken up into the cell through processes like endocytosis. For polymer gene delivery, these polyplex particles must then escape the endosome while also passing through the complex cytoskeletal network in the cell cytoplasm on their way to the nucleus. Then ultimately the polyplex must pass the nuclear envelope while also releasing its DNA for successful gene transcription of its payload.[148-151] The cationic polymer, polyethylenimine (PEI) has proven to be one of the most successful polymers for gene transfection and is often considered a benchmark for polymeric gene delivery. The high charge density of PEI, however, also means it is cytotoxic and therefore may not be sufficiently biocompatible for clinical applications.[152] To mediate this cytotoxicity, as well as to optimize gene delivery, a common strategy has been to modify PEI through reaction with the primary and secondary amines on the PEI backbone. Grafting different functional groups to PEI mediates polymer-DNA interactions, altering the binding and release of DNA by the modified PEIs, and often reduces the cytotoxicity of the polymer.

In prior work with acetylated and succinylated PEI, it was shown that modifications result in weakened binding to DNA, and the competitive release of DNA from polyplexes increases with increasing modification. In these newly synthesized zPEI and acPEI series, we again see the same behavior. By ethidium bromide exclusion assay

(**Figure 3.2**), we show that more polymer is needed to fully condense DNA with increasing levels of modification by both succinylation and acetylation. Using a dextran sulfate displacement assay (**Figure 3.3**), we also see acetylation and succcinylation weaken polymer-DNA interactions resulting in more DNA released by competitive displacement by dextran sulfate. Although secondary amines are more nucleophilic than primary amines,[153] it is generally assumed that PEI modification occurs mostly at primary amines due to steric hinderance of the secondary amines in the PEI chain.[88, 97] Using 2D-NMR, we experimentally tested this (**Figure 3.2**) and found that both acetylation and succinylation actually occur preferentially at secondary amines, especially at lower levels (≤10%) of modification. At higher levels of modification, we see an increase in modification of primary amines yet secondary amines are still modified more. The colloidal and charge properties of the resulting polyplex nanoparticles were also investigated by DLS and zeta potential measurement (**Table 3.1**). Acetylation at all levels was found to result in polyplex nanoparticles nearly identical in size to bPEI/DNA. Acetylation also decreases the particle surface charge slightly by 10% modification, and zeta potential decreased further at higher levels of modification. zPEI polyplexes in general were observed to be larger (~2x) than both bPEI/DNA and acPEI/DNA. This may reflect more aggregation is occurring in the zPEI formation. Surprisingly, the incorporation of the negatively charged succinate groups for zPEI did not affect zeta potential very much up to ~20% modification. The decrease in zeta potential in zPEI is quite similar to acPEI up until 30% modification where zPEI 30/DNA reversed sign and negative particle surface charge was observed. This correlates well with the very poor transfection efficacy of zPEI 30/DNA at all weight-to-weight ratios (**Figure 3.4**).

In prior work, it was reported from our group and others that acPEI and zPEI result in enhanced transfection in both the absence and presence of serum proteins.[88, 99] Forrest, et. al reported a 21-fold increase in acPEI transfection in serum, while we recently showed even minimally succinylated zPEIs as low as 2% can result in 260- to 480-fold enhancement in the transgene expression when compared to unmodified PEI. Although the mechanism is still unclear, both modifications suggest that altering the protonation properties of PEI enhances gene delivery activity. These new series of acPEI and zPEI were also tested for their transfection efficacy in HeLa cells in the presence of serum proteins for direct comparison to our biophysical characterizations and the results are given in **Figure 3.4**. In agreement with our most recent manuscript, succinylation at modifications $\leq 10\%$ showed a large enhancement in transgene expression compared to bPEI/DNA in the presence of serum proteins. With increasing polymer/DNA (wt/wt) ratio, bPEI/DNA gene expression decreased. In contrast, zPEI 5 and zPEI 10 show increasing transgene expression at higher polymer loading with zPEI 5 being 318-472x higher transgene expression at wt/wt 4 and 5 compared to bPEI at the same loading. In contrast, acPEI did not show an enhancement for transgene expression in the presence of serum in these experiments. acPEI/DNA performed worse in nearly all weight:weight ratios when compared to bPEI/DNA. The exact mechanism for this enhancement of zPEI/DNA in the presence of serum is still not fully understood. However, a similar enhancement of transfection in serum was reported using a biodegradable PEI-mimetic polymer, similar to linear PEI, where the ratio of primary, secondary and tertiary amines was controlled.[154] Similar to zPEI, these PEI-mimetic polymers showed only slightly higher efficacy without serum that increased when serum proteins were present. In their

polymers, a ratio of 1:4:1 for primary:secondary:tertiary amines was found to be optimal for gene transfection. In contrast, our zPEIs, based on branched PEI, are primarily modified at their secondary amines most likely decreasing the ratios of secondary amines below the optimal ratios for the PEI-mimetic polymers.

We next used X-ray experiments to examine the nanostructured ordering of the DNA helices condensed in the polyplexes. As discussed in the introduction, cations of net charge +3 or higher, can self-assemble with DNA to form highly compacted structures. Upon condensing, DNA is typically ordered into hexagonal arrays where ~5-15 Å water layer separates the DNA helices.[126, 155] This water layer represents a balance between the attractive and repulsive forces within the condensed cation/DNA phase. In previous work, osmotic pressure combined with small-angle X-ray scattering experiments to experimentally determine the attractive and repulsive contributions to the free energy for a variety of linear polycation-DNA systems.[127-129, 156] Using small arginine peptides, it was reported that the incorporation of uncharged amino acids, such as alanine or serine, and the incorporation of anionic amino acids, such as glutamic acid or phosphorylated serine, had the effect of increasing the repulsive interactions while simultaneously, but to a lower extent, decreasing the attractive interactions.[128] The net result of these effects was to alter peptide-DNA interactions leading to larger DNA-DNA spacings in the modified peptide/DNA systems. In particular, the incorporation of a negative moiety, significantly increased repulsions, and the resulting DNA-DNA spacings were much larger compared to the incorporation of an uncharged amino acid. Based on these results, we hypothesized that both acPEI and zPEI would result in lower DNA packaging densities in comparison to bPEI. Higher degrees of modifications would be expected to further decrease

attractions and increase repulsion leading to more loosely structured polyplexes with zPEI/DNA having the largest DNA-DNA spacings. We observed similar trends with a succinylated PAMAM dendrimer system where only primary amines of the dendrimer were succinylated.[157-158] Succinylated PAMAMs were still able to condense DNA up to 40% modification. The succinylated PAMAMs showed more modification resulted in decreased DNA packaging and even a phase transition from a columnar hexagonal to a columnar square lattice at the highest modifications. Tuning DNA-dendrimer interactions in this way was an effective tool to tune the resulting DNA packaging resulting in DNA-DNA spacings ranging from 28 Å for unmodified PAMAM to 40 Å for 40% succinylated PAMAM. PAMAM is also similar to bPEI as being a heavily branched polycation that would not likely coordinate in the grooves of the DNA helix in a manner comparable to linear polycations. Here, we see different behavior. Acetylation does show a monotonic increase in the DNA-DNA spacings with increasing levels of modification (**Figure 3.5**). The change in Bragg spacings, however, was smaller varying from 24.8 Å to 28.8 Å by 50% acetylation. These results are similar to what we observed in the short arginine peptides where incorporating a non-charged amino acid had relatively small effects on the attractive and repulsive forces within the condensate. The most significant difference was with zPEI (**Figure 3.5 b**). At low levels of succinylation (<10%) we do see DNA-DNA spacings increase. 5% succinylation has a similar effect as 10-20% acetylation in the resulting DNA packaging inside the polyplexes. Surprisingly, though at still higher levels of succinylation, the SAXS measured DNA-DNA spacings monotonically decrease for modifications of 10 to 30%. Despite this apparent tightening of the DNA-DNA spacing, we show (Figure 3.2/3.3) that high modification of zPEI greatly reduces

95

polymer-DNA interactions creating polyplexes that are easier to dissociate. By 40% modification, zPEI was no longer able to condense DNA. The decrease in DNA spacings for moderate succinylation would suggest that zPEI is decreasing the water layers between DNA helices. Another possibility is if DNA changes form upon condensation to form a small diameter helix (such as Z-form DNA). Generally double stranded DNA is in B-form resulting in a double helix with a diameter of 2 nm. Even after condensation, most experiments have shown DNA maintains B-form. To verify that zPEI/DNA maintains B-form DNA, we performed circular dichroism (CD) experiments (supplementary information, **Figure 3.27**). The spectrum for zPEI/DNA is comparable to free DNA strongly suggesting zPEI is not altering the DNA upon binding. Using time course studies (**Figure 3.6**), we also show that the resulting polyplexes are able to reorganize themselves over the course of days to create more tightly packaged DNA assemblies were relatively small (~1.5-2.5%) over the course of 30 days and most of the rearrangements occurred in the first 24 hours. This suggest polyplexes like PEI-DNA get trapped in nonequilibrium states due to the strong binding of the polycation but can get to more equilibrium state over time. Interestingly, zPEI 30 showed less rearrangement (~0.5%) potentially suggesting the high level of succinylation decreased polymer-DNA interactions sufficiently to more readily reach equilibrium. Acetylation, even at 50% modification, did not show this effect.

Lastly, we examined the effect of pH on the unmodified bPEI and modified PEI polyplex DNA packaging. During transfection, polyplexes would be expected to experience different pH depending on their location. Typically, polyplexes are first formulated in water or in buffers such as HEPES, PBS or Tris with pH near 7. If injected

into the body, polyplexes would see similar pH in blood (~7.35-7.45). Once endocytosed into cells, however, the polyplexes would experience lower pH ranging from ~6.5 in early endosomes to pH 5.5 in late endosomes. When maturing into lysosomes, pH is even lower at 4.5. To mimic the pH range experienced in vivo, we therefore looked at PEI polyplexes packaging in pH 7.5 buffer (Tris) and in pH 4.0 buffer (acetate). DNA packaging in the polyplexes was measured by X-ray diffraction (**Figure 3.7**). bPEI is known to have only about 20% of its amines charged at neutral pH but this charge state can increase to approximately 60% by pH 4. As shown in Figure 3.7, we show that the pH at which condensation occurs can have a large effect on the resulting internal packaging of the DNA. For all three polymer systems (bPEI, zPEI and acPEI), condensing at low pH resulted in significantly higher DNA packaging densities in the resulting polyplex as compared to condensation at pH 7.5. Previous studies have shown that using acidic culture medium enhanced polymeric transfection efficiency but acidic transfection medium reduce efficacy.[142] To mimic the effect of acidification of polyplexes in late endosomes and lysosomes, we also looked at DNA packaging that was preformed at near neutral pH (Tris pH 7.5), equilibrated for 1 hour, and then transferred the polyplex to acidic pH 4 buffer. These samples are labeled as pH 7.5-4 in **Figure 3.7**. Due to the presence of uncharged amines in PEI, a hypothesis for the relative high transfection with PEI is known as the "proton sponge effect".[144, 159] This hypothesis is based on the pH-buffering capacity of PEI. It is argued that having PEI present in endosomes during acidification will result in increased osmotic pressure as the PEI increases in charge and more anions are required to neutralize the PEI charge.[160] This increased osmotic pressure is argued then to help rupture endosomes allowing more

PEI/DNA polyplexes to be released in the cytoplasm. Commonly, it is also proposed that the PEI in polyplexes overcharges in an acidic effect causing enhanced repulsions and leading to the polyplex structure either swelling or loosening in the endosome.[79, 144-145] This hypothesis is disputed, however, with recent experimental and theoretical data seemingly both supporting[79, 149, 161] and not supporting it.[150, 162-163] Others have also argued that PEI, either free or bound in polyplexes, may interact with the endosome membrane in some manner that results in endosomal rupture.[162, 164-166] By SAXS experiments, we find that once formed, unmodified and modified PEI is able to reorganize its structure to tighten, not loosen, DNA packaging. The pH 7.5-4 samples achieved intermediate DNA packaging when compared to samples condensed directly at pH 7.5 or pH 4. This likely is due to the pK_as of the complexed PEI, acPEI and zPEIs being different than the unbound polymers resulting in the PEIs not achieving the same charge state inside the polyplex that they achieve in free solution. Interestingly, the succinylated zPEI showed the largest sensitivity to changing the pH which may aid in its transfection efficiency. The tightening of the DNA-PEI complex due to acidification is in good agreement with recent all-atom molecular dynamic simulation results by Antila, et al.[167] Their simulations suggest upon acidification PEI chains do not swell or fall apart due to overcharging but may lead to more PEI chains being freed from the polyplex and that these chains may contribute to release from endosomes by other mechanisms.

3.5   CONCLUSION

In summary, we have investigated the effect of acetylation and succinylation of branched PEI on the resulting biophysical properties, transfection efficiency, and nanoscopic internal structure of the resulting condensates. Through 2D-NMR studies, we

show that both modifications are preferential to secondary amines on the bPEI with primary PEI amines being modified only at higher percent modifications. As expected, higher degrees of modification reduce polymer−DNA interactions resulting in less stable polyplexes. Transfections in the presence of serum proteins show enhancement by the succinylated PEIs (zPEI), while acetylated PEI (acPEI) performed the same or worse than unmodified bPEI/DNA. Inter-DNA spacings were examined by SAXS experiments as a function of degree of modification. Acetylation resulted in a monotonic increase in Bragg spacings inside the acPEI polyplexes, while zPEI showed a surprising crossover behavior where DNA-DNA spacings increase at low modification but then decreased at higher modification. We also examined the pH dependence of the PEI and modified PEI polyplexes at pHs relevant to transfection conditions. We show that changing the pH at which the polyplex is condensed alters the resulting DNA packaging in all the polyplexes. Lowering pH, resulting in a more highly charged PEI polymer, results in significantly tighter DNA packaging. Lastly, we took preformed polyplexes condensed at near neutral pH and then exposed them to low pH buffer (pH 4), similar to pH a polyplex might encounter in a lysosome. The polyplexes become more tightly packaged upon acidification with a DNA packaging intermediate than observed for polyplexes directly condensed at neutral or low pH. The succinylated PEIs showed the largest response to changes in the solution pH with significant restructuring of their internal structure upon exposure to low pH buffer. These studies highlight how tuning polymer-DNA interactions through PEI modification and pH is a valuable tool to engineer optimized PEI based gene delivery agents.

3.6 Supplementary Information

3.6.1 Characterization of polymers with FT-IR (ATR)

All the zPEIs and acPEIs were characterized for functional groups with an iS50 FT-IR equipped with a diamond ATR (at 4000-400 cm^{-1}) on solid polymer stocks through OMNIC software (ThermoFisher Scientific; Waltham, MA). FT-IR spectra are plotted in **Figure 3.8 & 3.9** with the stretch and bend peaks for ethylene, amine, amide, and carboxyl functional groups identified. Polymer modification success was determined by inspecting the spectrum near the fingerprint region. Peaks at 1599 and 1455 cm^{-1} indicates -N-H (amine) and -C-H (ethyl) bend peak of bPEI while at 1635 cm^{-1} and 1565 cm^{-1} were assigned for carbonyl stretch and N-H bend (amide, CO-NH), respectively. Within the spectrum, the C-O-H bending mode for carboxylic acid was identified at 1386 cm^{-1} while
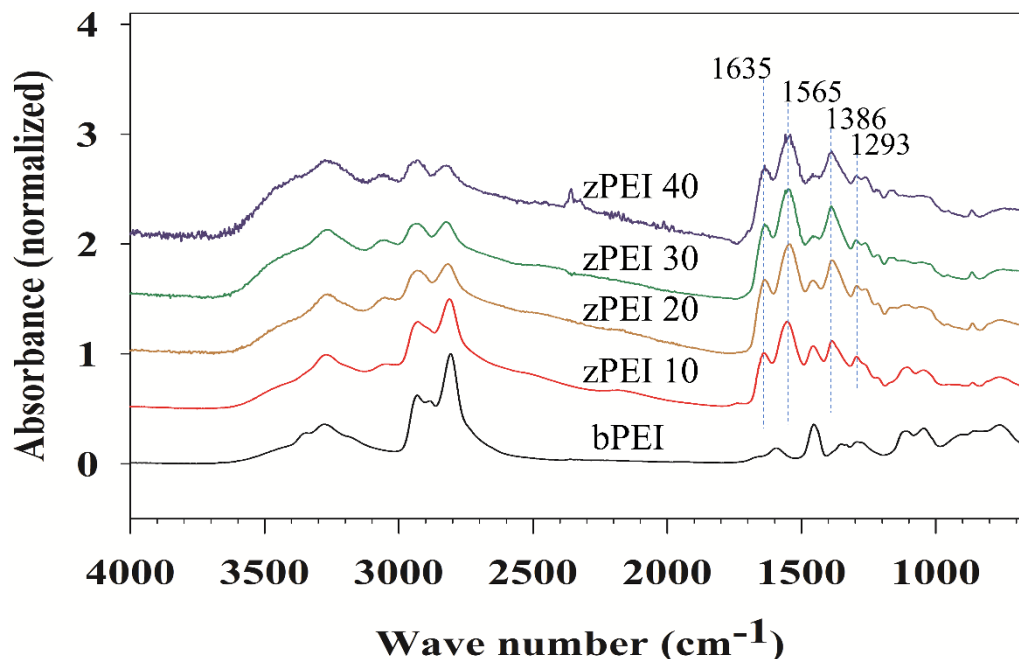
Figure 3.8. FT-IR of zPEIs with modification regions labelled
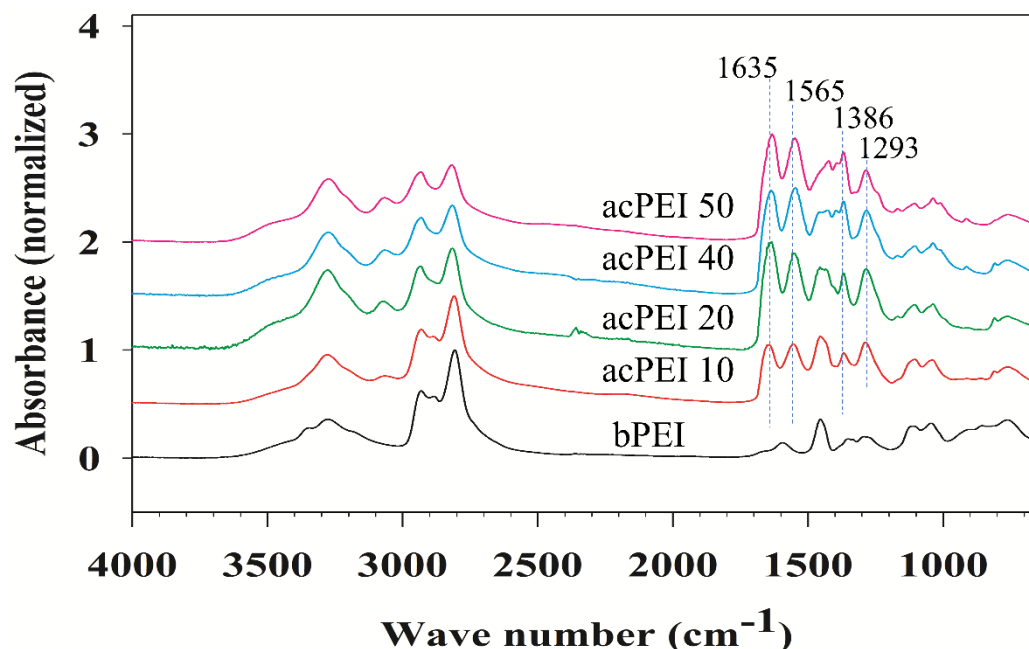
Figure 3.9. FT-IR of acPEIs with modification regions labelled

C-O of carboxylic acid and C-C stretch at 1293 cm^{-1} further proves the succinylation and acetylation reactions to be successful.

3.6.2 Characterization of polymers with NMR (H-NMR, HMBC, HSQC)

Both 1D and 2D-NMR characterization was conducted on an Avance Neo spectrometer (400 MHz) instrument on approximately 6.5 mg polymer dissolved in 0.65 ml D$_2$O, and data were analyzed with topspin 4.0.3 data analysis software. From the ^{1}H-NMR spectrum, three chemical shift regions supporting the Branched PEI methylene protons base peaks were identified at δ2.6-3.6 ppm while the peak region δ2.3-2.4 ppm was for succinyl methylene protons and 1.8-2.1 ppm for three protons of the methyl group conjugation with acetylation (**Figure 3.10-3.19**). As the mole ratio of succinic anhydride or acetic anhydride to branched PEI increased to get higher % modification,

the peak area also increased proportionally. The modification region in the 1D-NMR spectrum for acetylation has more than two peaks which made the characterization challenging, so 2D-NMR with HMBC was performed. The coordinates at F1: 181.3 ppm, F2: 1.78 ppm was assigned for 2°-amides, while 3°- amide show isomerism at F1: 174.1 ppm, F2: 1.86 ppm for trans amide, while F1: 174.1 ppm, F2: 2.0 ppm for cis amide (**Figure 3.20**). The % degree of modification was calculated using the integral areas of succinyl peak divided by bPEI amine base peaks. Thus, nearly a quantified modification series of 8, 21, 29 and 35% zPEIs and 11, 22, 41 and 53% acPEIs were characterized. The percent modification is tabulated in **Table 3.2**.

The chemical structure in **Figure 3.20** shows the most important peak assignments for succinylation. HMBC spectra of zPEI 20 shows the long range ^{1}H-^{13}C correlation which are three or two bonds away. So, proton (b at 2.45 ppm) is correlated to the carbonyl carbon (C-4, at 181.4 ppm) of the 2°-amide group by three bonds. For the same reason, proton H^b show strong correlation to C-5 (at 174.1 ppm) of the 3°-amide carbonyl carbon. Protons H^a and H^b also correlated between each other via two bonds at 32.45 (C-3) and 32.55 ppm (C-2) respectively along the F-1 axis (vertical axis). Inset correlation peak showing two carbons at 32.5 ppm (F1-axis) as a proof that the proton peaks between amide and carboxyl groups are merged along F-2 axis (**Figure 3.20**, inset). This shows a similar chemical environment imparting on two adjacent methylene protons (-CH$_2$-CH$_2$-) due to amide and carboxyl groups respectively. Both H^d and H^e are strongly correlated to amide carbonyl (C-4 & C-5) is a proof of a successful conjugation to both primary and secondary amines (further proved with HMBC spectra of acPEIs). H^d and H^e also forms two bond correlation peaks with PEI base carbons at around 50-60

ppm (F1 horizontal axis). Unfortunately, peaks for the H^e could not be resolved from this HMBC spectra. HSQC spectra of zPEI 5 and zPEI 20 further supports the successful succinyl conjugation by showing 1-bond ^{1}H-^{13}C correlation between F1: 32.45/32.55 ppm and F2: 2.45 ppm (**Figure 3.21 & Figure 3.22**). Because of single bond ^{1}H-^{13}C correlation, we do not see any contour plot arising at downfield region (F1- axis, at 170-185 ppm) with C-4 or C-5 carbons.

Inset chemical structure in **Figure 3.23** shows the most important peak assignments for acPEI 40. HMBC spectra shows the long range ^{1}H-^{13}C correlation which are three or two bonds away. Here, the peaks arising with the modification must have two bond ^{1}H-^{13}C correlation. So, protons 'a' at 1.86 ppm are correlated to the carbonyl carbon C-2, at 181.4 ppm of the 2°-amide group by two bonds. For the same reason, proton H^e & H^{e*} show strong correlation to C-3 (at 174.1 ppm) of the 3°-amide carbon. Unlike zPEI, these protons do not show any correlation peak around the modification region (up field~30.0-35.0 ppm along F-1 horizontal axis), proving the differences in chemical environment originating due to succinyl and acetyl functionality. HSQC spectra further supports the difference in chemical environment due to the attachment of three different types of -CH$_3$ groups (**Figure 3.24**). Both H^e and H^{e*} show different ^{1}H-^{13}C single bond correlation peaks depicting a possible presence of isomerism which could not be identified by current experiment. HMBC experiment was further conducted at very low pH (~2) to see whether the conjugation peaks shift to up/downfield. The reason was to identify any possibility of carboxyl group in the acPEIs. This experiment shows the position of the correlation peaks at the modification region, although merged, of acetyl group remains unchanged (**Figure 3.25**). Because of the high electron withdrawal effect

of Cl⁻, the PEI base peaks shifts to 2.9-3.8 ppm. Unfortunately, the presence of carboxylic acid, if present, could not be explicitly distinguished from these spectrums because of their similar resonance to amide carbonyl carbons. However, these spectrums confirm that the secondary amines of the branched PEI start to conjugate first followed by primary amines. The argument is supported by the HMBC spectra of acPEI 20, where we see the integral area of the peak at 1.86 ppm is almost negligible (correlated to F1: 181.4 ppm) (**Figure 3.26**). With an increasing degree of modification shown in acPEI 40 (**Figure 3.23**), the integral area of this peak increases linearly.

Table 3.2 Composition of modified PEIs[a]

Polymer ID	Reagent/amine*100%, feed	[b] Modification degree, %
zPEI 2	2	2
zPEI 5	5	4.8
zPEI 10	10	8
zPEI 20	20	21
zPEI 30	30	29
zPEI 40	40	35
acPEI 10	10	11.2
acPEI 20	20	22
acPEI 40	40	41
acPEI 50	50	53

[a] The nomenclature of the polymers is expressed as follows: xPEI-y, where x represents the reagent by which PEI was modified (x = z or ac, where z = succinic anhydride and ac = acetic anhydride, respectively) and y represents the modification degree of amins used as feed ratio. Throughout the manuscript the feed ratio was used for consistency.

[b] Modification degree of amines measured by ¹H-NMR
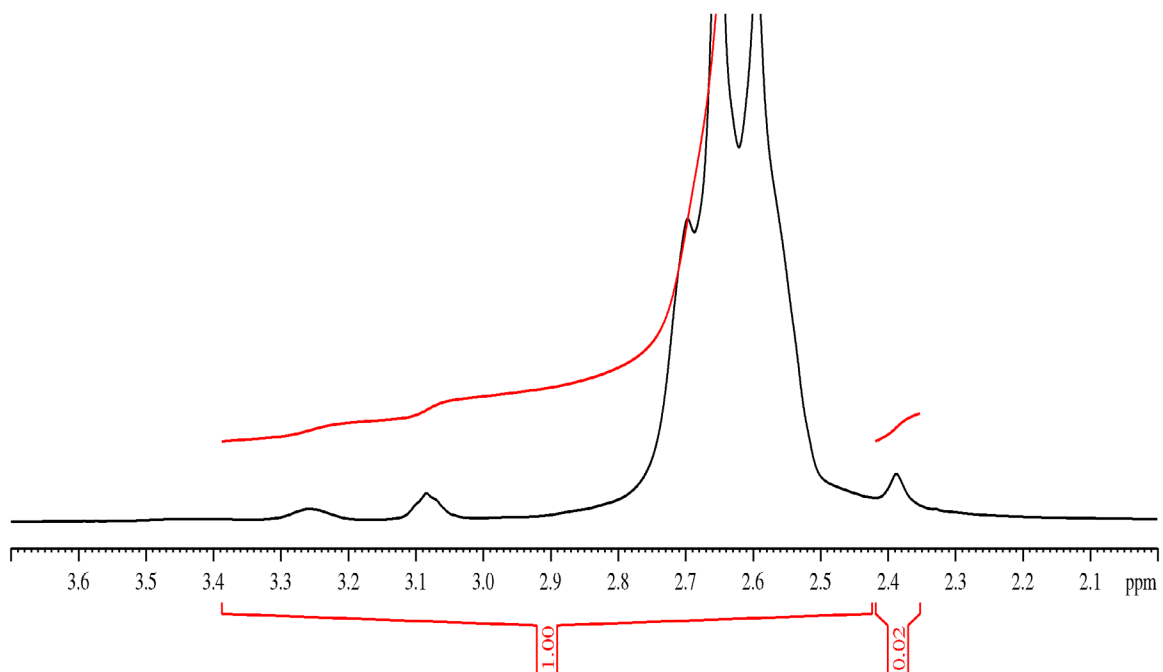
Figure 3.10. ^{1}H-NMR of zPEI 2
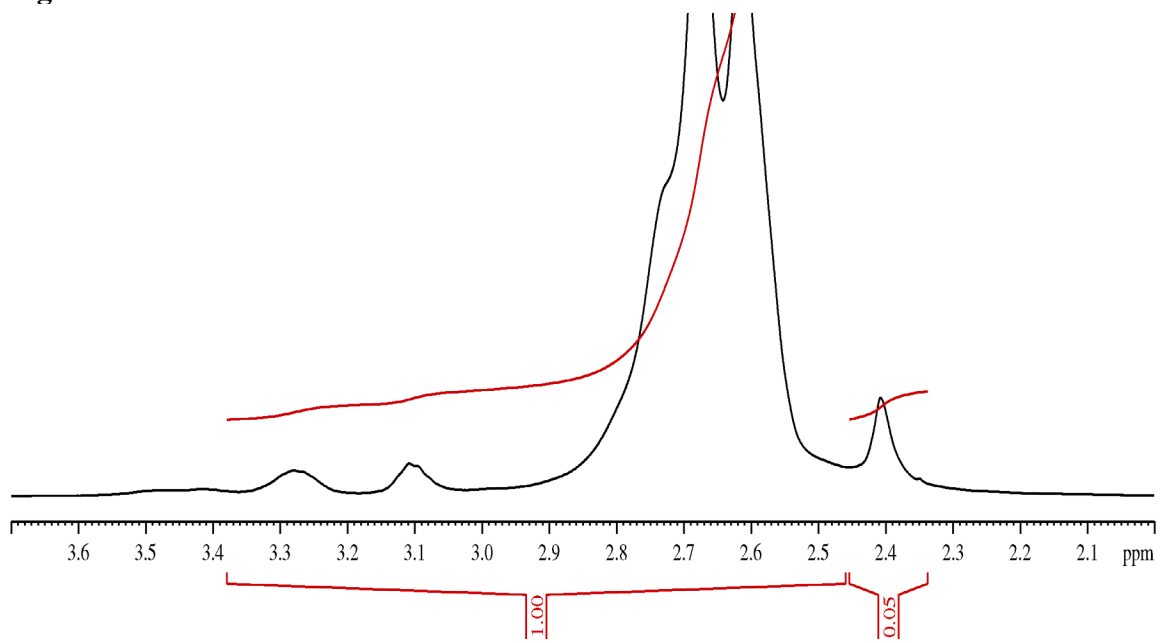
Figure 3.11. ^{1}H-NMR of zPEI 5
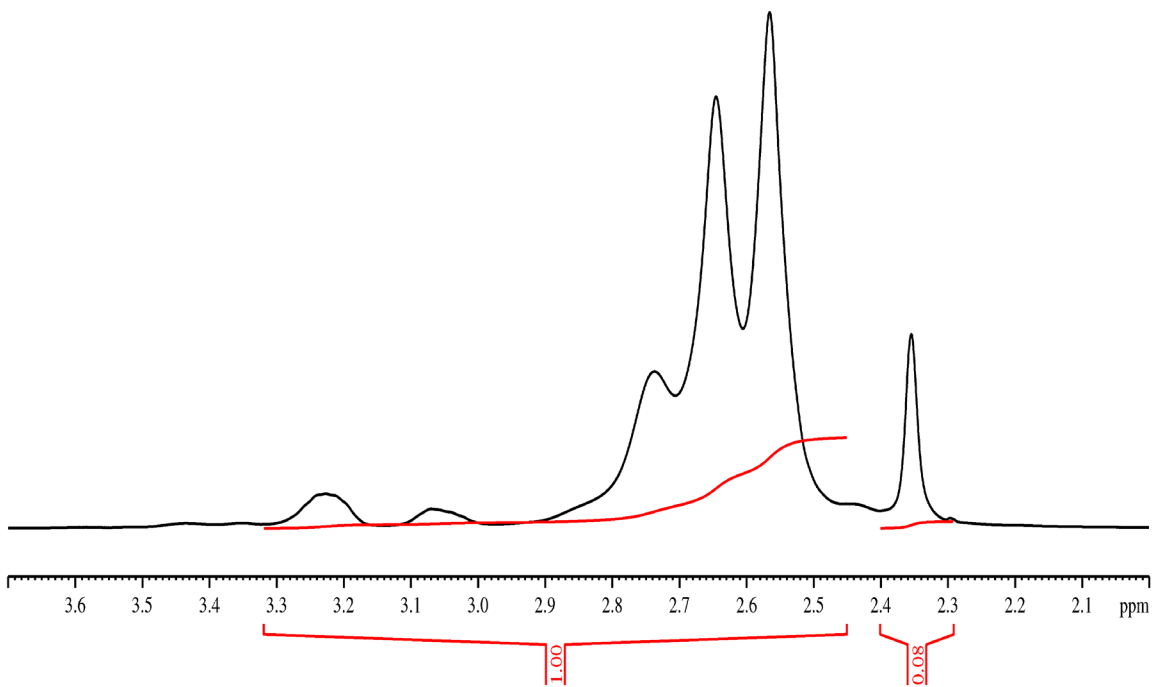
Figure 3.12. ^{1}H-NMR of zPEI 10
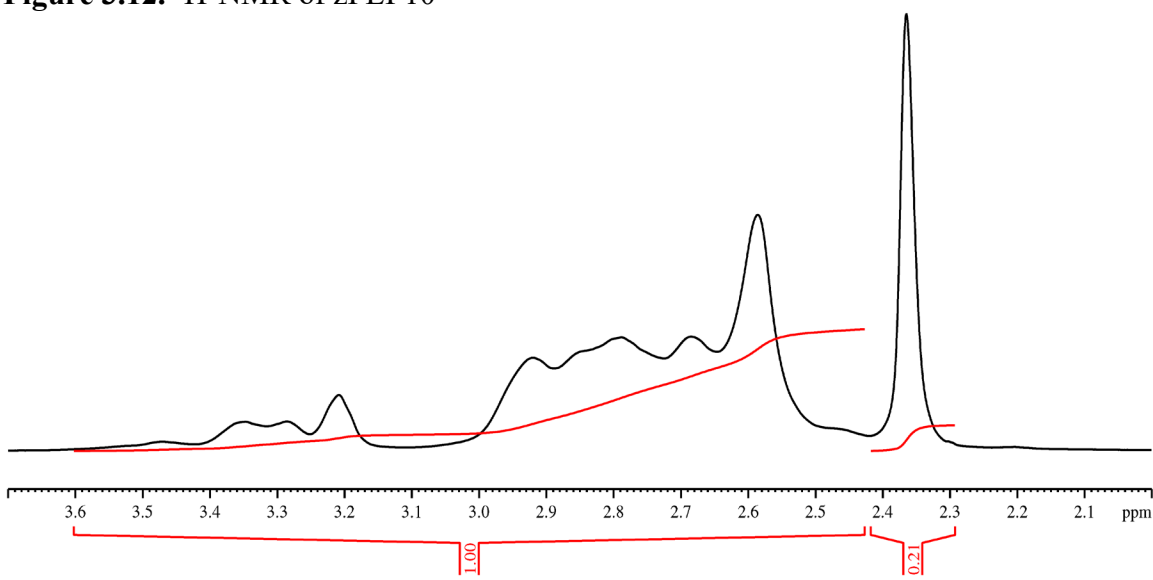
Figure 3.13. ^{1}H-NMR of zPEI 20
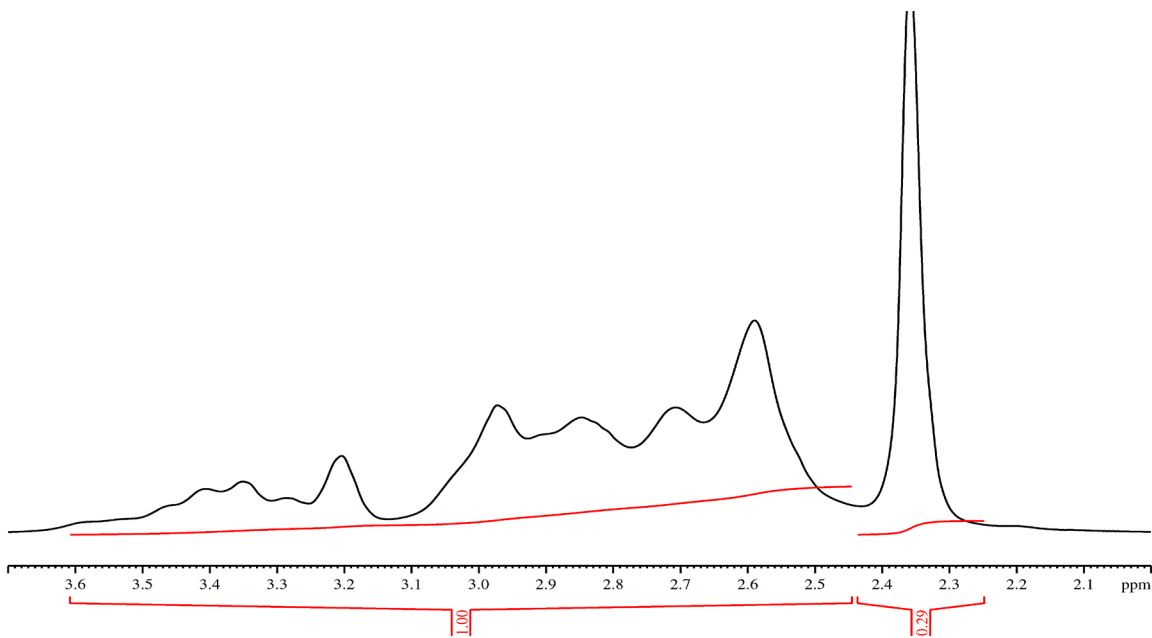
Figure 3.14. ^{1}H-NMR of zPEI 30
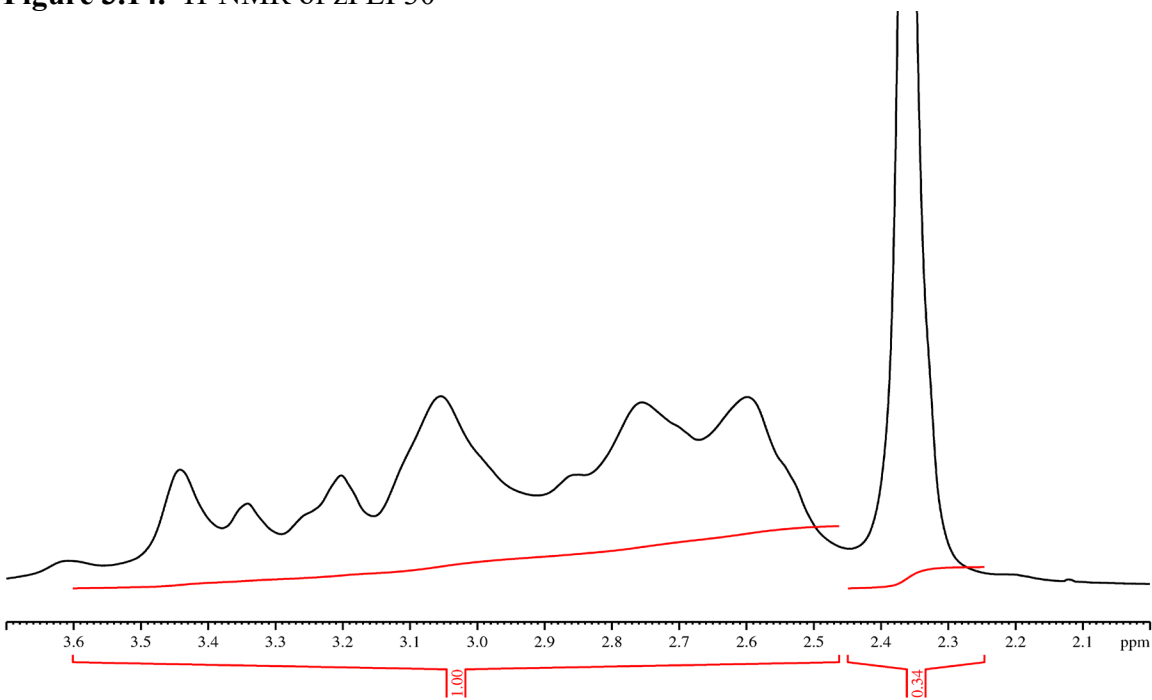
Figure 3.15. ^{1}H -NMR of zPEI 40
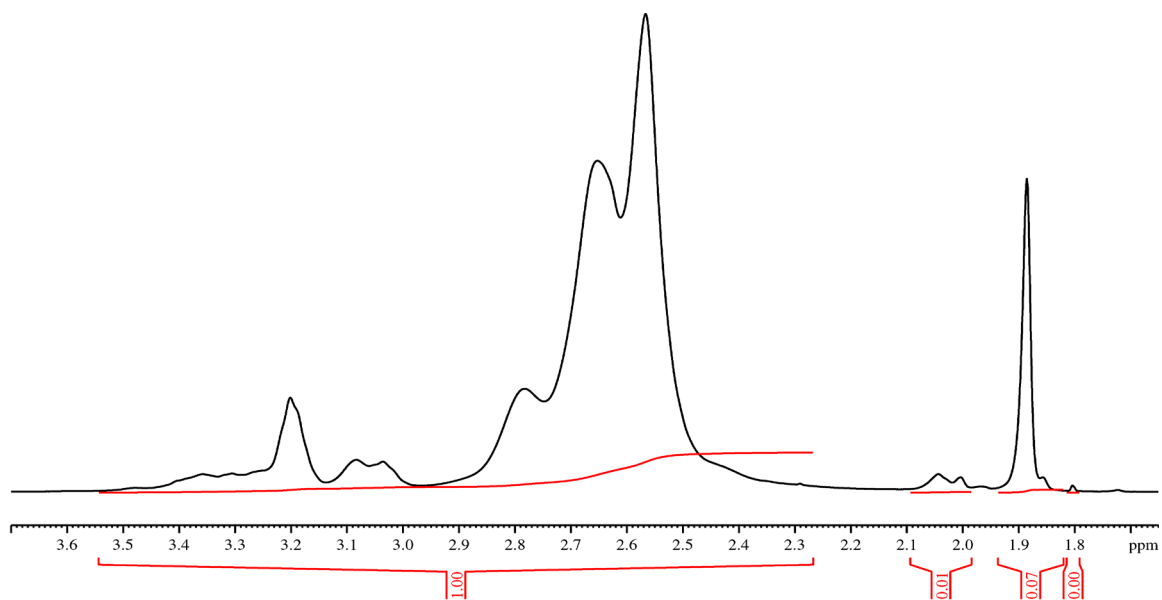
Figure 3.16. ^{1}H-NMR of acPEI 10
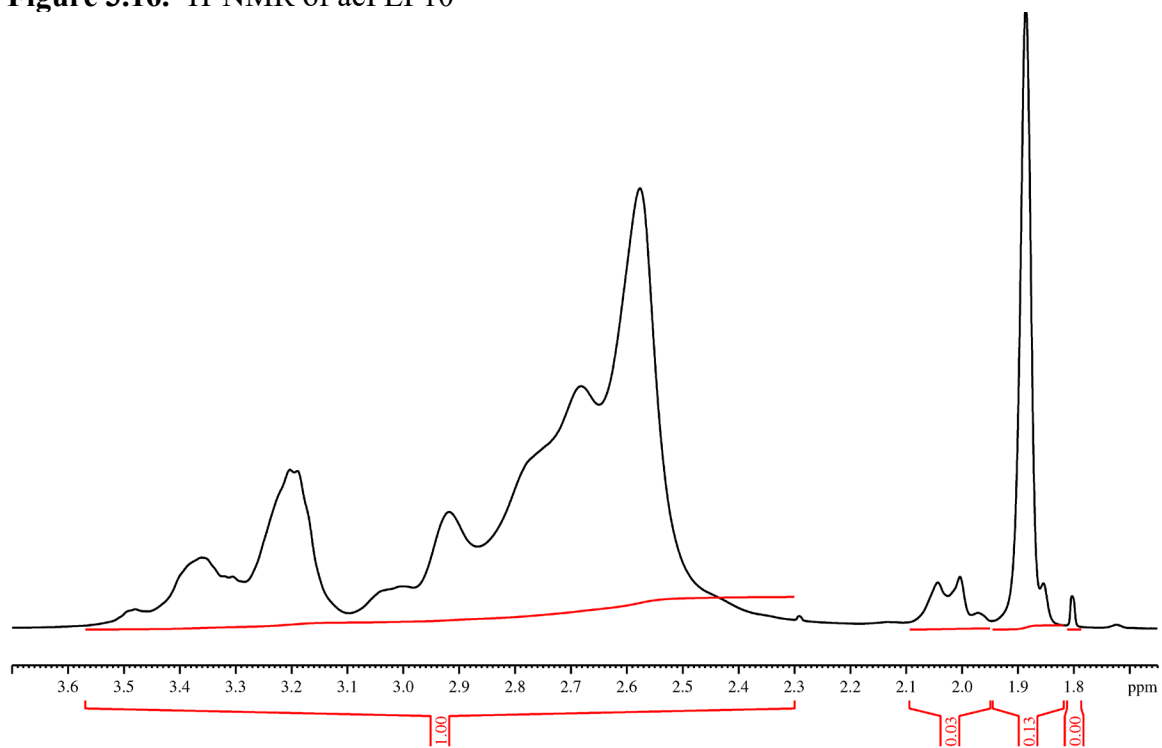
Figure 3.17. ^{1}H-NMR of acPEI 20
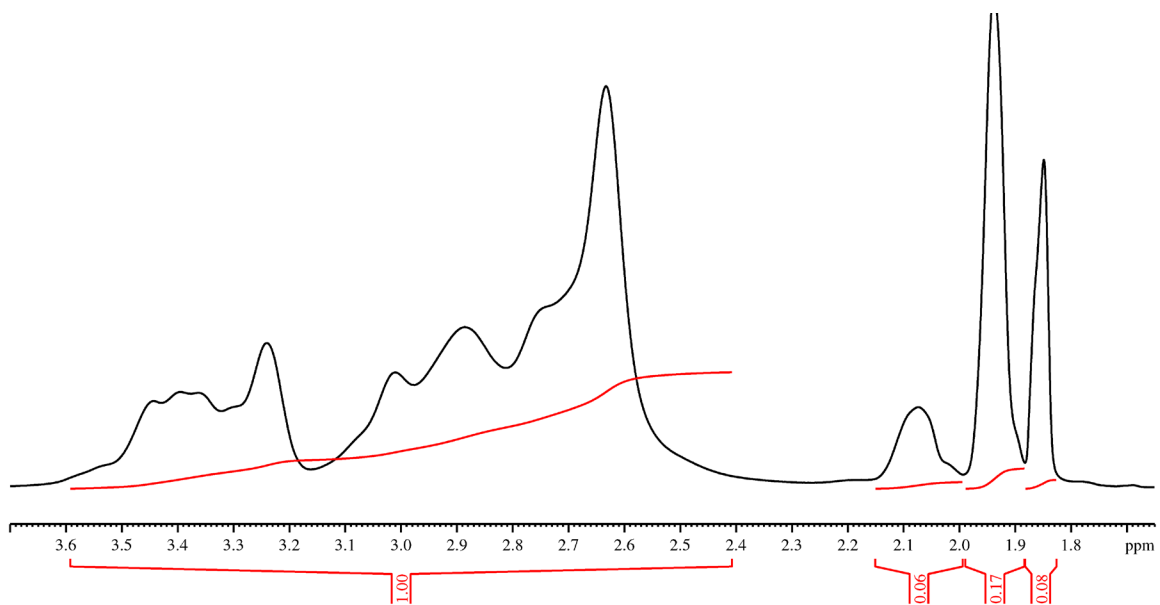
Figure 3.18. ^{1}H-NMR of acPEI 40
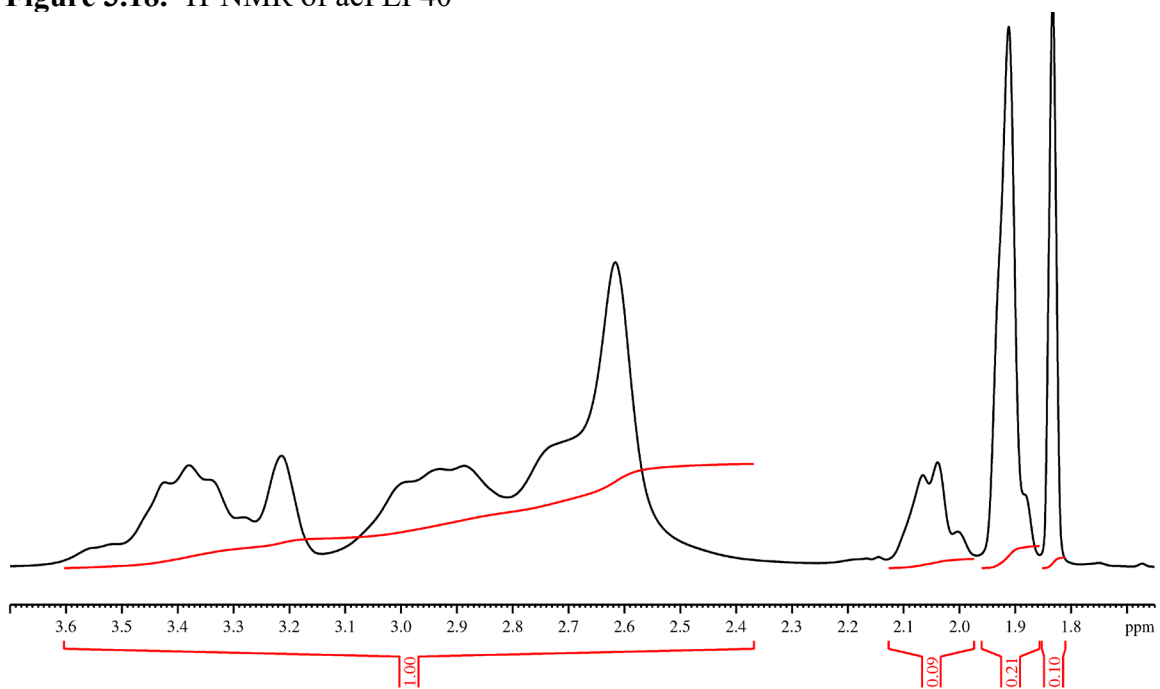
Figure 3.19. ^{1}H-NMR of acPEI 50
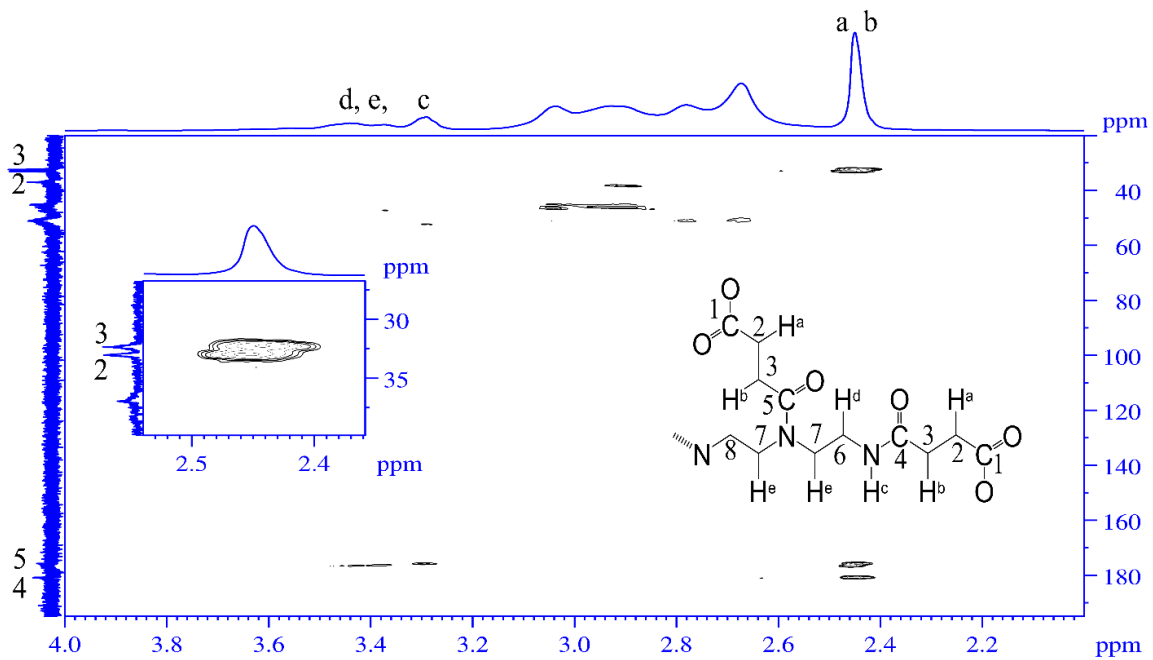
Figure 3.20. HMBC-NMR (2D) of zPEI 20
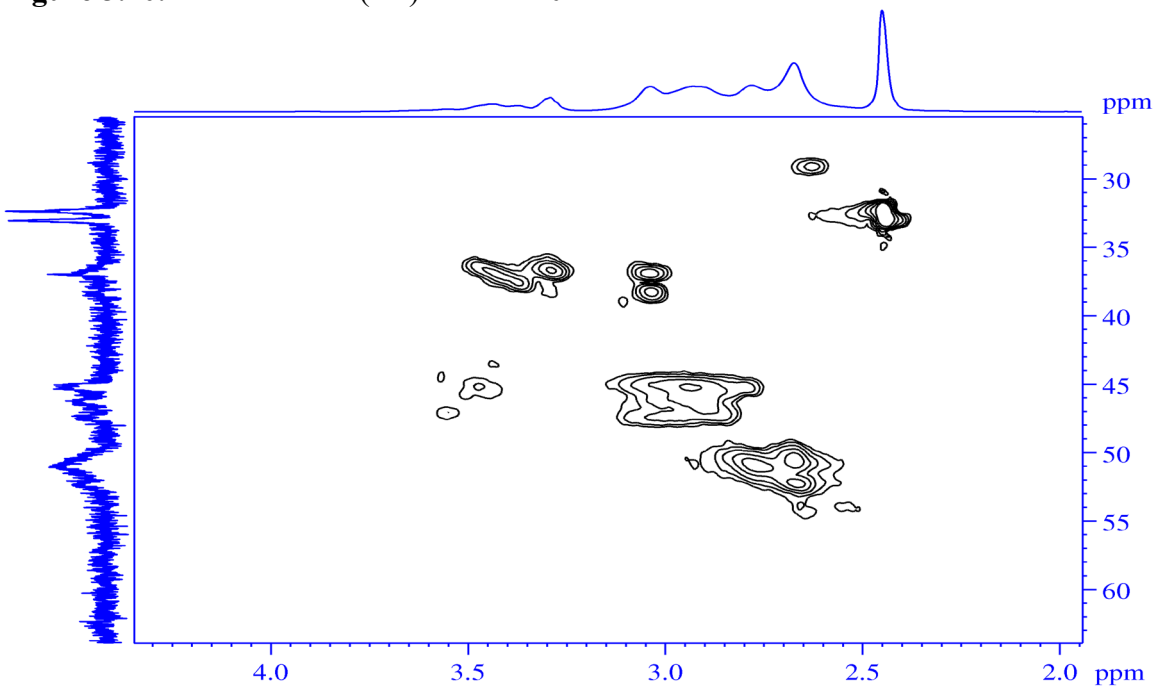
Figure 3.21. HSQC-NMR of zPEI 20
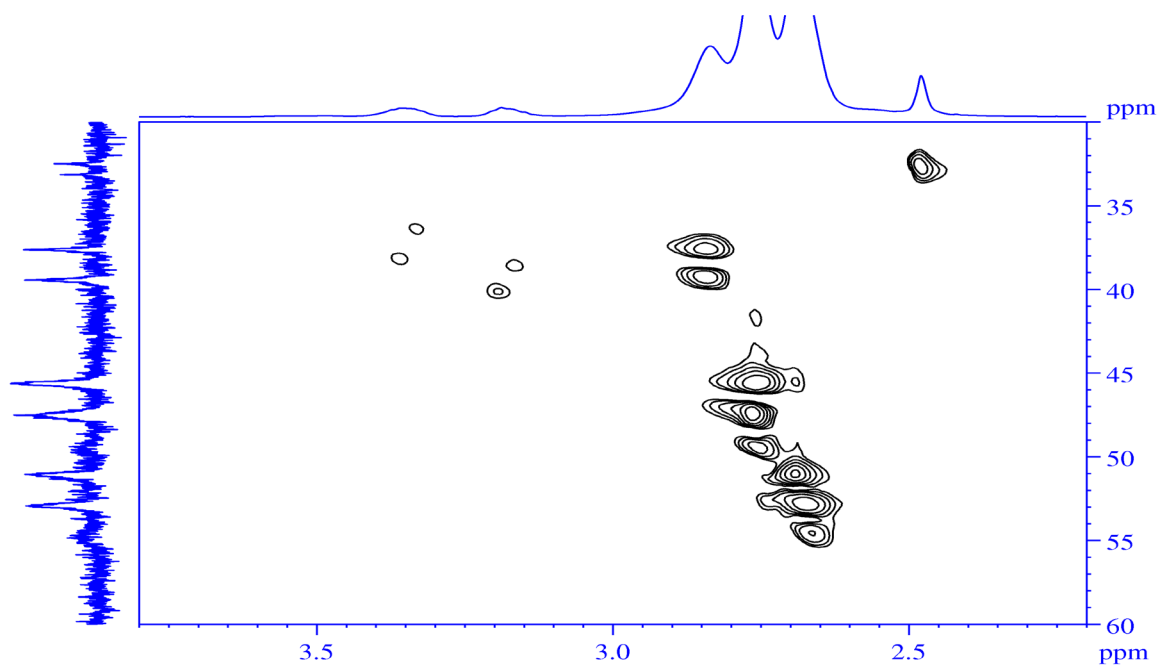
Figure 3.22. HSQC-NMR of zPEI 5
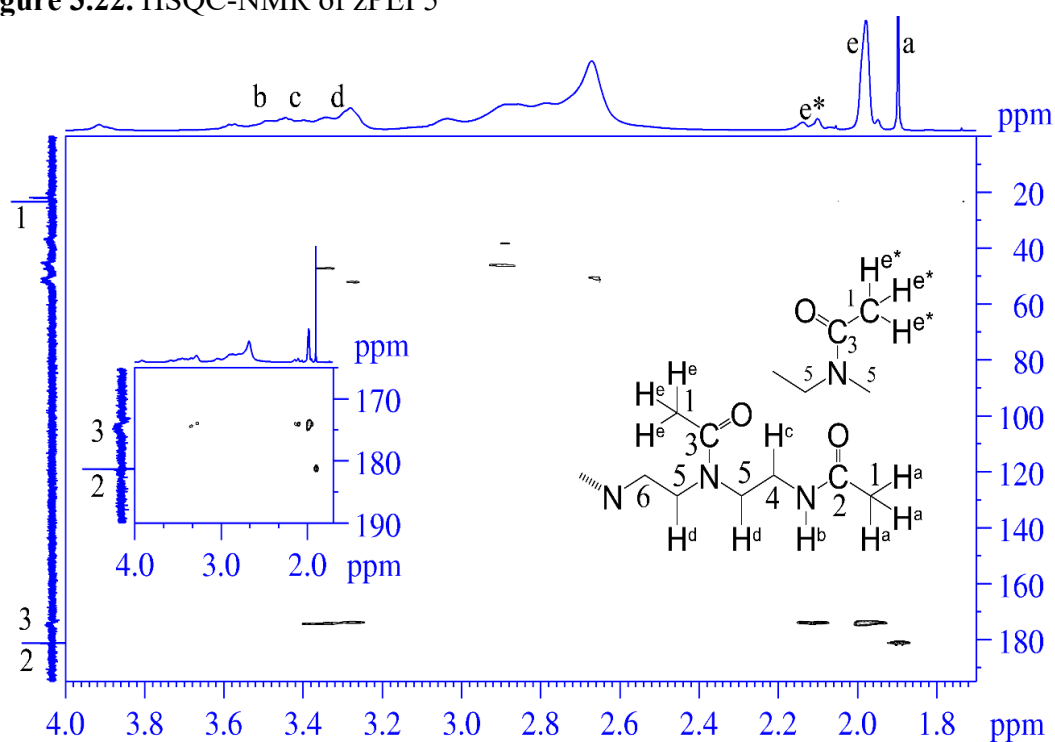
Figure 3.23. HMBC-NMR (2D) of acPEI 40

Figure 3.24. HSQC-NMR (2D) of acPEI 40

Figure 3.25. HMBC-NMR (2D) of acPEI 40 at pH 2.0
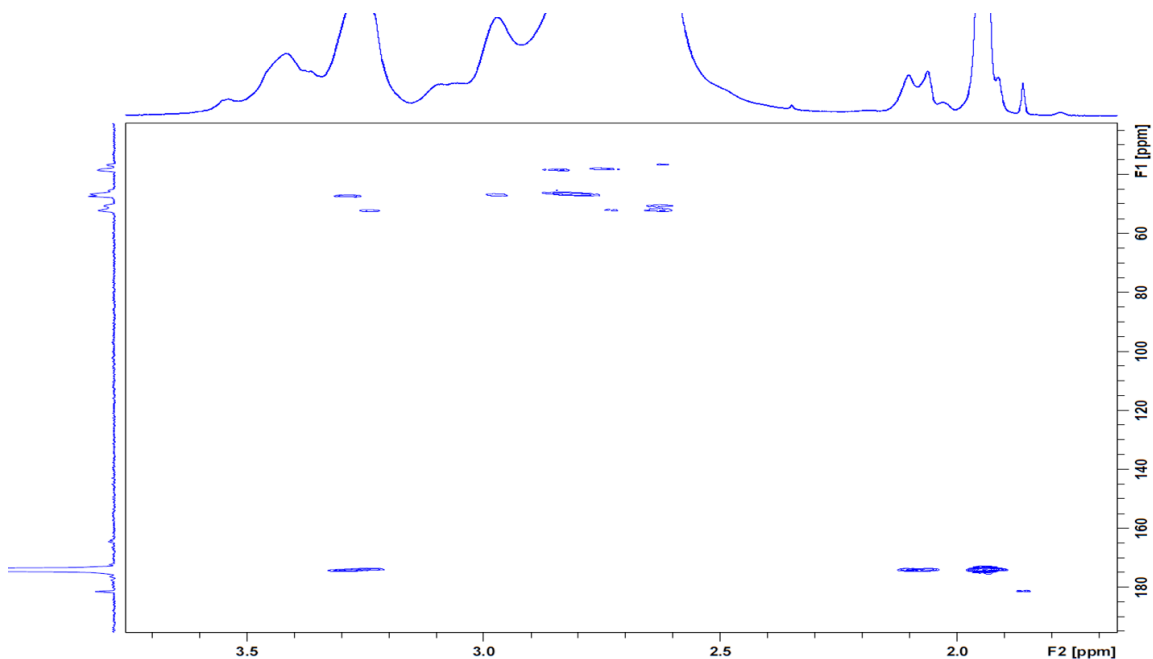
Figure 3.26. HMBC-NMR (2D) of acPEI 20 as reference, showing the conjugation reaction preference for secondary amines of branched PEI followed by primary amine conjugation. With higher modification, the integral area of the peak at F2 1.86 ppm & F1 181.4 ppm coordinates get higher as shown in Figure 3.23.

3.6.3   Circular Dichroism (CD)

Samples of calf thymus DNA polyplexes with acPEI 40 and zPEI 30 were prepared at wt/wt ratio 3.0 and 6.0, respectively, and placed in a quartz cuvette with an optical path of 1 cm. The CD spectra of these polyplexes were compared to CD spectra of uncondensed DNA. Samples were analyzed with a Jasco J-815 spectropolarimeter. CD spectra were collected from 220 to 300 nm at a scanning speed of 100 nm/min. A total of 3 scans were collected and averaged for each sample. Apart from hypsochromic shift with acPEI, both polymers showed similar spectra typical to that of ctDNA, most frequently observed for B-conformation, as a proof of no DNA transition occurs.
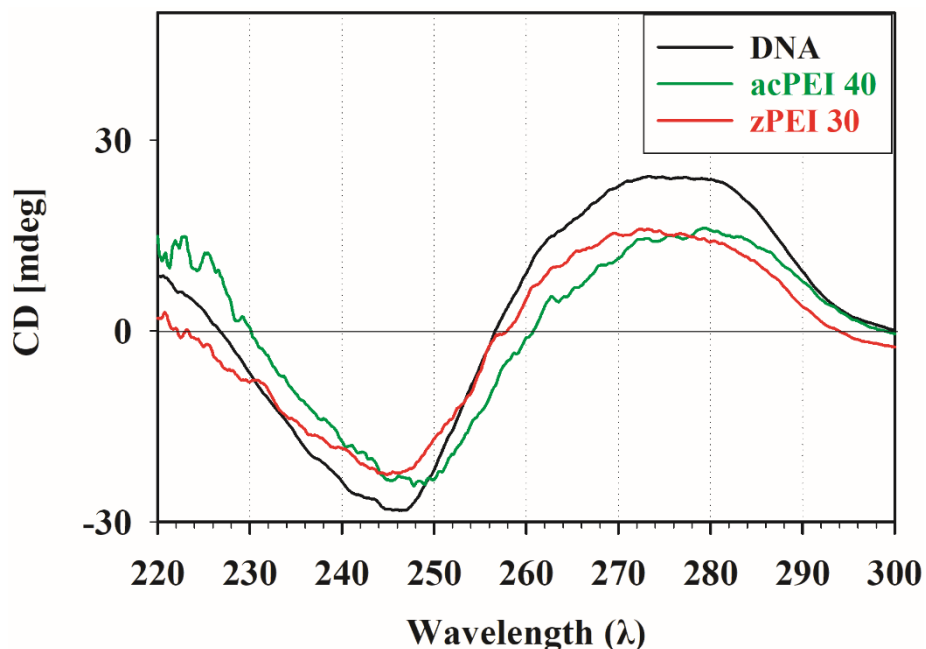
Figure 3.27. Circular Dichroism spectra of calf thymus DNA. The spectra obtained with JASCO (J-815) CD spectrometer (Japan) and analyzed with JASCO spectra manager software. The spectrum obtained at room temperature for 0.1X PBS buffer solution of ctDNA complexed with acPEI 40 and zPEI 30 at a polymer/DNA weight ratio obtained from EtBr exclusion assay.

3.6.4   Electrophoretic mobility shift assay at DNA condensation weight ratio

Agarose gel electrophoresis was used to assess each modified polymers' relative polyplex stability at specific polymers' condensation weight ratio determined by EtBr exclusion assay (**Figure 3.3b**). Polymers were condensed at polymer/DNA weight ratio 0.5, 1, 1, 1, 3, 6 by the PEI, zPEI 2, zPEI 5, zPEI 10, zPEI 20, and zPEI 30 while 1, 1.5, 3.0, and 3.0 weight ratio for acPEI 10, 20, 40 and 50 respectively. At this threshold condensation weight ratio, polymers can hardly withstand competitive counterion. Because of a negative COO⁻ moiety added to bPEI, polyplexes formed with zPEI maintain weak electrostatic interaction between polymer and DNA. Hence, the zPEI polymers release DNA from condensed polyplex by a DS/DNA weight ratio of 0.5-1.0.

114

In contrast, acPEIs show relatively strong polyplex packaging. Thus, DNA release occurs at DS/DNA weight ratio between 1.0-2.0.
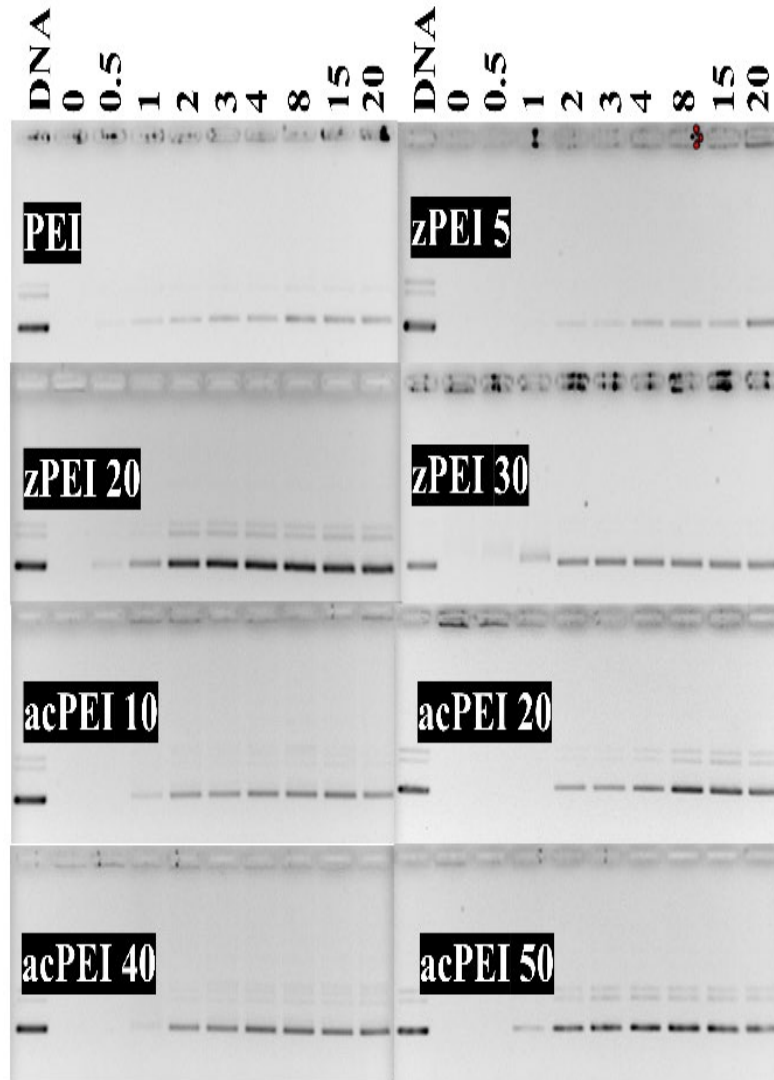
Figure 3.28. Dextran sulfate (DS) displacement assay at polymer/DNA condensation weight ratio obtained from EtBr exclusion assay.

Table 3.3. D_{Bragg} changes over time and polymer modification

Polymer	D_{Bragg} (1hr) Å	D_{Bragg} (30 day) Å	Delta D (D 1hr - D 30) Å	% Change [delta D / D Bragg (1hr)]
bPEI	24.71	24.28	0.43	1.74
zPEI 2	25.1	24.75	0.35	1.4
zPEI 5	26.7	26.06	0.64	2.4
zPEI 10	26.21	25.54	0.67	2.56
zPEI 20	25.636	25.25	0.39	1.52
zPEI 30	25.19	25.06	0.13	0.52
acPEI 10	26.525	26.05	0.48	1.8
acPEI 20	27.01	26.5	0.51	1.9
acPEI 40	27.68	27.4	0.28	1.01
acPEI 50	28.83	28.23	0.6	2.08

3.6.5   pH effects on the observed SAXS Bragg peaks and calculated D_{Bragg} values

Polyplexes of bPEI, acPEI 10 and zPEI 10 were formed at different pHs and measured by SAXS to evaluate changes in the internal structure of the resulting polyplexes. Samples were either formed in 10 mM Tris (pH 7.5) or 10 mM acetate buffer (pH 4) or were preformed for 1 hour in Tris then transferred to the acetate buffer for equilibration (pH 7.5-4). All complexes resulted in a single diffraction peak being observed and the corresponding Q and D_{Bragg} values are tabulated in **Table 3.4.**

Table 3.4. Role of pH in interhelical spacings within condensed DNA. Here, sample ID 1 and 2 represents as mean±0.2 (n =2) while sample ID 3 (n =1)

Sample ID	pH	**After 1-hour equilibration		**After 24-hour equilibration	
		$Q(nm^{-1})$	D_{Bragg} (Å)	$Q(nm^{-1})$	D_{Bragg} (Å)
PEI-1	7.5	2.53	24.8	2.57	24.5
PEI-2	7.5-4.0	2.53	24.8	2.62	24.0
PEI-3	4.0	2.69	23.4	2.71	23.2
zPEI 10-1	7.5	2.39	26.3	2.44	25.7
zPEI 10-2	7.5-4.0	2.44	25.7	2.61	24.1
zPEI 10-3	4.0	2.7	23.3	2.71	23.2
acPEI 10-1	7.5	2.36	26.5	2.38	26.3
acPEI 10-2	7.5-4.0	2.4	26.1	2.48	25.3
acPEI 10-3	4.0	2.61	24.0	2.65	23.7

*pH 7.4: Pellets were transferred to the same fresh buffer, pH 7.4-4.0: Pellets were transferred from pH 7.4 to 4.0 and pH 4.0: When polymer solution was prepared with 10 mM acetate buffer as a solvent and then condensed pellets formed with subsequent transfer of these pellet to fresh pH 4.0 buffer.

**Time for equilibration after pellets are transferred to respective buffer solutions to attain stable packaging.

CHAPTER 4. ROLE OF VARYING PROTEIN CONCENTRATION AND PRE-TREATED POLYPLEXES ON SUCCINYLATED POLYETHYLENIMINE MEDIATED GENE TRANSFECTION

Preface: This work was performed in collaboration with the group of Dr. Daniel Pack of the Departments of Chemical & Materials Engineering and Pharmaceutical Sciences at the University of Kentucky. All polymer synthesis, characterization, and gene transfections were completed by the author. The fluorescence imaging experiments were performed by Dr. Logan Warriner in the laboratory of Dr. Daniel Pack.

4.1   Introduction

Polymer-based therapeutics holds the promise to treat almost any disease through the emerging fields of gene silencing, protein expression, drug and RNA delivery, or genetic modification. Over the past few decades, intense efforts have been made to optimize and understand the mechanism of nanoparticle (NP)-based formulations for effective payload delivery. Complexes involving polymers for therapeutics, for example polycation-DNA complexes (or polyplexes) used for nonviral gene delivery, typically result in the formation of nanoparticles. In vivo, these nanoparticles come into contact with high concentrations of serum proteins that can adsorb onto the nanoparticle surface to form a protein layer called a protein corona.[168] This protein corona often determines how the nanoparticle then interacts with the surrounding biological materials.[168] The protein-nanoparticle interactions, in turn, determine the particles' size, shape, aggregation state, pharmacokinetics, and therapeutic efficacy in vivo, that can vary with patient physiology to form the so-called personalized protein corona.[168-170] Proteins are also not the only binding agent found on the surface of the corona with cholesterol and triglycerides known to also potentially adsorb on the surface to form a corona.[169, 171-172] For example, apolipoproteins, cholesterol, and triglycerides were found to show a high

affinity to bind effectively to the surface of the carboxylated polystyrene nanoparticles.[171] In a study with gold nanoparticles, major serum proteins such as immunoglobulin G, fibrinogen, apolipoprotein A and albumin exhibited aggregation at low concentration but show colloidal stability at higher concentrations due to complete corona formation.[173] The difference in corona type significantly impacts nanoparticle-cell membrane interaction, endosomal uptake, intracellular trafficking, and subsequent release pathways.[174-176] Literature reports that specific proteins in the original corona were retained on the surface of polymeric nanoparticles until they accumulated in lysosomes and degraded.[177] One significant finding of this study was that the serum proteins could exhibit different intracellular processing when carried inside cells as part of the nanoparticle corona, as compared to unbound proteins in the extracellular medium.[177] Another study suggests that the protein coronas formed on engineered particles either increased or mitigated the secretion of a specific cytokine, depending on the environment where the protein corona was formed.[178] According to the study, protein coronas could be engineered as drug carriers for elongated circulation, enhanced biocompatibility, and lower toxicity by triggering a specific immune response.[178]

Among the various cationic polymers used for therapeutics, polyethylenimine (PEI) and modified PEIs are still some of the most widely studied systems especially for the delivery of DNA, RNA and siRNAs.[179-180] PEIs therefore serve as a benchmark for polymeric therapeutics and can serve as an excellent model for investigating delivery mechanisms. For example, in vitro processes of PEI-based polyplexes have been systematically studied to understand cellular internalization, intracellular trafficking, and release.[58, 181] However, the overall goal in nonviral gene delivery is to develop nonviral

transfecting agents suitable for in vivo applications where PEI polyplex nanoparticles encounter and interact with proteins and other biological macromolecules. Polyplexes in vivo, like other nanoparticles, also encounter nonspecific protein binding often forming large aggregates as well as coronas.[182-183] The formation of a protein corona formed with PEI/DNA polyplexes reduces its interaction with cell membrane by several orders of magnitude.[183] It has been proposed that nonspecific protein interactions dissociate the polyplex prematurely resulting in the unpackaging of the particle cargo and negatively impacting the cellular internalization process. In contrast, there are also reports of protein coronas positively impacting nanoparticle efficacy. For example, mechanistic studies show that pre-formed corona on PEI/DNA polyplex with bovine serum albumin activates the caveolae-mediated endocytosis pathway resulting in enhanced gene transfection or silencing.[184-185]

In chapter 2, we have discussed the gene transfection efficacy with minimally succinylated PEI even at only 2% modification. Luciferase expression with zPEI 2 was found to be 260- to 480-fold higher than unmodified PEI in HEK 293 and HeLa cells, respectively, when transfected in the presence of serum proteins.[124] Especially for zPEI 2, we saw no significant change in the protein-DNA interactions nor cytotoxicity, yet still obtained a large enhancement in transgene expression compared to unmodified bPEI. We hypothesized that one possibility for this enhancement could be that zPEI modifies the ability of the polyplex to form coronas either by forming coronas faster or altering the protein make-up within the corona. Recently, another study showed that bPEI polyplexes precoated with BSA resulted in enhanced transfection.[109] Using other nanoparticles, prior

studies showed that a strategic choice of materials can greatly influence the types of protein adsorbed on nanoparticles and improve gene delivery efficiency.[186] [187]

Delivery of polyplexes in vivo results in nanoparticles being exposed to high concentrations of serum proteins in the blood. In this work, we investigated the effect of varying bovine serum albumin (BSA) concentrations in gene transfection with succinylated PEI (zPEI)/DNA polyplexes and compared the efficacy with unmodified PEI. Albumin is a major component (50-60%) of the blood plasma proteins and therefore a good model for intravenous delivery of polyplexes. Transgene expression was investigated for zPEI/DNA at a variety of polymer:DNA weight ratios. Finally, to test if these conditions may lead to the formation of a protein corona on the nanoparticles, we also measured the transgene expression of polyplexes pre-treated to form a protein corona on un-treated polyplexes.

4.2 Materials and Methods

4.2.1 Materials

Succinylated PEIs (2-11.5%) were used for all transfection experiments from the previously synthesized series described in detail in chapter 2.[124] HEK293 cell line was purchased from the American Type Culture Collection and cryopreserved in-house for further need. Cell lines were cultured at 37 °C, 5% CO_2, and in the presence of 10% fetal bovine serum (FBS) per ATCC recommendations. The pGL3 luciferase expression vector was purchased from Elim BioPharm (Hayward, CA).

4.2.2 Polyplex transfection

HEK 293 cell line was cultured in EMEM supplemented with 10% FBS according to ATCC recommendations. Cell lines were seeded in 24-well plates at 7.5 x 10^4 cells/well 24 h before transfection. Polymer/DNA complexes were formed by diluting 20 μL of 0.1 μg/μL DNA solution with 80 μL of PBS (1X) in a 1.5 mL microcentrifuge tube. Polymer solutions (100 μL) at various concentrations were added dropwise to the DNA solution under constant agitation to achieve the desired polymer: DNA weight ratio. Particles were allowed to incubate at room temperature for 20 min. Immediately before transfection, 200 μL polyplex solution was deposited into 1.8 mL of transfection medium depending on the particular need of the experiment. For the first part of the project, varying bovine serum albumin (BSA) concentration (0, 1, 3, 6, and 10 mg/mL) was used as a transfection medium. The regular growth medium was aspirated from cells and replaced with 500 μL of polyplex/growth medium solution (0.5 μg DNA/well). After four hours, the transfection medium was replaced with a serum-supplemented growth

medium. Transfection efficiency was quantified via luciferase expression 24 h post-transfection. A Promega luciferase assay kit (Madison, WI) was used to measure protein activity in relative light units (RLU) using a Synergy 2 plate reader (BioTek, Winooski, VT). The results were normalized to total cell protein using a bicinchoninic acid (BCA) assay from G-Biosciences (St. Louis, MO).

The second part of the project where pre-treated BSA was used for gene delivery followed one of the two possible formulations. After 200 μL polymer-DNA mixing & incubation, an equi-volume i) 1 mg/mL BSA or ii) 5% fetal bovine serum (FBS) was further mixed with incubating for another 20 minutes to form a protein coat. Immediately before transfection, 400 μL protein- treated polyplex solution was deposited into 1.6 mL of transfection medium (serum-free, 10% FBS, or 100% FBS) depending on the particular need of the experiment. After four hours, the transfection medium was replaced with a serum-supplemented growth medium followed by luciferase expression quantified, as discussed above.

4.2.3 Particle size measurement with DLS

Polymer/DNA complexes for DLS study were formed in 0.1x phosphate-buffered saline (PBS) at the optimum transfection weight ratio for each modified and unmodified polymer. After the 30 min incubation, the polyplexes were diluted to 1 μg of DNA/mL using 0.1x PBS. The solution was then immediately read using a 90Plus/BI-MAS automatic particle sizer (Brookhaven Instruments, Holtsville, NY). Each measurement was taken in triplicate (n =3).

4.2.4 Imaging of protein and polyplex interactions via fluorescently labeled BSA and pDNA

Plasmid DNA was labeled with Cy5 (red) according to the protocol specified by the manufacturer (Mirus Bio, Madison, WI). BSA conjugated with FITC (green) was obtained from Invitrogen (Waltham, MA). HEK293 cells were seeded in 24-well glass-bottom plates at 7.5 x 10^4 cells/well 24 h prior to transfection. Polymer/DNA complexes were formed by diluting 20 μL of 0.1 μg/μL Cy5-labeled DNA solution with 80 μL of PBS in a 1.5 mL microcentrifuge tube. The equi-volume polymer solution was added dropwise to the DNA solution under constant agitation to achieve the desired carrier/DNA weight ratio. Particles were allowed to incubate at room temperature for 30 min. Immediately before transfection, 200 μL polyplex solution was added to 1.8 mL of EMEM containing 3 mg/mL of BSA, approximately the equivalent protein concentration of 10% FBS. To prevent signal oversaturation, only 25% of the BSA solution was the FITC conjugated form. Immediately after, the normal growth medium was aspirated from cells and replaced with 0.5 mL of polyplex/BSA-FITC containing medium (0.5 μg DNA/well). Transfection was allowed to proceed for 30 min in order to capture the early trafficking stages of the particles. From here, the transfection media was aspirated, and the cells were gently washed twice with PBS. The cell membrane was then stained using BioTracker 400 Cytoplasmic Membrane Dye (blue) according to the suggested protocol from the manufacturer (Sigma Aldrich, St. Louis, MO). After, the cells were washed three more times to remove excess dye and then immediately imaged using a Cytation 7 multimode plate reader (BioTek, Winooski, VT).

4.2.5   Statistical testing

Results were presented as average ± SD and the number of replicates ($n \geq 3$). Statistical significances were analyzed using one way ANOVA. All pairwise multiple comparison procedures were conducted with Holm-Sidak method where an overall significance level = 0.05. Significance levels were indicated with the following symbols: [#,] * $p \leq 0.05$; ** $p \leq 0.01$; and *** $p \leq 0.001$.

4.3   Results and Discussion

4.3.1   Gene transfection at varying BSA concentration

As mentioned before, the first part of the project was to investigate the effect of varying protein concentrations in gene transfection mediated by minimally modified zPEIs and compare the efficacy with unmodified PEI (**Figure 4.1**).   Previously, we transfected in 10% fetal bovine serum (FBS) solution (~3.5 mg/mL total protein), but protein concentrations in blood are significantly higher (approximately 60-80 mg/mL) with over half of the proteins present being albumin. FBS is the supernatant after blood from a bovine fetus coagulates and therefore is a complex mixture of proteins that can vary in content from batch to batch. For simplicity, we performed these experiments in pure bovine serum albumin (BSA) solutions. Luciferase activity in the cell lysate is reported as RLU normalized by the mass of total protein in the lysate. From prior results, bPEI and zPEI 2 performed best for transgene expression at a polymer/DNA wt ratio of 1:1.[159] Therefore, we examined the transgene expression of bPEI and zPEI 2 at this weight ratio as a function of increasing BSA concentration (**Figure 4.1 a/b**). BSA at the lowest concentration (1 mg/mL or ~5% FBS equivalent) moderately improves the transfection efficiency of both uPEI and zPEIs. Two possible explanations for this could be (1) that the presence of a small amount of serum protein leads to higher transfections due to serum protein-cell interactions when compared to serum-free (BSA 0 mg/mL) conditions or (2) because polyplexes are made with an excess of cation, and free PEI is cytotoxic to cells, adding a small amount of BSA may preferentially complex this free bPEI enhancing cell viability. However, when BSA concentration in the EMEM was higher than 3 mg/mL, we see a drop in luciferase expression for bPEI (**Figure 4.1a**)

126

while zPEI 2-mediated luciferase expression remains high up to 6 mg/mL but drops some by 10 mg/mL BSA (**Figure 4.1b**). We next examined a series of minimally succinylated PEIs (zPEIs 2-11.5%) for their resulting luciferase expression at different BSA concentrations at the same polymer:DNA (wt:wt) loading ratio of 1. The results are plotted in **Figure 4.1c**. Similar to results discussed in Chapter 2, the higher degree of succinylation (>9%) transfected poorly. Similar to transfection in FBS, bPEI-DNA luciferase expression decreases at BSA concentrations >1 mg/mL. zPEI 2 performs better at higher BSA concentrations particularly at 3 and 6 mg/mL. The low protein expression for higher zPEI modifications is presumably due to the poor complexation of these polyplexes at wt:wt ratio 1.
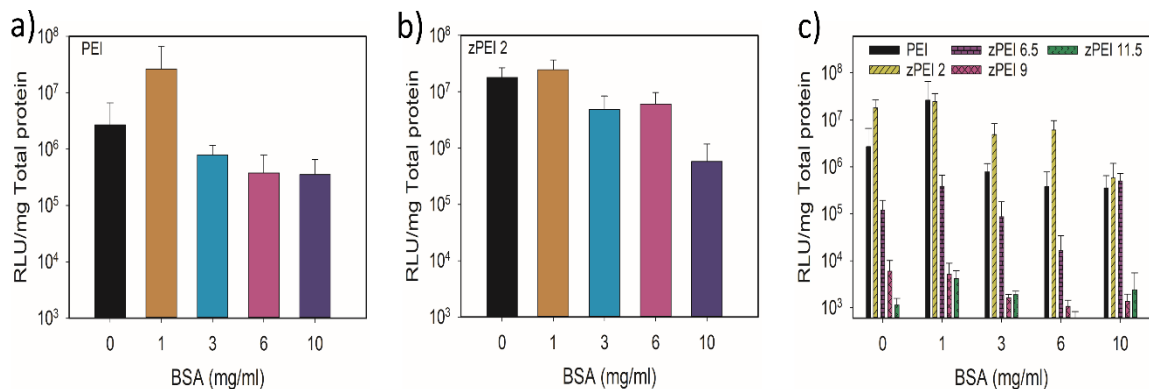
Figure 4.1. Comparative gene transfection efficacy mediated by **a)** bPEI, **b)** zPEI 2 and **c)** zPEI 0-11.5% in the presence of varying BSA concentrations (0, 1, 3, 6, 10 mg/mL). The efficacy was measured as relative light unit RLU/ total mg of protein. Polyplex was prepared at polymer/DNA weight ratio 1. All the experiments were triplicated (n=1).

We next compared the in vitro transfection efficiency of our bPEI, zPEI 2, and zPEI 6.5 polyplexes in HEK293 cells at different polymer:DNA (wt:wt) loading ratios in the presence of varying amounts of BSA protein (**Figure 4.2**). All experiments were done in triplicates with error bars representing the standard deviation. Each polymer had

mediated highest transgene expression at 1 mg/mL BSA concentration (**Figure 4.2 a, b, c**) similar to results in Figure 4.1. The maximum gene expression for bPEI/DNA occurs at 1 mg/mL but only for wt:wt 1 potentially supporting the idea that low concentrations of BSA initially complex the uncomplexed PEI in solution. At higher wt:wt ratios, where BSA is likely to interact with the polyplex after binding all the free bPEIs, the luciferase drops significantly. For bPEI/DNA, at higher BSA concentrations, all weight ratios show lower luciferase expression. In contrast, zPEI 2 and 6.5 mediate higher transgene expression than bPEI at all weight ratios. zPEI 6.5 is lowest at wt:wt 1 but increases with higher polymer loading and is relatively constant for all wt:wt ratios > 1. Because succinylation adds a negative charge on PEI amines, more zPEI 6.5 polymers are required to fully condense the DNA so wt:wt 1 is likely an incomplete condensation of the DNA in the polyplexes. At higher wt:wt, a fully condensed zPEI 6.5 polyplex is formed and all show enhanced transfection. zPEI 2, on the other hand, only modifies approximately 12 of the 582 amines in a 25kDa PEI so does not significantly change the polymer interactions with DNA compared to unmodified PEI. As shown in Chapter 2, both form fully condensed polyplexes by wt:wt 1. Overall, the data shows zPEI 2 and 6.5 have better transfection efficacy over higher level of BSA concentrations when compared to the unmodified bPEI. **Figure 4.2d** shows the statistical significance of the transgene expression obtained with bPEI at varying low BSA concentrations (0-3 mg/mL) to further explore the maximum observed at 1 mg/mL in Figure 4.2a. Although we see unmodified PEI apparently aids in transgene expression in Figure 4.2d at 0.5 and 1 mg/mL BSA in EMEM medium, these values are statistically not significant compared to the control (0 mg/mL protein) with an overall significance level 0.05. Differences in mean transgene
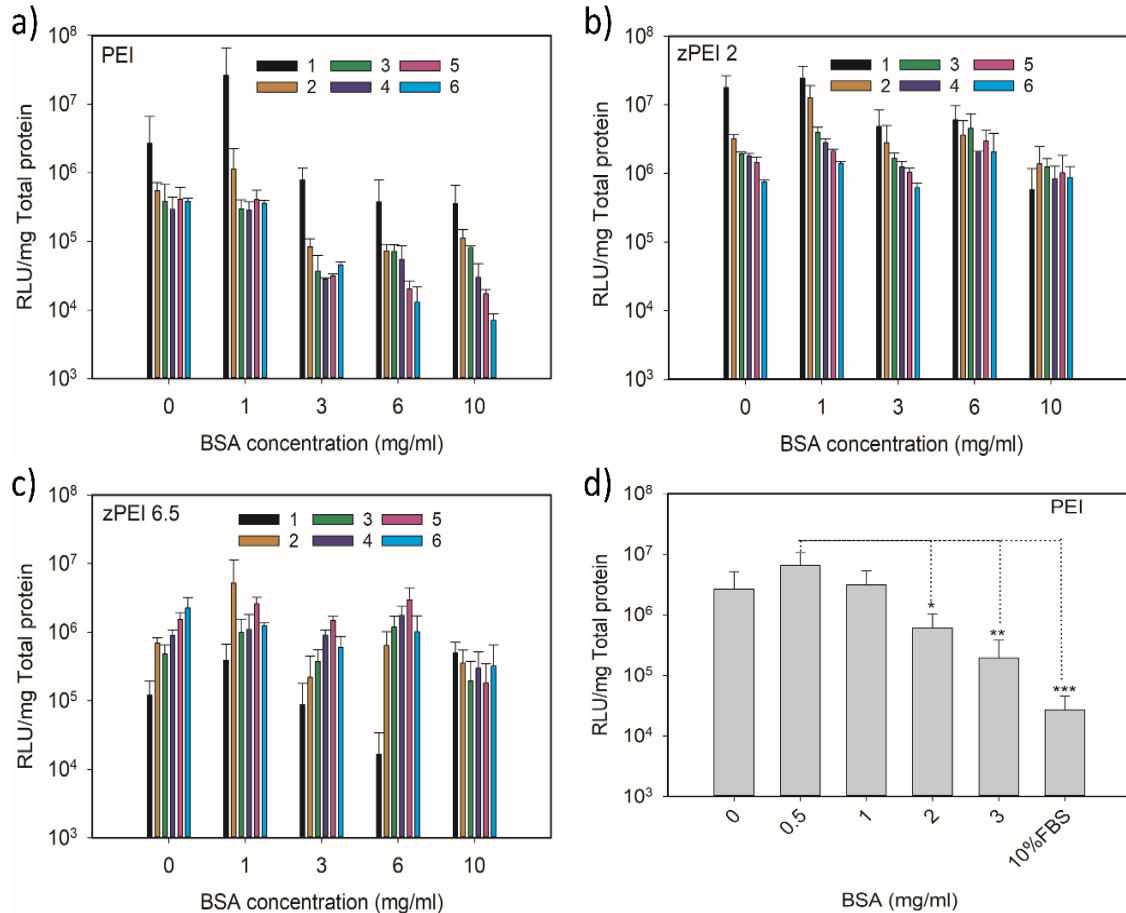
Figure 4.2. Gene transfection ability at varying BSA concentration and polymer/DNA weight ratio with a) bPEI, b) zPEI 2, and c) zPEI 6.5, respectively. The numbers in the legends are the polymer/DNA weight ratio (representative color, from left to right). Figure 2d shows the relationship between luciferase expression and BSA concentration mediated by bPEI. All the experiments were triplicated (n≥3).

expression in bPEI/DNA are statistically significant when comparing transfections in 0.5 mg/mL BSA to transfections at 2 mg/mL (* $p < 0.05$), 3 mg/mL (** $p < 0.01$) and 10% FBS (*** $p < 0.001$). So, we conclude the low BSA concentration (<1 mg/mL) are statistically similar in transfection efficacy compared to the control (0 mg/mL), and only at higher BSA concentrations do we observe the proteins having a negative impact on bPEI-mediated transgene expression. This data contradicts previously published findings

that increasing protein concentration does not have a harmful effect on gene transfection.[184-185]

4.3.2 Colocalization Studies by Fluorescence Microscopy

We used fluorescence microscopy to visualize the internalization of bPEI/DNA and zPEI 2/DNA polyplexes into HEK293 cells. For these experiments, polyplexes containing Cy5-labeled DNA (red emission) were complexed with polymer to a polymer:DNA wt:wt ratio of 1. Immediately before transfection, polyplexes were added to a 3 mg/mL BSA solution. This concentration of BSA was chosen as it corresponds to the approximate BSA concentration in 10% FBS which was used previously in chapter 2 and chapter 3 for all transfections in serum. FITC-labelled BSA (green emission) was added at a 1:3 weight ratio with unlabeled BSA to enable colocalization studies to be performed. This ratio of labelled BSA was chosen to avoid oversaturation in our microscopy images. Our goal in these experiments was to examine the early trafficking stages in HEK293 by these two systems. The results are shown in **Figure 4.3**. In general, we found that zPEI 2/DNA forms smaller homogeneous particles, as indicated by the yellowish green particles near the cell membranes (**Figure 4.3b**). The yellow color is a result of colocalization of the green-labeled BSA and red-labeled DNA most likely due to BSA complexed with the zPEI 2/DNA polyplexes.[188-189] This suggests the formation of a partial or complete BSA protein coating. Unmodified bPEI/DNA, in contrast, was observed to form large aggregates in the same 3 mg/mL BSA transfection medium (**Figure 4.3a**). One possible explanation for this finding is that zPEI 2/DNA is more readily forming a stable, protective BSA protein corona as compared to bPEI. Another

possible explanation is that the uncomplexed bPEI and zPEI 2 in the polyplex solution interact differently with BSA enhancing the interaction and uptake of zPEI polyplexes into cells. More studies are required to differentiate between these cellular internalization and trafficking mechanisms.
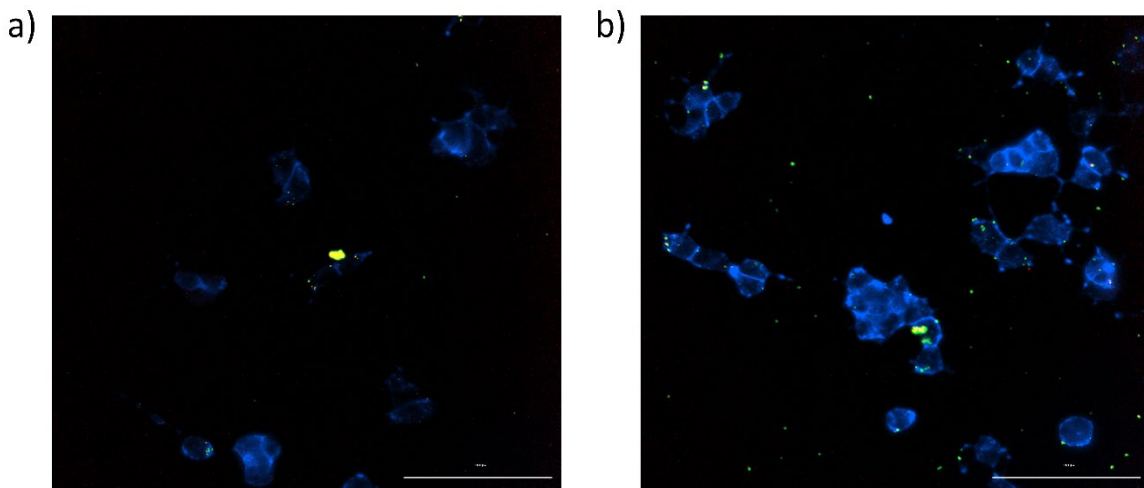
Figure 4.3. Imaging of protein and polyplex interactions via fluorescently labeled BSA and pDNA. The figure shows the confocal fluorescence microscopy images of a) bPEI and b) zPEI 2 captured 30 minutes after initial transfection on HEK 293 cell line. The images are a composite of three different fluorescent channels associated with Cytation 7: Cy5 (red), GFP (green), DAPI (blue). Standard transfection protocol was used with 10% FBS as a medium. Scale bar = 300 μm.

4.3.3 Particle size of protein pre-treated polyplexes

DLS was used to measure the effective hydrodynamic diameter of the complexes formed at the polymer/DNA weight ratio of 3, which resulted in full DNA condensation for all zPEI formulations (0-11.5% modification). Results are given in **Table 4.1**. Polyplexes were formed in phosphate buffered saline (0.1x PBS, pH 7.4) and equilibrated for 30 mins. Nanoparticle diameters ranged from 70 to 186 nm for these polyplexes with the smallest particles being unmodified PEI/DNA. With increasing degrees of

succinylation, zPEI/DNA polyplex nanoparticles were observed to increase in size. In another set of experiments, we formed polyplexes in the same manner in PBS and then added an equal volume of 1 mg/mL BSA and incubated for 20 minutes. In all cases, BSA complexed with the polyplexes to form larger aggregates (~400-860 nm in diameter). Interestingly, the trend in the size of BSA-polyplex complexes is reversed that was observed for the polyplexes alone. The largest complex sizes were observed for bPEI-DNA with BSA. With increasing succinylation, the BSA-zPEI-DNA complexes formed with smaller diameters. While the mechanism for this observation is still not known, we hypothesize that the presence of the succinyl groups on the PEI alter the interactions

Table 4.1. Particle size comparing bPEI and zPEI polyplexes formed in PBS buffer or in the presence of 1 mg/mL BSA

Name of polymer	Particle diameter in PBS (nm)	Particle diameter in 1 mg/mL BSA* (nm)
bPEI	70±2.1	857.1±14.2
zPEI 2	73.6±3.7	787.2±11.5
zPEI 6.5	105.5±0.8	491.2±8.6
zPEI 9	132.8±3.6	466.8±7.3
zPEI 11.5	186.4±2	403±6.4

*After polyplex formation, an equi-volume 1 mg/mL BSA was mixed and allowed to incubate for 20 minutes before diluting to 1 ml with 0.1x PBS.

of the mixed charge zPEI polymers with BSA proteins which is net negatively charged but also has both positive and negatively charged moieties. This may result in a faster formation of neutral but stable BSA protein coating on the nanoparticle or could create

BSA-zPEI 'ghost particles' that help mitigate the aggregation of the polyplexes more than BSA-bPEI complexes.

4.3.4   Gene transfection with pre-treated polyplex

Recent studies have suggested that pre-coating bPEI/DNA polyplexes can result in enhanced gene transfection.[109, 190] As it is unclear currently if our transfections in BSA (**Figure 4.1/4.2**) result in complete protein corona formation or not, we conducted experiments to test the effect of pre-treating polyplexes of bPEI and zPEI 2 with BSA protein. For these experiments, polyplexes were formed in the same manner as before but then treated with 1 mg/mL BSA or 5% FBS serum and incubated for an additional 20 minutes. Zhu et al. showed that this concentration of protein and incubation time was sufficient to form a corona around bPEI/DNA polyplexes.[109, 190] Immediately before transfection into HEK293 cells, these pre-treated polyplexes were mixed with the transfection medium specific to the experiment and added to cells. When pre-treated with 1 mg/mL BSA, this results in a polymer/DNA/BSA weight ratio of 1/1/100 in the incubated solution. In **Figure 4.4,** we show the results of experiments comparing pre-treated polyplexes directly to non-treated polyplexes. Specifically, the luciferase expression was measured for non-treated and BSA treated polyplexes in two different transfection conditions with the medium being either serum free medium or a 'in serum' medium consisting of 10% FBS solution. It is well known that unmodified bPEI/DNA is an excellent transfecting agent in serum-free conditions, but the efficacy goes down significantly in the presence of serum proteins. This is exactly what we see in **Figure 4.4a** when comparing bPEI/DNA in serum free (black) vs in serum (red) where the

luciferase expression drops by more than 100-fold. Similar to the results of Zhu et al,[109] we also see that pre-treating the bPEI/DNA polyplexes with 1 mg/mL BSA for 20 min increases the luciferase expression modestly for serum-free conditions (orange) but significantly for transfection in serum (purple). Similarly, pre-treating with 5% FBS solution also results in better transfection in serum-free conditions (dark blue), but FBS treated bPEI/DNA performed worse in serum (light blue). In contrast, the non-treated zPEI 2/DNA polyplexes transfected higher than bPEI/DNA in serum-free conditions and significantly higher for in serum similar to results discussed in chapter 2.
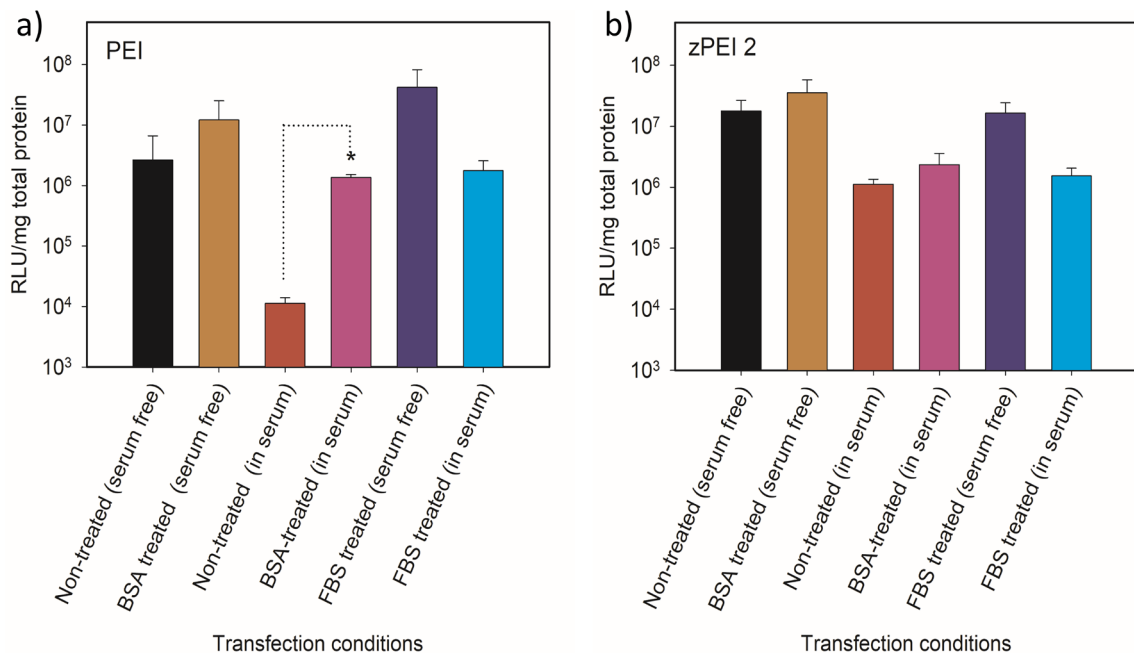
Figure 4.4. Gene transfection of pre-treated vs. non-treated particles with **a)** bPEI and **b)** zPEI 2 at different transfection conditions. BSA pre-treating was done at 1 mg/mL BSA in EMEM, while FBS pre-treating was done at 5% FBS in EMEM media. In serum means where 10% FBS was used as transfection media ($P<0.05$), serum-free means no serum present in the media. Polyplex formed at polymer/DNA weight ratio 1. All the data was obtained in triplicates (n=3).

Pre-treating the zPEI 2/DNA polyplexes with BSA resulted in similar high transgene expression both in serum and serum free conditions. FBS pre-treated zPEI/DNA polyplexes behaved similar to bPEI/DNA in both serum free and in serum conditions. One point to note here is that zPEI 2 shows a lesser gene expression in serum than gene expression in the absence of serum. While compared to the gene expression mediated by bPEI in the absence of serum seems comparable to zPEI 2. The data presented herein, **Figure 4.4b**, was obtained at polymer/DNA wt ratio one, where bPEI performs the best. However, this data is similar to what we observed in chapter 2, where zPEI 2 shows higher gene expression with a higher polymer/DNA loading wt ratio. The most important finding from this experiment is that gene transfection efficiency of bPEI decreases more than a hundred-fold while zPEI 2 maintains a significant transfectability both in the presence or absence of serum.

Taken together, these results suggest that both bPEI and zPEI polyplexes when pre-treated with BSA or FBS protein solutions give comparable transgene expression. This may suggest that when a protein corona is fully formed, the transfection efficacy is controlled more by the interaction of the cells with the corona proteins and is not as sensitive to the small modification differences between bPEI and zPEI 2. The most significant differences were found when comparing BSA treated and non-treated bPEI and zPEI 2 in either serum-free or in serum conditions. For bPEI, pre-treating polyplexes with BSA greatly enhances transfection in serum while zPEI 2 shows similar results in both untreated and BSA treated samples. One possible explanation for these results is that succinylated polyplexes may form a more complete protein coating faster when compared to bPEI/DNA. More experiments are needed to better understand these results.

One other thing to note is that the results in pre-coating with BSA and precoating with the more complex mixture of proteins in 5% FBS still resulted in similar transfection results in both bPEI and zPEI 2. This may be due to the FBS corona being predominantly formed by BSA depositing on the polyplexes or may suggest that the identity of protein composition do not have significant impact in gene expression. In future studies, it could be interesting to examine transgene expression in preformed coronas consisting of proteins not common to serum.

4.3.5   Gene transfection with pre- treated polyplex at higher serum conditions

In a final set of experiments, we next examined the effect of non- treated and pre-treated polyplexes at varying polymer:DNA wt ratios (1-6) under three different transfection conditions. In **Figure 4.5a**, we show bPEI, zPEI 2, and zPEI 6.5 polyplexes transfected in 10% FBS medium. In **Figure 4.5b**, we looked at the same polyplexes transfected in 10% FBS after pre-treating the polyplexes with 1 mg/mL BSA. In **Figure 4.5c**, we again pre-treated the polyplexes with 1 mg/mL BSA but then transfected in 100% FBS. In non-treated polyplexes, we see nearly identical results to the 10% FBS (or "in serum") transfections discussed in chapter 2. At all polymer:DNA ratios, zPEI 2 shows significantly higher (~100-fold) transgene expression when compared to bPEI/DNA. We do note, in these experiments we do see lower transfection for zPEI 2 than in chapter 2 however we do note that FBS is complex solution of proteins that is
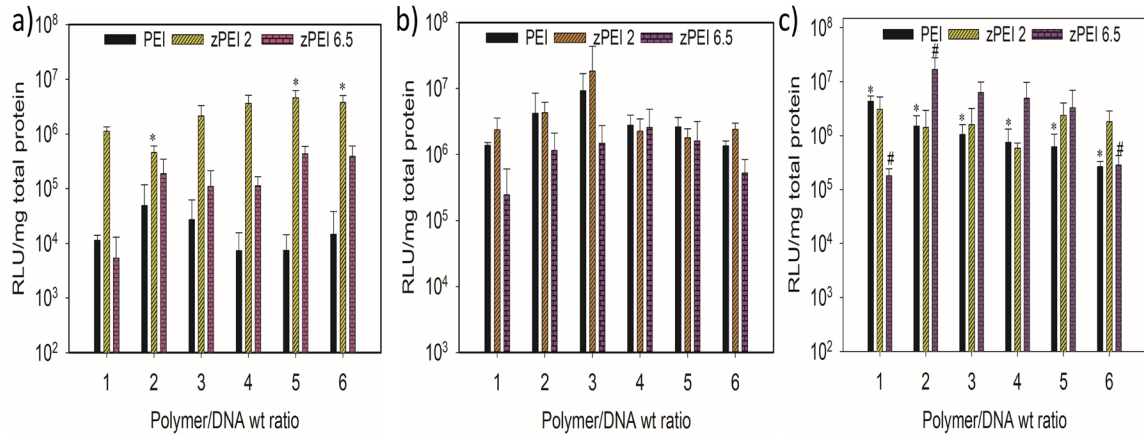
Figure 4.5. Comparative gene transfection efficacy in a) standard in serum (10% FBS in EMEM) b) pre-treated with 1 mg/mL BSA and transfection in serum (10% FBS in EMEM) & c) pre- treated with 1 mg/mL BSA and transfection in 100% serum with bPEI, zPEI 2 and zPEI 6.5 respectively. All the data collected as a triplicate (n = 3 and $P<0.05$).

known to have significant differences in the serum constituents that vary from batch to batch and therefore show different interaction behavior with polyplexes.[124, 191-192] Except the polymer/DNA wt ratio 2, zPEI 2 show no significant variability in gene expression with increasing loading ratio (**Figure 4.5a**, *$P<0.05$). zPEI 6.5 shows similar enhanced transfection over bPEI but only at polymer/DNA ratios (wt:wt) of 2 and above.

When we pre-treat the polyplexes with BSA (**Figure 4.5b**), the transgene expression is nearly identical at all three polyplexes. Surprisingly even at high polymer:DNA ratios, where there is more free polycation available to potentially complex and bind with BSA and thus presumably less BSA available to be incorporated into the pre-treated protein polyplex, the transgene expression seem stable up to wt:wt 6. However, as we discussed at polymer:DNA ratio 1, having a concentration of 1 mg/mL BSA is still sufficient to have nearly 100 BSAs available per polyplex. Therefore even at wt:wt 6, there is still a large excess of BSA available to form the corona. We also cannot exclude the possibility of ghost particles of BSA-PEI also being incorporated in the

137

protein corona surrounding the PEI and zPEI polyplexes. For the first time, we also performed transfections in 100% FBS medium or 10-fold higher protein concentration in the transfection medium compared to our previous 'in serum' experiments. Transfection in 100% FBS is not common, but as our ultimate goal is for in vivo gene transfection, 100% FBS should more closely resemble the protein concentrations experienced by polyplexes in the body. Again, the pretreated polyplexes are quite similar for all three systems except some variability observed in bPEI- and zPEI 6.5-mediated gene expression due to polymer/DNA loading ratio (**Figure 4.5c**, *, #$P<0.05$). The one exception is zPEI 6.5 at wt:wt 1 but as discussed these are not fully formed polyplexes and at higher polymer concentrations we see zPEI 6.5 expression increase back to comparable or higher levels than the pre-treated bPEI and zPEI 2 polyplexes. While these results do not explain the mechanism of enhanced transfection for minimally succinylated PEIs in the presence of serum, they are in good agreement with the recent results of Zhu et al., suggesting pre-coating polyplexes, whether bPEI or zPEI, results in enhanced gene transfection in serum even at 100% FBS concentrations.

4.4   Conclusion

These experiments investigated the effect of varying BSA concentrations (0, 1, 3, 6, 10 mg/mL) on gene transfection mediated by unmodified bPEI as well as minimally modified zPEIs. We find that transgene expression decreases with increasing BSA concentration for bPEI/DNA. zPEI 2 and zPEI 6.5 however show higher gene transfection over a wider range of BSA concentrations (0-6 mg/mL). Lastly, a series of experiments were performed to compare polyplexes pre-treated with BSA compared to

the non-treated polyplexes transfected in the presence of protein solution medium. For bPEI/DNA, the presence of pre-formed BSA corona showed clear enhancement of transgene expression when compared to transfection by bPEI/DNA polyplexes that did not have a pre-formed corona. In all three systems, the treatment with varying concentrations of proteins to favor pre-formed corona, transfection efficacy was quite similar, suggesting that transgene expression may be more dominated by the corona-cell interactions and not significantly influenced by low levels of succinylation. zPEI/DNA, in contrast, showed high transgene expression both with and without a pretreated protein. More experiments are needed to investigate the complex correlation between zPEI-DNA particles with protein coating to facilitate enhanced gene expression.

CHAPTER 5. CONCLUSION AND FUTURE RESEARCH DIRECTION

With this work, a series of minimally succinylated PEI were synthesized and evaluated for their transgene expression efficacy in vitro. In chapter 2, the transfection efficacy of these succinylated PEI (zPEI 2-11.5) was compared with unmodified branched PEI and commercial PEGylated PEI. The in-vitro efficacy mediated by zPEI 2 was reported 260- to 480-folds higher than that of unmodified PEI and more than 50-folds higher than PEGylated PEI in the presence of serum in HEK293 and HeLa cells, respectively. zPEI 2 was also able to repair a gene via CRISPR/Cas9 homology-directed repair mechanism, which was more than 16-folds higher than bPEI and Lipofectamine (2kDa) in the presence of serum. We concluded that this enhanced transgene expression efficacy with minimally succinylated PEI was not correlated to serum protein interaction; instead, a controlled interaction could benefit stable transgene expression.

In the future, a mechanistic study should be conducted to investigate how zPEI interacts with the cell membrane. In the second chapter, we hypothesized succinylation could potentially incorporate succinate receptor-mediated endocytosis. If this hypothesis is true, it could open another cell- specific therapy customized for certain organs such as the kidney. In situ physicochemical properties of the polyplexes should also be investigated. One vital question to consider is can zPEI alter intracellular trafficking? or how zPEI differs in cargo release compared to unmodified PEI? or does zPEI alters the rate of nucleic acid release from its cargo? For these types of intracellular trafficking experiments, a super-resolution imaging experiment should be incorporated. The CRISPR/Cas9 homology-directed repair was conducted on HEK 293 cell line. In the future, actual cancer cell line should be used to verify what level of correction we can

achieve. A new set of gene should be developed to modify cancer cells. We haven't checked the mRNA delivery efficacy with minimally succinylated PEI yet, but discussions are ongoing with a company so the DeRouchey and Pack labs may test mRNA delivery in the near future. Work by summer REU students in 2021 also explored the use of minimally succinylated PEI to transfect hard-to-transfect cell lines such as macrophage cells. The initial results were very promising and more work along these lines should be pursued in the future.

In chapter 3, we examined how the DNA packaging in PEI polyplexes changes due to polymer modification and pH. For this purpose, a new series of succinylated and acetylated PEI were synthesized and characterized with FT-IR and NMR spectroscopy. 2D-NMR (^{1}H-^{13}C HSQC, HMBC) experiments. Although modifications on PEI have often been assumed to occur preferentially on primary amines due to steric hinderance, using 2D-NMR we were able to show that both acetylation and succinylation actually occur primarily on the secondary amines of bPEI. This is reasonable as secondary amines are more nucleophilic than primary amines. In previous work, DeRouchey et al. showed that incorporation of either an uncharged amino acid or a negatively charged amino acid into short arginine peptides resulted in reduced attractions and increased repulsions ultimately reducing the packaging density of the DNA in the condensate. Acetylated PEI shows a similar trend with more loosely packaged DNA with increasing degrees of modification but zPEI shows a crossover behavior with DNA-DNA spacings first increasing and then decreasing at higher succinylation levels. Lastly, we showed that at low pH comparable to a lysosomal environment, polyplexes with PEI and modified PEIs all showed tighter DNA packaging.

Some complimentary future experiments to this work could include polyplex visualization by transmission electron microscopy to see if the polyplexes of the assorted succinylated and acetylated PEIs form similar or different complexes when compared to bPEI/DNA. These modifications could result in polyplexes that have more open structures or form more fibrous elongated nanoparticles when compared to bPEI/DNA which is known to form tightly compacted spherical or toroidal nanoparticles. zPEI/DNA was observed to loosen structure at low modification but tighten the DNA packaging at high modification, yet competition experiments show the highly modified zPEI complexes were more unstable. In contrast the condensation of DNA by PEI at low pH resulted in significantly tighter DNA packaging and presumably more stable polyplexes. This was not tested however so an interesting follow-up experiment would be to look at DNA condensation and release with polyplexes formed at low pH. Molecular dynamic simulations also suggested acidification of PEI/DNA may lead to more polycation being released from the complex and this could be experimentally validated. Lastly, since the formation of coronas on polyplexes have been observed, other groups have suggested that the proteins of the corona may interact and alter the DNA packaging of the polyplex nanoparticles. This could also be experimentally determined using X-ray diffraction experiments to determine DNA packaging in PEI and modified PEI polyplexes in the presence of serum proteins or lysosomal enzymes. In the future, it is critical to know how both pH and enzymes interplay in changing intra-helical spacings and the lysosomal release. X-ray experiments should also incorporate live-cell imaging to support whether polyplexes can evade lysosomal degradation due to polymer chemistry. Such experiments

may shed light on the mechanism of why zPEI acts as a better gene transfecting agent in the presence of serum proteins.

In chapter 4, gene transfection was conducted with bPEI and minimally modified zPEIs polyplexes at varying BSA concentrations (0, 1, 3, 6, 10 mg/mL) in the transfecting medium. The results of this chapter are very preliminary but offers some insight into how bPEI/DNA and zPEI/DNA transfect in these high protein concentrations. Most clearly, we see significant differences in bPEI/DNA when they are pretreated with BSA as compared to transfections performed with non-treated polyplexes in the presence of serum proteins. In contrast, zPEI/DNA shows little difference perhaps suggesting the succinylation is enabling the formation of a stable protein corona in a shorter time scale compared to bPEI/DNA. When pre- treated, both bPEI and zPEI shows high stability in transgene expression in both 10 and 100% FBS solution. This preliminary work used confocal fluorescence microscopy to observe colocalization of BSA and DNA in cells.

In future work, super-resolution microscopy could be incorporated to observe particle trafficking within the cell. Much more work could be done to explore how pre-treating polyplexes enhances gene transfection as well as distinguishing if there are differences depending on the polycation used in the original polyplex. For instance, bPEI and zPEI 2 seemed quite similar due presumably to a similar BSA corona formed on both polyplexes but would this still be true if one significantly altered the polycation-DNA interactions by using more highly succinylated or acetylated polymers in the pre-treated polyplexes. Such particles should much more readily disassemble inside the cells altering the DNA release dynamics. In addition, using different proteins than BSA could be explored to see how non-serum proteins alter the uptake of pre-treated polyplexes into

cells. Particularly integrating ligands into the protein corona to enhance cell target should be performed. Mechanistic studies to understand how the presence of corona alters the polyplex cell entry could also be pursued.

APPENDICES

APPENDIX 1. Synthesis of polymers (PEI/reactant mole ratio calculation)

To conjugate x% succinyl/acetl group to the bPEI polymer (25kDa), first, the total moles of nitrogen atoms were determined in the polymer. For simplification, a calculation follows:

For 2% succinylation:

*Half a gram of PEI (500 mg) requires $\frac{500mg \times 582\ mmol\ N\ atom}{25000g \times 1\ mmol\ PEI}$= 11.64 mmols N atoms

*For 2% succinylation, total N atoms should be modified = 0.02 x 11.64 = 0.2328 mmol succinic anhydride should be reacted.

So, the amount of succinic anhydride will be => $\frac{w}{100.07g}$= 0.2328 mmol x $\frac{10^{-3}}{1\ mmol}$=

0.023296296 ~0.0233 g = 23.3 mg

APPENDIX 2. Polymer/DNA wt/wt ratio converting to nitrogen/phosphate (N/P) ratio calculation

As an example, polymer/DNA wt ratio one is used. In this example, 200 ng pDNA and 200 ng bPEI (25kDa) polymer was used.

The calculation is as follows:

200 ng pDNA => 2 x 10^{-7} g DNA = 2 x 10^{-7} g x $\frac{One\ mol\ DNA}{660\ g/mol}$ = 3.03 x 10^{-10} mol DNA

Each base pair contains two phosphate groups, so, mols of phosphate in this DNA = 3.03 x 10^{-10} mol DNA x 2 PO^{4-} = 6.06 x 10^{-10} mol PO^{4-}

200 ng bPEI = $\dfrac{200\ x\ 10^{-9}\ g\ PEI}{42\frac{g}{mol}\ per\ N\ atom\ based\ on\ aziridine\ group}$ = 4.7619 x 10^{-9} mol N atom

So, the N/P ratio = $\dfrac{4.7619\ x\ 10^{-9}\ N}{6.06\ x\ 10-10\ P}$ = 7.86 ~ 8.

APPENDIX 3. NMR characterization parameters sample (H-NMR/HSQC/HMBC)

```
Data Parameters for H-NMR
NAME                 acPEI 40

F2 - Acquisition Parameters

INSTRUM   Avance NEO 400
PROBHD    Z163739_0007 (
PULPROG            zg30
TD                65536
SOLVENT             D2O
NS                  256
DS                    2
SWH          8196.722 Hz
FIDRES       0.250144 Hz
AQ          3.9976959 sec
RG                  101
DW             61.000 usec
DE             13.54 usec
TE              298.0 K
D1         2.00000000 sec
TD0                   1
SFO1      400.1524709 MHz
NUC1                 1H
P0               3.33 usec
P1              10.00 usec
PLW1       14.84899998 W

F2 - Processing parameters
SI                65536
SF        400.1499725 MHz
WDW                  EM
SSB                   0
LB               0.30 Hz
GB                    0
PC                 1.00
```

```
Data Parameters for 1H-13 HSQC
NAME                acPEI 40

F2 - Acquisition Parameters

INSTRUM   Avance NEO 400
PROBHD    Z163739_0007 (
PULPROG   hsqcedetgpsp.3
TD                    2048
SOLVENT                D2O
NS                       8
DS                      16
SWH            5882.353 Hz
FIDRES         5.744485 Hz
AQ            0.1740800 sec
RG                     101
DW              85.000 usec
DE               6.50 usec
TE              294.7 K
CNST2       145.0000000
D0          0.00000300 sec
D1          1.50000000 sec
D4          0.00172414 sec
D11         0.03000000 sec
D16         0.00020000 sec
D21         0.00360000 sec
INO         0.00002761 sec
TDav                   1
SFO1       400.1524009 MHz
NUC1                  1H
P1              10.00 usec
P2              20.00 usec
P28           1000.00 usec
PLW1        14.84899998 W
SFO2       100.6268531 MHz
NUC2                 13C
CPDPRG[2          garp4
P3              10.00 usec
P14            500.00 usec
P31           2119.00 usec
PCPD2           80.00 usec
PLW0                 0 W
PLW2        63.61999893 W
PLW12        0.99406999 W
SPNAM[3] Crp60,0.5,20.1
SPOAL3           0.500
SPOFFS3              0 Hz
SPW3         9.72049999 W
SPNAM[18  Crp60_xfilt.2
SPOAL18          0.500
SPOFFS18             0 Hz
SPW18        1.87259996 W
GPNAM[1]     SMSQ10.100
GPZ1            80.00 %
GPNAM[2]     SMSQ10.100
GPZ2            20.10 %
P16           1000.00 usec

F1 - Acquisition parameters
TD                   256
SFO1        100.6269 MHz
FIDRES      141.498749 Hz
SW            179.990 ppm
FnMODE     Echo-Antiecho

F2 - Processing parameters
SI                  2048
SF         400.1500000 MHz
WDW                QSINE
SSB                    2
LB                   0 Hz
GB                   0
PC                1.40

F1 - Processing parameters
SI                  1024
MC2         echo-antiecho
SF         100.6177975 MHz
WDW                QSINE
SSB                    2
LB                   0 Hz
GB                   0
```

```
Data Parameters for 1H-13C HMBC
NAME              acPEI-40


F2 - Acquisition Parameters

INSTRUM   Avance NEO 400
PROBHD    Z163739_0007 (
PULPROG     hmbcetgpl3nd
TD                   4096
SOLVENT               D2O
NS                      8
DS                     16
SWH              5882.353 Hz
FIDRES           2.872243 Hz
AQ              0.3481600 sec
RG                    101
DW                 85.000 usec
DE                   6.50 usec
TE                  294.3 K
CNST6         120.0000000
CNST7         170.0000000
CNST13          8.0000000
D0              0.00000300 sec
D1              1.50000000 sec
D6              0.06250000 sec
D16             0.00020000 sec
IN0             0.00002161 sec
TDav                    1
SFO1           400.1526010 MHz
NUC1                   1H
P1                  10.00 usec
P2                  20.00 usec
PLW1            14.84899998 W
SFO2           100.6288655 MHz
NUC2                  13C
P3                  10.00 usec
P24               2000.00 usec
PLW2            63.61999893 W
SPNAM[7]       Crp60comp.4
SPOAL7               0.500
SPOFFS7                 0 Hz
SPW7            9.72049999 W
GPNAM[1]        SMSQ10.100
GPZ1                80.00 %
GPNAM[3]        SMSQ10.100
GPZ3                14.00 %
GPNAM[4]        SMSQ10.100
GPZ4                -8.00 %
GPNAM[5]        SMSQ10.100
GPZ5                -4.00 %
GPNAM[6]        SMSQ10.100
GPZ6                -2.00 %
P16               1000.00 usec
CNST30           0.598113


F1 - Acquisition parameters
TD                    512
SFO1            100.6289 MHz
FIDRES          90.396294 Hz
SW               229.968 ppm
FnMODE      Echo-Antiecho


F2 - Processing parameters
SI                   4096
SF             400.1499679 MHz
WDW                  SINE
SSB                     0
LB                      0 Hz
GB                      0
PC                   1.40


F1 - Processing parameters
SI                   2048
MC2         echo-antiecho
SF             100.6177975 MHz
WDW                 QSINE
SSB                     2
LB                      0 Hz
GB                      0
```

148

BIBLIOGRAPHY

1.   Wilson James, M., A History Lesson for Stem Cells. *Science (New York, N.Y.)* **2009,** *324* (5928), 727-728.
2.   Ginn, S. L.; Amaya, A. K.; Alexander, I. E.; Edelstein, M.; Abedi, M. R., Gene therapy clinical trials worldwide to 2017: An update. *The journal of gene medicine* **2018,** *20* (5), e3015.
3.   Alhakamy, N. A.; Curiel, D. T.; Berkland, C. J., The era of gene therapy: From preclinical development to clinical application. *Drug Discovery Today* **2021,** *26* (7), 1602-1619.
4.   Singh, V.; Khan, N.; Jayandharan, G. R., Vector engineering, strategies and targets in cancer gene therapy. *Cancer Gene Therapy* **2021**.
5.   Arjmand, B.; Larijani, B.; Sheikh Hosseini, M.; Payab, M.; Gilany, K.; Goodarzi, P.; Parhizkar Roudsari, P.; Amanollahi Baharvand, M.; Hoseini Mohammadi, N. s., The Horizon of Gene Therapy in Modern Medicine: Advances and Challenges. In *Cell Biology and Translational Medicine, Volume 8: Stem Cells in Regenerative Medicine*, Turksen, K., Ed. Springer International Publishing: Cham, 2020; pp 33-64.
6.   Lin, Q.; Wang, D.-G.; Zhang, Z.-Q.; Liu, D.-P., Applications of Virus Vector–Mediated Gene Therapy in China. *Human Gene Therapy* **2017,** *29* (2), 98-109.
7.   Naso, M. F.; Tomkowicz, B.; Perry, W. L., 3rd; Strohl, W. R., Adeno-Associated Virus (AAV) as a Vector for Gene Therapy. *BioDrugs : clinical immunotherapeutics, biopharmaceuticals and gene therapy* **2017,** *31* (4), 317-334.
8.   Hirsch, M. L.; Wolf, S. J.; Samulski, R. J., Delivering Transgenic DNA Exceeding the Carrying Capacity of AAV Vectors. *Methods Mol Biol* **2016,** *1382*, 21-39.
9.   Robbins, P. D.; Ghivizzani, S. C., Viral vectors for gene therapy. *Pharmacology & therapeutics* **1998,** *80* (1), 35-47.
10.   Lundstrom, K., RNA Viruses as Tools in Gene Therapy and Vaccine Development. *Genes (Basel)* **2019,** *10* (3), 189.
11.   Escors, D.; Breckpot, K., Lentiviral vectors in gene therapy: their current status and future potential. *Arch Immunol Ther Exp (Warsz)* **2010,** *58* (2), 107-119.
12.   Milone, M. C.; O'Doherty, U., Clinical use of lentiviral vectors. *Leukemia* **2018,** *32* (7), 1529-1541.
13.   Munis, A. M., Gene Therapy Applications of Non-Human Lentiviral Vectors. *Viruses* **2020,** *12* (10), 1106.
14.   Zheng, P.-P.; Kros, J. M.; Li, J., Approved CAR T cell therapies: ice bucket challenges on glaring safety risks and long-term impacts. *Drug Discovery Today* **2018,** *23* (6), 1175-1182.
15.   Lundstrom, K., Viral Vectors in Gene Therapy. *Diseases (Basel, Switzerland)* **2018,** *6* (2).
16.   Gene therapy needs a long-term approach. *Nature medicine* **2021,** *27* (4), 563-563.
17.   Wilson, J. M.; Flotte, T. R., Moving Forward After Two Deaths in a Gene Therapy Trial of Myotubular Myopathy. *Human Gene Therapy* **2020,** *31* (13-14), 695-696.
18.   Mietzsch, M.; Eddington, C.; Jose, A.; Hsi, J.; Chipman, P.; Henley, T.; Choudhry, M.; McKenna, R.; Agbandje-McKenna, M., Improved Genome Packaging

Efficiency of Adeno-associated Virus Vectors Using Rep Hybrids. *Journal of virology* **2021,** *95* (19), e0077321.

19.   Giles, A. R.; Sims, J. J.; Turner, K. B.; Govindasamy, L.; Alvira, M. R.; Lock, M.; Wilson, J. M., Deamidation of Amino Acids on the Surface of Adeno-Associated Virus Capsids Leads to Charge Heterogeneity and Altered Vector Function. *Mol Ther* **2018,** *26* (12), 2848-2862.

20.   Bryant, D. H.; Bashir, A.; Sinai, S.; Jain, N. K.; Ogden, P. J.; Riley, P. F.; Church, G. M.; Colwell, L. J.; Kelsic, E. D., Deep diversification of an AAV capsid protein by machine learning. *Nature Biotechnology* **2021,** *39* (6), 691-696.

21.   Kumar, R.; Santa Chalarca, C. F.; Bockman, M. R.; Bruggen, C. V.; Grimme, C. J.; Dalal, R. J.; Hanson, M. G.; Hexum, J. K.; Reineke, T. M., Polymeric Delivery of Therapeutic Nucleic Acids. *Chemical reviews* **2021**.

22.   Buschmann, M. D.; Carrasco, M. J.; Alishetty, S.; Paige, M.; Alameh, M. G.; Weissman, D., Nanomaterial Delivery Systems for mRNA Vaccines. *Vaccines* **2021,** *9* (1).

23.   Park, J. W.; Lagniton, P. N. P.; Liu, Y.; Xu, R.-H., mRNA vaccines for COVID-19: what, why and how. *Int J Biol Sci* **2021,** *17* (6), 1446-1460.

24.   Shin, M. D.; Shukla, S.; Chung, Y. H.; Beiss, V.; Chan, S. K.; Ortega-Rivera, O. A.; Wirth, D. M.; Chen, A.; Sack, M.; Pokorski, J. K.; Steinmetz, N. F., COVID-19 vaccine development and a potential nanomaterial path forward. *Nature Nanotechnology* **2020,** *15* (8), 646-655.

25.   Uludag, H.; Ubeda, A.; Ansari, A., At the Intersection of Biomaterials and Gene Therapy: Progress in Non-viral Delivery of Nucleic Acids. *Frontiers in Bioengineering and Biotechnology* **2019,** *7*, 131.

26.   Wang, M.; Glass, Z. A.; Xu, Q., Non-viral delivery of genome-editing nucleases for gene therapy. *Gene therapy* **2017,** *24* (3), 144-150.

27.   Zhang, Y.-M.; Huang, Z.; Zhang, J.; Wu, W.-X.; Liu, Y.-H.; Yu, X.-Q., Amphiphilic polymers formed from ring-opening polymerization: a strategy for the enhancement of gene delivery. *Biomaterials Science* **2017,** *5* (4), 718-729.

28.   Shi, J.; Schellinger, J. G.; Johnson, R. N.; Choi, J. L.; Chou, B.; Anghel, E. L.; Pun, S. H., Influence of histidine incorporation on buffer capacity and gene transfection efficiency of HPMA-co-oligolysine brush polymers. *Biomacromolecules* **2013,** *14* (6), 1961-1970.

29.   Loczenski Rose, V.; Mastrotto, F.; Mantovani, G., Phosphonium polymers for gene delivery. *Polymer Chemistry* **2017,** *8* (2), 353-360.

30.   Nie, X.; Zhang, Z.; Wang, C.-H.; Fan, Y.-S.; Meng, Q.-Y.; You, Y.-Z., Interactions in DNA Condensation: An Important Factor for Improving the Efficacy of Gene Transfection. *Bioconjugate Chemistry* **2019,** *30* (2), 284-292.

31.   Kauffman, A. C.; Piotrowski-Daspit, A. S.; Nakazawa, K. H.; Jiang, Y.; Datye, A.; Saltzman, W. M., Tunability of Biodegradable Poly(amine- co-ester) Polymers for Customized Nucleic Acid Delivery and Other Biomedical Applications. *Biomacromolecules* **2018,** *19* (9), 3861-3873.

32.   Liu, Z.; Zhang, Z.; Zhou, C.; Jiao, Y., Hydrophobic modifications of cationic polymers for gene delivery. *Progress in Polymer Science* **2010,** *35* (9), 1144-1162.

33.   Thapa, B.; Plianwong, S.; Remant Bahadur, K. C.; Rutherford, B.; Uludağ, H., Small hydrophobe substitution on polyethylenimine for plasmid DNA delivery: Optimal substitution is critical for effective delivery. *Acta biomaterialia* **2016,** *33*, 213-24.

34.   Ansari, A. S.; K, C. R.; Jiang, X.; Uludağ, H., Investigation of water-insoluble hydrophobic polyethylenimines as RNAi vehicles in chronic myeloid leukemia therapy. *Journal of biomedical materials research. Part A* **2021,** *109* (11), 2306-2321.

35.   Liu S, H. W., Jin M, Wang Q, Zhang G, Wang X, Shao S, Gao Z, High gene delivery efficiency of alkylated low-molecular-weight polyethylenimine through gemini surfactant-like effect. *Int J Nanomedicine.* **2014,** *9* (1), 3567-3581.

36.   Tian, H.; Chen, J.; Chen, X., Nanoparticles for Gene Delivery. *Small* **2013,** *9* (12), 2034-2044.

37.   Piest, M.; Engbersen, J. F. J., Effects of charge density and hydrophobicity of poly(amido amine)s for non-viral gene delivery. *Journal of controlled release : official journal of the Controlled Release Society* **2010,** *148* (1), 83-90.

38.   Pereira-Silva, M.; Jarak, I.; Alvarez-Lorenzo, C.; Concheiro, A.; Santos, A. C.; Veiga, F.; Figueiras, A., Micelleplexes as nucleic acid delivery systems for cancer-targeted therapies. *Journal of controlled release : official journal of the Controlled Release Society* **2020,** *323*, 442-462.

39.   Ooi, Y. J.; Wen, Y.; Zhu, J.; Song, X.; Li, J., Surface Charge Switchable Polymer/DNA Nanoparticles Responsive to Tumor Extracellular pH for Tumor-Triggered Enhanced Gene Delivery. *Biomacromolecules* **2020,** *21* (3), 1136-1148.

40.   Mishra, S.; Webster, P.; Davis, M. E., PEGylation significantly affects cellular uptake and intracellular trafficking of non-viral gene delivery particles. *European journal of cell biology* **2004,** *83* (3), 97-111.

41.   Ke, X.; Wei, Z.; Wang, Y.; Shen, S.; Ren, Y.; Williford, J. M.; Luijten, E.; Mao, H. Q., Subtle changes in surface-tethered groups on PEGylated DNA nanoparticles significantly influence gene transfection and cellular uptake. *Nanomedicine : nanotechnology, biology, and medicine* **2019,** *19*, 126-135.

42.   Uz, M.; Bulmus, V.; Alsoy Altinkaya, S., Effect of PEG Grafting Density and Hydrodynamic Volume on Gold Nanoparticle–Cell Interactions: An Investigation on Cell Cycle, Apoptosis, and DNA Damage. *Langmuir* **2016,** *32* (23), 5997-6009.

43.   Gabizon, A.; Szebeni, J., Complement Activation: A Potential Threat on the Safety of Poly(ethylene glycol)-Coated Nanomedicines. *ACS Nano* **2020,** *14* (7), 7682-7688.

44.   Huckaby, J. T.; Jacobs, T. M.; Li, Z.; Perna, R. J.; Wang, A.; Nicely, N. I.; Lai, S. K., Structure of an anti-PEG antibody reveals an open ring that captures highly flexible PEG polymers. *Communications Chemistry* **2020,** *3* (1), 124.

45.   Kozma, G. T.; Shimizu, T.; Ishida, T.; Szebeni, J., Anti-PEG antibodies: Properties, formation, testing and role in adverse immune reactions to PEGylated nano-biopharmaceuticals. *Advanced drug delivery reviews* **2020,** *154-155*, 163-175.

46.   Hoang Thi, T. T.; Pilkington, E. H.; Nguyen, D. H.; Lee, J. S.; Park, K. D.; Truong, N. P., The Importance of Poly(ethylene glycol) Alternatives for Overcoming PEG Immunogenicity in Drug Delivery and Bioconjugation. *Polymers (Basel)* **2020,** *12* (2).

47.   Maan, A. M. C.; Hofman, A. H.; de Vos, W. M.; Kamperman, M., Recent Developments and Practical Feasibility of Polymer-Based Antifouling Coatings. *Advanced Functional Materials* **2020**, *30* (32), 2000936.

48.   Suh, J.; Paik, H. J.; Hwang, B. K., Ionization of Poly(ethylenimine) and Poly(allylamine) at Various pH′s. *Bioorganic Chemistry* **1994**, *22* (3), 318-327.

49.   Wang, X.; Niu, D.; Hu, C.; Li, P., Polyethylenimine-Based Nanocarriers for Gene Delivery. *Current pharmaceutical design* **2015**, *21* (42), 6140-56.

50.   Pinilla-Torres, A. M.; Carrión-García, P. Y.; Sánchez-Domínguez, C. N.; Gallardo-Blanco, H.; Sánchez-Domínguez, M., Modification of Branched Polyethylenimine Using Mesquite Gum for Its Improved Hemocompatibility. *Polymers* **2021**, *13* (16), 2766.

51.   Wang, Q.; Jiang, H.; Li, Y.; Chen, W.; Li, H.; Peng, K.; Zhang, Z.; Sun, X., Targeting NF-kB signaling with polymeric hybrid micelles that co-deliver siRNA and dexamethasone for arthritis therapy. *Biomaterials* **2017**, *122*, 10-22.

52.   Chen, L.; Ji, F.; Bao, Y.; Xia, J.; Guo, L.; Wang, J.; Li, Y., Biocompatible cationic pullulan-g-desoxycholic acid-g-PEI micelles used to co-deliver drug and gene for cancer therapy. *Materials science & engineering. C, Materials for biological applications* **2017**, *70* (Pt 1), 418-429.

53.   Wu, Y.; Zhang, Y.; Zhang, W.; Sun, C.; Wu, J.; Tang, J., Reversing of multidrug resistance breast cancer by co-delivery of P-gp siRNA and doxorubicin via folic acid-modified core-shell nanomicelles. *Colloids and surfaces. B, Biointerfaces* **2016**, *138*, 60-9.

54.   Dunbar, C. E.; High, K. A.; Joung, J. K.; Kohn, D. B.; Ozawa, K.; Sadelain, M., Gene therapy comes of age. *Science* **2018**, *359* (6372), eaan4672.

55.   Goswami, R.; Subramanian, G.; Silayeva, L.; Newkirk, I.; Doctor, D.; Chawla, K.; Chattopadhyay, S.; Chandra, D.; Chilukuri, N.; Betapudi, V., Gene Therapy Leaves a Vicious Cycle. *Frontiers in Oncology* **2019**, *9* (297).

56.   Bae, Y. H.; Park, K., Targeted drug delivery to tumors: myths, reality and possibility. *J Control Release* **2011**, *153* (3), 198-205.

57.   Kotterman, M. A.; Chalberg, T. W.; Schaffer, D. V., Viral Vectors for Gene Therapy: Translational and Clinical Outlook. *Annual Review of Biomedical Engineering* **2015**, *17* (1), 63-89.

58.   Yin, H.; Kanasty, R. L.; Eltoukhy, A. A.; Vegas, A. J.; Dorkin, J. R.; Anderson, D. G., Non-viral vectors for gene-based therapy. *Nature Reviews Genetics* **2014**, *15* (8), 541-555.

59.   Bouard, D.; Alazard-Dany, D.; Cosset, F. L., Viral vectors: from virology to transgene expression. *Br J Pharmacol* **2009**, *157* (2), 153-65.

60.   Ayuso, E., Manufacturing of recombinant adeno-associated viral vectors: new technologies are welcome. *Molecular Therapy - Methods & Clinical Development* **2016**, *3*.

61.   Thomas, C. E.; Ehrhardt, A.; Kay, M. A., Progress and problems with the use of viral vectors for gene therapy. *Nature Reviews Genetics* **2003**, *4* (5), 346-358.

62.   Uren, A. G.; Kool, J.; Berns, A.; van Lohuizen, M., Retroviral insertional mutagenesis: past, present and future. *Oncogene* **2005**, *24* (52), 7656-7672.

63.   Somia, N.; Verma, I. M., Gene therapy: trials and tribulations. *Nature Reviews Genetics* **2000**, *1* (2), 91-99.

64.	Kay, M. A.; Glorioso, J. C.; Naldini, L., Viral vectors for gene therapy: the art of turning infectious agents into vehicles of therapeutics. *Nature Medicine* **2001,** *7* (1), 33-40.

65.	Niidome, T.; Huang, L., Gene therapy progress and prospects: nonviral vectors. *Gene Ther* **2002,** *9* (24), 1647-52.

66.	Pack, D. W.; Hoffman, A. S.; Pun, S.; Stayton, P. S., Design and development of polymers for gene delivery. *Nature reviews. Drug discovery* **2005,** *4* (7), 581-93.

67.	Morille, M.; Passirani, C.; Vonarbourg, A.; Clavreul, A.; Benoit, J. P., Progress in developing cationic vectors for non-viral systemic gene therapy against cancer. *Biomaterials* **2008,** *29* (24-25), 3477-96.

68.	Gulei, D.; Berindan-Neagoe, I., CRISPR/Cas9: A Potential Life-Saving Tool. What's next? *Molecular Therapy - Nucleic Acids* **2017,** *9*, 333-336.

69.	Zhang, P.; Wagner, E., History of Polymeric Gene Delivery Systems. *Topics in Current Chemistry* **2017,** *375* (2), 26.

70.	Wang, Y.; Ye, M.; Xie, R.; Gong, S., Enhancing the In Vitro and In Vivo Stabilities of Polymeric Nucleic Acid Delivery Nanosystems. *Bioconjugate Chemistry* **2019,** *30* (2), 325-337.

71.	Zhang, Y.; Satterlee, A.; Huang, L., In vivo gene delivery by nonviral vectors: overcoming hurdles? *Mol Ther* **2012,** *20* (7), 1298-304.

72.	Grigsby, C. L.; Leong, K. W., Balancing protection and release of DNA: tools to address a bottleneck of non-viral gene delivery. *J R Soc Interface* **2010,** *7 Suppl 1* (Suppl 1), S67-S82.

73.	Duncan, R.; Richardson, S. C. W., Endocytosis and Intracellular Trafficking as Gateways for Nanomedicine Delivery: Opportunities and Challenges. *Molecular Pharmaceutics* **2012,** *9* (9), 2380-2402.

74.	Shi, J.; Choi, J. L.; Chou, B.; Johnson, R. N.; Schellinger, J. G.; Pun, S. H., Effect of Polyplex Morphology on Cellular Uptake, Intracellular Trafficking, and Transgene Expression. *ACS Nano* **2013,** *7* (12), 10612-10620.

75.	Remant Bahadur, K. C.; Uludağ, H., 2 - PEI and its derivatives for gene therapy. In *Polymers and Nanomaterials for Gene Therapy*, Narain, R., Ed. Woodhead Publishing: 2016; pp 29-54.

76.	Pandey, A. P.; Sawant, K. K., Polyethylenimine: A versatile, multifunctional non-viral vector for nucleic acid delivery. *Materials Science and Engineering: C* **2016,** *68*, 904-918.

77.	Lungwitz, U.; Breunig, M.; Blunk, T.; Göpferich, A., Polyethylenimine-based non-viral gene delivery systems. *European Journal of Pharmaceutics and Biopharmaceutics* **2005,** *60* (2), 247-266.

78.	Fischer, D.; Bieber, T.; Li, Y.; Elsässer, H.-P.; Kissel, T., A Novel Non-Viral Vector for DNA Delivery Based on Low Molecular Weight, Branched Polyethylenimine: Effect of Molecular Weight on Transfection Efficiency and Cytotoxicity. *Pharmaceutical Research* **1999,** *16* (8), 1273-1279.

79.	Akinc, A.; Thomas, M.; Klibanov, A. M.; Langer, R., Exploring polyethylenimine-mediated DNA transfection and the proton sponge hypothesis. *The journal of gene medicine* **2005,** *7* (5), 657-63.

80.	Godbey, W. T.; Wu, K. K.; Mikos, A. G., Poly(ethylenimine) and its role in gene delivery. *J Control Release* **1999,** *60* (2-3), 149-60.

81.   Hall, A.; Lächelt, U.; Bartek, J.; Wagner, E.; Moghimi, S. M., Polyplex Evolution: Understanding Biology, Optimizing Performance. *Mol Ther* **2017,** *25* (7), 1476-1490.

82.   Ogris, M.; Brunner, S.; Schüller, S.; Kircheis, R.; Wagner, E., PEGylated DNA/transferrin-PEI complexes: reduced interaction with blood components, extended circulation in blood and potential for systemic gene delivery. *Gene Ther* **1999,** *6* (4), 595-605.

83.   Ernsting, M. J.; Murakami, M.; Roy, A.; Li, S. D., Factors controlling the pharmacokinetics, biodistribution and intratumoral penetration of nanoparticles. *J Control Release* **2013,** *172* (3), 782-94.

84.   Fischer, D.; Li, Y.; Ahlemeyer, B.; Krieglstein, J.; Kissel, T., In vitro cytotoxicity testing of polycations: influence of polymer structure on cell viability and hemolysis. *Biomaterials* **2003,** *24* (7), 1121-31.

85.   Read, M. L.; Bremner, K. H.; Oupický, D.; Green, N. K.; Searle, P. F.; Seymour, L. W., Vectors based on reducible polycations facilitate intracellular release of nucleic acids. *J Gene Med* **2003,** *5* (3), 232-45.

86.   Itaka, K.; Harada, A.; Yamasaki, Y.; Nakamura, K.; Kawaguchi, H.; Kataoka, K., In situ single cell observation by fluorescence resonance energy transfer reveals fast intra-cytoplasmic delivery and easy release of plasmid DNA complexed with linear polyethylenimine. *J Gene Med* **2004,** *6* (1), 76-84.

87.   Kircheis, R.; Wightman, L.; Wagner, E., Design and gene delivery activity of modified polyethylenimines. *Advanced Drug Delivery Reviews* **2001,** *53* (3), 341-358.

88.   Forrest, M. L.; Meister, G. E.; Koerber, J. T.; Pack, D. W., Partial Acetylation of Polyethylenimine Enhances In Vitro Gene Delivery. *Pharmaceutical Research* **2004,** *21* (2), 365-371.

89.   Gabrielson, N. P.; Pack, D. W., Acetylation of Polyethylenimine Enhances Gene Delivery via Weakened Polymer/DNA Interactions. *Biomacromolecules* **2006,** *7* (8), 2427-2435.

90.   Kircheis, R.; Blessing, T.; Brunner, S.; Wightman, L.; Wagner, E., Tumor targeting with surface-shielded ligand--polycation DNA complexes. *J Control Release* **2001,** *72* (1-3), 165-70.

91.   Knop, K.; Hoogenboom, R.; Fischer, D.; Schubert, U. S., Poly(ethylene glycol) in drug delivery: pros and cons as well as potential alternatives. *Angew Chem Int Ed Engl* **2010,** *49* (36), 6288-308.

92.   Nguyen, H. K.; Lemieux, P.; Vinogradov, S. V.; Gebhart, C. L.; Guérin, N.; Paradis, G.; Bronich, T. K.; Alakhov, V. Y.; Kabanov, A. V., Evaluation of polyether-polyethylenimine graft copolymers as gene transfer agents. *Gene Ther* **2000,** *7* (2), 126-38.

93.   Oupicky, D.; Ogris, M.; Howard, K. A.; Dash, P. R.; Ulbrich, K.; Seymour, L. W., Importance of lateral and steric stabilization of polyelectrolyte gene delivery vectors for extended systemic circulation. *Mol Ther* **2002,** *5* (4), 463-72.

94.   Tseng, W. C.; Jong, C. M., Improved stability of polycationic vector by dextran-grafted branched polyethylenimine. *Biomacromolecules* **2003,** *4* (5), 1277-84.

95.   Liu, X.; Yang, J. W.; Miller, A. D.; Nack, E. A.; Lynn, D. M., Charge-Shifting Cationic Polymers That Promote Self-Assembly and Self-Disassembly with DNA. *Macromolecules* **2005,** *38* (19), 7907-7914.

96.   Liu, X.; Yang, J. W.; Lynn, D. M., Addition of "charge-shifting" side chains to linear poly(ethyleneimine) enhances cell transfection efficiency. *Biomacromolecules* **2008,** *9* (7), 2063-2071.

97.   Zintchenko, A.; Philipp, A.; Dehshahri, A.; Wagner, E., Simple modifications of branched PEI lead to highly efficient siRNA carriers with low toxicity. *Bioconjug Chem* **2008,** *19* (7), 1448-55.

98.   Khalvati, B.; Sheikhsaran, F.; Sharifzadeh, S.; Kalantari, T.; Behzad Behbahani, A.; Jamshidzadeh, A.; Dehshahri, A., Delivery of plasmid encoding interleukin-12 gene into hepatocytes by conjugated polyethylenimine-based nanoparticles. *Artificial cells, nanomedicine, and biotechnology* **2017,** *45* (5), 1036-1044.

99.   Warriner, L. W.; Duke, J. R.; Pack, D. W.; DeRouchey, J. E., Succinylated Polyethylenimine Derivatives Greatly Enhance Polyplex Serum Stability and Gene Delivery In Vitro. *Biomacromolecules* **2018,** *19* (11), 4348-4357.

100.   Ziebarth, J. D.; Kennetz, D. R.; Walker, N. J.; Wang, Y., Structural Comparisons of PEI/DNA and PEI/siRNA Complexes Revealed with Molecular Dynamics Simulations. *J Phys Chem B* **2017,** *121* (8), 1941-1952.

101.   Zhang, J.-H. Y., H.-Z.; Zhang, J.; Liu, Y.-H.; He, X.; Xiao, Y.-P.; Yu, X.-Q., Biodegradable Gene Carriers Containing Rigid Aromatic Linkage with Enhanced DNA Binding and Cell Uptake. *Polymers* **2018,** *10* (1), 1080-96.

102.   Mislick, K. A.; Baldeschwieler, J. D., Evidence for the role of proteoglycans in cation-mediated gene transfer. *Proc Natl Acad Sci U S A* **1996,** *93* (22), 12349-12354.

103.   von Harpe, A.; Petersen, H.; Li, Y.; Kissel, T., Characterization of commercially available and synthesized polyethylenimines for gene delivery. *Journal of Controlled Release* **2000,** *69* (2), 309-322.

104.   Fitzsimmons, R. E.; Uludağ, H., Specific effects of PEGylation on gene delivery efficacy of polyethylenimine: interplay between PEG substitution and N/P ratio. *Acta Biomater* **2012,** *8* (11), 3941-55.

105.   Banan, M., Recent advances in CRISPR/Cas9-mediated knock-ins in mammalian cells. *Journal of Biotechnology* **2020,** *308*, 1-9.

106.   Medda, L.; Monduzzi, M.; Salis, A., The molecular motion of bovine serum albumin under physiological conditions is ion specific. *Chemical Communications* **2015,** *51* (30), 6663-6666.

107.   Mi, L.; Jiang, S., Integrated Antimicrobial and Nonfouling Zwitterionic Polymers. *Angewandte Chemie International Edition* **2014,** *53* (7), 1746-1754.

108.   Chen, S.; Li, L.; Zhao, C.; Zheng, J., Surface hydration: Principles and applications toward low-fouling/nonfouling biomaterials. *Polymer* **2010,** *51* (23), 5283-5293.

109.   Zhu, D.; Yan, H.; Zhou, Z.; Tang, J.; Liu, X.; Hartmann, R.; Parak, W. J.; Shen, Y.; Feliu, N., Influence of the Modulation of the Protein Corona on Gene Expression Using Polyethylenimine (PEI) Polyplexes as Delivery Vehicle. *Advanced Healthcare Materials n/a* (n/a), 2100125.

110.   Przemyslaw, S.; Mirna, S.; David, H.; Karine, Z.; Jean-Sébastien, J.; Jang-Hyeon, C.; Jean-Claude, H.; Elsa, K.-D.; Daya, R. V.; Sophie, T.; Martin, L.; Lenka, R.; Pierre, H.; William, H. K.; Xiuqian, M.; Orval, M.; Pierre, L.; Adriana Di, P.; Christian, B.; Gregor, A.; Grant, M.; Florian, S.; Sylvain, C., The succinate receptor GPR91 in neurons has a major role in retinal angiogenesis. *Nature medicine* **2008,** *14* (10), 1067.

111.   Ariza, A. C.; Deen, P.; Robben, J., The Succinate Receptor as a Novel Therapeutic Target for Oxidative and Metabolic Stress-Related Conditions. *Frontiers in Endocrinology* **2012,** *3* (22).

112.   Ginn, S. L.; Alexander, I. E.; Edelstein, M. L.; Abedi, M. R.; Wixon, J., Gene therapy clinical trials worldwide to 2012 - an update. *The journal of gene medicine* **2013,** *15* (2), 65-77.

113.   Liu, M.-X.; Ma, L.-L.; Liu, X.-Y.; Liu, J.-Y.; Lu, Z.-L.; Liu, R.; He, L., Combination of [12]aneN3 and Triphenylamine-Benzylideneimidazolone as Nonviral Gene Vectors with Two-Photon and AIE Properties. *ACS Applied Materials & Interfaces* **2019,** *11* (46), 42975-42987.

114.   Mintzer, M. A.; Simanek, E. E., Nonviral vectors for gene delivery. *Chemical reviews* **2009,** *109* (2), 259-302.

115.   Schwarz, B., Merkel, O. M. , Functionalized PEI and Its Role in Gene Therapy. *Material Matters* **2017,** *12* (2), 63-66.

116.   Lächelt, U.; Wagner, E., Nucleic Acid Therapeutics Using Polyplexes: A Journey of 50 Years (and Beyond). *Chemical reviews* **2015,** *115* (19), 11043-11078.

117.   Guan, X.; Guo, Z.; Wang, T.; Lin, L.; Chen, J.; Tian, H.; Chen, X., A pH-Responsive Detachable PEG Shielding Strategy for Gene Delivery System in Cancer Therapy. *Biomacromolecules* **2017,** *18* (4), 1342-1349.

118.   Wen, S.; Zheng, F.; Shen, M.; Shi, X., Surface modification and PEGylation of branched polyethylenimine for improved biocompatibility. *Journal of Applied Polymer Science* **2013,** *128* (6), 3807-3813.

119.   He, Y.; Cheng, G.; Xie, L.; Nie, Y.; He, B.; Gu, Z., Polyethylenimine/DNA polyplexes with reduction-sensitive hyaluronic acid derivatives shielding for targeted gene delivery. *Biomaterials* **2013,** *34* (4), 1235-45.

120.   Sadeghpour, H.; Khalvati, B.; Entezar-Almahdi, E.; Savadi, N.; Hossaini Alhashemi, S.; Raoufi, M.; Dehshahri, A., Double domain polyethylenimine-based nanoparticles for integrin receptor mediated delivery of plasmid DNA. *Scientific reports* **2018,** *8* (1), 6842.

121.   Hashemi, M.; Parhiz, B. H.; Hatefi, A.; Ramezani, M., Modified polyethylenimine with histidine–lysine short peptides as gene carrier. *Cancer Gene Therapy* **2011,** *18* (1), 12-19.

122.   Moffatt, S.; Wiehle, S.; Cristiano, R. J., A multifunctional PEI-based cationic polyplex for enhanced systemic p53-mediated gene therapy. *Gene therapy* **2006,** *13* (21), 1512-1523.

123.   Liu, C.; Liu, F.; Feng, L.; Li, M.; Zhang, J.; Zhang, N., The targeted co-delivery of DNA and doxorubicin to tumor cells via multifunctional PEI-PEG based nanoparticles. *Biomaterials* **2013,** *34* (10), 2547-64.

124.   Gabrielson, N. P.; Pack, D. W., Acetylation of polyethylenimine enhances gene delivery via weakened polymer/DNA interactions. *Biomacromolecules* **2006,** *7* (8), 2427-35.

125.   Forrest, M. L.; Meister, G. E.; Koerber, J. T.; Pack, D. W., Partial acetylation of polyethylenimine enhances in vitro gene delivery. *Pharmaceutical research* **2004,** *21* (2), 365-71.

126.   Warriner, L. W.; Duke, J. R.; Pack, D. W.; Derouchey, J. E., Succinylated Polyethylenimine Derivatives Greatly Enhance Polyplex Serum Stability and Gene Delivery In Vitro. *Biomacromolecules* **2018,** *19* (11), 4348--4357.

127.   Uddin, N.; Warriner, L. W.; Pack, D. W.; DeRouchey, J. E., Enhanced Gene Delivery and CRISPR/Cas9 Homology-Directed Repair in Serum by Minimally Succinylated Polyethylenimine. *Molecular pharmaceutics* **2021,** *18* (9), 3452-3463.

128.   Wong, G. C.; Pollack, L., Electrostatics of strongly charged biological polymers: ion-mediated interactions and self-organization in nucleic acids and proteins. *Annual review of physical chemistry* **2010,** *61*, 171-89.

129.   Bloomfield, V. A., DNA condensation by multivalent cations. *Biopolymers* **1997,** *44* (3), 269-82.

130.   DeRouchey, J.; Hoover, B.; Rau, D. C., A Comparison of DNA Compaction by Arginine and Lysine Peptides: A Physical Basis for Arginine Rich Protamines. *Biochemistry* **2013,** *52* (17), 3000-3009.

131.   DeRouchey, J. E.; Rau, D. C., Role of amino acid insertions on intermolecular forces between arginine peptide condensed DNA helices: implications for protamine-DNA packaging in sperm. *The Journal of biological chemistry* **2011,** *286* (49), 41985-92.

132.   DeRouchey, J.; Parsegian, V. A.; Rau, D. C., Cation charge dependence of the forces driving DNA assembly. *Biophysical journal* **2010,** *99* (8), 2608-2615.

133.   Todd, B. A.; Parsegian, V. A.; Shirahata, A.; Thomas, T. J.; Rau, D. C., Attractive forces between cation condensed DNA double helices. *Biophysical journal* **2008,** *94* (12), 4775-4782.

134.   Ha, B. Y.; Liu, A. J., Counterion-Mediated Attraction between Two Like-Charged Rods. *Physical Review Letters* **1997,** *79* (7), 1289-1292.

135.   Shklovskii, B. I., Wigner Crystal Model of Counterion Induced Bundle Formation of Rodlike Polyelectrolytes. *Physical Review Letters* **1999,** *82* (16), 3268-3271.

136.   Kornyshev, A. A.; Leikin, S., Electrostatic interaction between helical macromolecules in dense aggregates: An impetus for DNA poly- and meso-morphism. *Proceedings of the National Academy of Sciences* **1998,** *95* (23), 13579.

137.   Kornyshev, A. A.; Leikin, S., Electrostatic Zipper Motif for DNA Aggregation. *Physical Review Letters* **1999,** *82* (20), 4138-4141.

138.   Kornyshev, A. A.; Lee, D. J.; Leikin, S.; Wynveen, A., Structure and interactions of biological helices. *Reviews of Modern Physics* **2007,** *79* (3), 943-996.

139.   Ouameur, A. A.; Tajmir-Riahi, H. A., Structural analysis of DNA interactions with biogenic polyamines and cobalt(III)hexamine studied by Fourier transform infrared and capillary electrophoresis. *The Journal of biological chemistry* **2004,** *279* (40), 42041-54.

140.   Prieto, M. C.; Maki, A. H.; Balhorn, R., Analysis of DNA-protamine interactions by optical detection of magnetic resonance. *Biochemistry* **1997,** *36* (39), 11944-51.

141.   Hud, N. V.; Milanovich, F. P.; Balhorn, R., Evidence of novel secondary structure in DNA-bound protamine is revealed by Raman spectroscopy. *Biochemistry* **1994,** *33* (24), 7528-35.

142.   DeRouchey, J.; Netz, R. R.; Rädler, J. O., Structural investigations of DNA-polycation complexes. *The European physical journal. E, Soft matter* **2005,** *16* (1), 17-28.

143.   Rezvani Amin, Z.; Rahimizadeh, M.; Eshghi, H.; Dehshahri, A.; Ramezani, M., The effect of cationic charge density change on transfection efficiency of polyethylenimine. *Iran J Basic Med Sci* **2013,** *16* (2), 150-156.

144.   Kang, H. C.; Samsonova, O.; Kang, S.-W.; Bae, Y. H., The effect of environmental pH on polymeric transfection efficiency. *Biomaterials* **2012,** *33* (5), 1651-1662.

145.   Lai, W. F.; Wong, W. T., Design of Polymeric Gene Carriers for Effective Intracellular Delivery. *Trends Biotechnol* **2018,** *36* (7), 713-728.

146.   Behr, J.-P., The Proton Sponge: a Trick to Enter Cells the Viruses Did Not Exploit. *CHIMIA International Journal for Chemistry* **1997,** *51* (1-2), 34-36.

147.   Nguyen, J.; Szoka, F. C., Nucleic acid delivery: the missing pieces of the puzzle? *Acc Chem Res* **2012,** *45* (7), 1153-62.

148.   Burke, R. S.; Pun, S. H., Extracellular barriers to in Vivo PEI and PEGylated PEI polyplex-mediated gene delivery to the liver. *Bioconjug Chem* **2008,** *19* (3), 693-704.

149.   Dean, L. F. G. a. D. A., Extracellular and Intracellular Barriers to Non-Viral Gene Transfer. *Novel Gene Therapy Approaches* **2013**.

150.   González-Domínguez, I.; Grimaldi, N.; Cervera, L.; Ventosa, N.; Gòdia, F., Impact of physicochemical properties of DNA/PEI complexes on transient transfection of mammalian cells. *New Biotechnology* **2019,** *49*, 88-97.

151.   Sonawane, N. D.; Szoka, F. C., Jr.; Verkman, A. S., Chloride accumulation and swelling in endosomes enhances DNA transfer by polyamine-DNA polyplexes. *The Journal of biological chemistry* **2003,** *278* (45), 44826-31.

152.   Funhoff, A. M.; van Nostrum, C. F.; Koning, G. A.; Schuurmans-Nieuwenbroek, N. M. E.; Crommelin, D. J. A.; Hennink, W. E., Endosomal Escape of Polymeric Gene Delivery Complexes Is Not Always Enhanced by Polymers Buffering at Low pH. *Biomacromolecules* **2004,** *5* (1), 32-39.

153.   Van Bruggen, C.; Hexum, J. K.; Tan, Z.; Dalal, R. J.; Reineke, T. M., Nonviral Gene Delivery with Cationic Glycopolymers. *Accounts of Chemical Research* **2019,** *52* (5), 1347-1358.

154.   Brunot, C.; Ponsonnet, L.; Lagneau, C.; Farge, P.; Picart, C.; Grosgogeat, B., Cytotoxicity of polyethylenimine (PEI), precursor base layer of polyelectrolyte multilayer films. *Biomaterials* **2007,** *28* (4), 632-640.

155.   Brotzel, F.; Chu, Y. C.; Mayr, H., Nucleophilicities of Primary and Secondary Amines in Water. *The Journal of Organic Chemistry* **2007,** *72* (10), 3679-3688.

156.   Xun, M.-M.; Zhang, J.-H.; Liu, Y.-H.; Zhang, J.; Xiao, Y.-P.; Guo, Q.; Li, S.; Yu, X.-Q., Polyethylenimine analogs for improved gene delivery: effect of the type of amino groups. *RSC Advances* **2016,** *6* (7), 5391-5400.

157.   Stanley, C.; Rau, D. C., Evidence for water structuring forces between surfaces. *Curr Opin Colloid Interface Sci* **2011,** *16* (6), 551-556.

158.   DeRouchey, J. E.; Rau, D. C., Salt Effects on Condensed Protamine–DNA Assemblies: Anion Binding and Weakening of Attraction. *The Journal of Physical Chemistry B* **2011,** *115* (41), 11888-11894.

159.   An, M.; Parkin, S. R.; DeRouchey, J. E., Intermolecular forces between low generation PAMAM dendrimer condensed DNA helices: role of cation architecture. *Soft Matter* **2014,** *10* (4), 590-599.

160.   An, M.; Yesilbag Tonga, G.; Parkin, S. R.; Rotello, V. M.; DeRouchey, J. E., Tuning DNA Condensation with Zwitterionic Polyamidoamine (zPAMAM) Dendrimers. *Macromolecules* **2017,** *50* (20), 8202-8211.

161.   Boussif, O.; Lezoualc'h, F.; Zanta, M. A.; Mergny, M. D.; Scherman, D.; Demeneix, B.; Behr, J. P., A versatile vector for gene and oligonucleotide transfer into cells in culture and in vivo: polyethylenimine. *Proc Natl Acad Sci U S A* **1995,** *92* (16), 7297-301.

162.   Vermeulen, L. M. P.; Brans, T.; Samal, S. K.; Dubruel, P.; Demeester, J.; De Smedt, S. C.; Remaut, K.; Braeckmans, K., Endosomal Size and Membrane Leakiness Influence Proton Sponge-Based Rupture of Endosomal Vesicles. *ACS Nano* **2018,** *12* (3), 2332-2345.

163.   Kichler, A.; Leborgne, C.; Coeytaux, E.; Danos, O., Polyethylenimine-mediated gene delivery: a mechanistic study. *The journal of gene medicine* **2001,** *3* (2), 135-44.

164.   Benjaminsen, R. V.; Mattebjerg, M. A.; Henriksen, J. R.; Moghimi, S. M.; Andresen, T. L., The Possible "Proton Sponge " Effect of Polyethylenimine (PEI) Does Not Include Change in Lysosomal pH. *Molecular Therapy* **2013,** *21* (1), 149-157.

165.   Bertschinger, M.; Backliwal, G.; Schertenleib, A.; Jordan, M.; Hacker, D. L.; Wurm, F. M., Disassembly of polyethylenimine-DNA particles in vitro: implications for polyethylenimine-mediated DNA delivery. *Journal of controlled release : official journal of the Controlled Release Society* **2006,** *116* (1), 96-104.

166.   Bus, T.; Traeger, A.; Schubert, U. S., The great escape: how cationic polyplexes overcome the endosomal barrier. *Journal of Materials Chemistry B* **2018,** *6* (43), 6904-6918.

167.   Vermeulen, L. M. P.; De Smedt, S. C.; Remaut, K.; Braeckmans, K., The proton sponge hypothesis: Fable or fact? *European journal of pharmaceutics and biopharmaceutics : official journal of Arbeitsgemeinschaft fur Pharmazeutische Verfahrenstechnik e.V* **2018,** *129*, 184-190.

168.   Walker, G. F.; Fella, C.; Pelisek, J.; Fahrmeir, J.; Boeckle, S.; Ogris, M.; Wagner, E., Toward synthetic viruses: endosomal pH-triggered deshielding of targeted polyplexes greatly enhances gene transfer in vitro and in vivo. *Mol Ther* **2005,** *11* (3), 418-25.

169.   Antila, H. S.; Härkönen, M.; Sammalkorpi, M., Chemistry specificity of DNA–polycation complex salt response: a simulation study of DNA, polylysine and polyethylenimine. *Physical Chemistry Chemical Physics* **2015,** *17* (7), 5279-5289.

170.   Corbo, C.; Molinaro, R.; Tabatabaei, M.; Farokhzad, O. C.; Mahmoudi, M., Personalized protein corona on nanoparticles and its clinical implications. *Biomater Sci* **2017,** *5* (3), 378-387.

171.   Singh, N.; Marets, C.; Boudon, J.; Millot, N.; Saviot, L.; Maurizi, L., In vivo protein corona on nanoparticles: does the control of all material parameters orient the biological behavior? *Nanoscale Advances* **2021,** *3* (5), 1209-1229.

172.   Akhter, M. H.; Khalilullah, H.; Gupta, M.; Alfaleh, M. A.; Alhakamy, N. A.; Riadi, Y.; Md, S., Impact of Protein Corona on the Biological Identity of Nanomedicine: Understanding the Fate of Nanomaterials in the Biological Milieu. *Biomedicines* **2021,** *9* (10).

173.   Lima, T.; Bernfur, K.; Vilanova, M.; Cedervall, T., Understanding the Lipid and Protein Corona Formation on Different Sized Polymeric Nanoparticles. *Scientific reports* **2020,** *10* (1), 1129.

174.   Bertrand, N.; Grenier, P.; Mahmoudi, M.; Lima, E. M.; Appel, E. A.; Dormont, F.; Lim, J.-M.; Karnik, R.; Langer, R.; Farokhzad, O. C., Mechanistic understanding of in vivo protein corona formation on polymeric nanoparticles and impact on pharmacokinetics. *Nature Communications* **2017,** *8* (1), 777.

175.   Ho, Y. T.; Azman, N.; Loh, F. W. Y.; Ong, G. K. T.; Engudar, G.; Kriz, S. A.; Kah, J. C. Y., Protein Corona Formed from Different Blood Plasma Proteins Affects the Colloidal Stability of Nanoparticles Differently. *Bioconjug Chem* **2018,** *29* (11), 3923-3934.

176.   Francia, V.; Yang, K.; Deville, S.; Reker-Smit, C.; Nelissen, I.; Salvati, A., Corona Composition Can Affect the Mechanisms Cells Use to Internalize Nanoparticles. *ACS Nano* **2019,** *13* (10), 11107-11121.

177.   Qin, M.; Zhang, J.; Li, M.; Yang, D.; Liu, D.; Song, S.; Fu, J.; Zhang, H.; Dai, W.; Wang, X.; Wang, Y.; He, B.; Zhang, Q., Proteomic analysis of intracellular protein corona of nanoparticles elucidates nano-trafficking network and nano-bio interactions. *Theranostics* **2020,** *10* (3), 1213-1229.

178.   Wang, C.; Chen, B.; He, M.; Hu, B., Composition of Intracellular Protein Corona around Nanoparticles during Internalization. *ACS Nano* **2021,** *15* (2), 3108-3122.

179.   Bertoli, F.; Garry, D.; Monopoli, M. P.; Salvati, A.; Dawson, K. A., The Intracellular Destiny of the Protein Corona: A Study on its Cellular Internalization and Evolution. *ACS Nano* **2016,** *10* (11), 10471-10479.

180.   Dai, Q.; Guo, J.; Yan, Y.; Ang, C. S.; Bertleff-Zieschang, N.; Caruso, F., Cell-Conditioned Protein Coronas on Engineered Particles Influence Immune Responses. *Biomacromolecules* **2017,** *18* (2), 431-439.

181.   Zakeri, A.; Kouhbanani, M. A. J.; Beheshtkhoo, N.; Beigi, V.; Mousavi, S. M.; Hashemi, S. A. R.; Karimi Zade, A.; Amani, A. M.; Savardashtaki, A.; Mirzaei, E.; Jahandideh, S.; Movahedpour, A., Polyethylenimine-based nanocarriers in co-delivery of drug and gene: a developing horizon. *Nano Rev Exp* **2018,** *9* (1), 1488497-1488497.

182.   Jiang, C.; Chen, J.; Li, Z.; Wang, Z.; Zhang, W.; Liu, J., Recent advances in the development of polyethylenimine-based gene vectors for safe and efficient gene delivery. *Expert opinion on drug delivery* **2019,** *16* (4), 363-376.

183.   Andersen, H.; Parhamifar, L.; Hunter, A. C.; Shahin, V.; Moghimi, S. M., AFM visualization of sub-50nm polyplex disposition to the nuclear pore complex without compromising the integrity of the nuclear envelope. *Journal of controlled release : official journal of the Controlled Release Society* **2016,** *244* (Pt A), 24-29.

184.   Xie, L.; Jiang, Q.; He, Y.; Nie, Y.; Yue, D.; Gu, Z., Insight into the efficient transfection activity of a designed low aggregated magnetic polyethylenimine/DNA complex in serum-containing medium and the application in vivo. *Biomaterials Science* **2015,** *3* (3), 446-456.

185.   Gräfe, C.; Weidner, A.; Lühe, M. V.; Bergemann, C.; Schacher, F. H.; Clement, J. H.; Dutz, S., Intentional formation of a protein corona on nanoparticles: Serum concentration affects protein corona mass, surface charge, and nanoparticle-cell interaction. *The international journal of biochemistry & cell biology* **2016,** *75*, 196-202.

186.   Syga, M. I.; Nicolì, E.; Kohler, E.; Shastri, V. P., Albumin Incorporation in Polyethylenimine-DNA Polyplexes Influences Transfection Efficiency. *Biomacromolecules* **2016,** *17* (1), 200-7.

187.   Herrera, L. C.; Shastri, V. P., Silencing of GFP expression in human mesenchymal stem cells using quaternary polyplexes of siRNA-PEI with glycosaminoglycans and albumin. *Acta biomaterialia* **2019,** *99*, 397-411.

188.   Zhu, D.; Yan, H.; Zhou, Z.; Tang, J.; Liu, X.; Hartmann, R.; Parak, W. J.; Shen, Y.; Feliu, N., Influence of the Modulation of the Protein Corona on Gene Expression Using Polyethylenimine (PEI) Polyplexes as Delivery Vehicle. *Advanced Healthcare Materials* **2021,** *10* (13), 2100125.

189.   Chen, D.; Ganesh, S.; Wang, W.; Amiji, M., Protein Corona-Enabled Systemic Delivery and Targeting of Nanoparticles. *The AAPS journal* **2020,** *22* (4), 83.

190.   Piella, J.; Bastús, N. G.; Puntes, V., Size-Dependent Protein-Nanoparticle Interactions in Citrate-Stabilized Gold Nanoparticles: The Emergence of the Protein Corona. *Bioconjug Chem* **2017,** *28* (1), 88-97.

191.   Dunn, K. W.; Kamocka, M. M.; McDonald, J. H., A practical guide to evaluating colocalization in biological microscopy. *Am J Physiol Cell Physiol* **2011,** *300* (4), C723-C742.

192.   Moser, B.; Hochreiter, B.; Herbst, R.; Schmid, J. A., Fluorescence colocalization microscopy analysis can be improved by combining object-recognition with pixel-intensity-correlation. *Biotechnol J* **2017,** *12* (1), 1600332.

193.   Zhu, D.; Yan, H.; Zhou, Z.; Tang, J.; Liu, X.; Hartmann, R.; Parak, W. J.; Feliu, N.; Shen, Y., Detailed investigation on how the protein corona modulates the physicochemical properties and gene delivery of polyethylenimine (PEI) polyplexes. *Biomaterials Science* **2018,** *6* (7), 1800-1817.

194.   Zheng, X.; Baker, H.; Hancock, W. S.; Fawaz, F.; McCaman, M.; Pungor, E., Jr., Proteomic analysis for the assessment of different lots of fetal bovine serum as a raw material for cell culture. Part IV. Application of proteomics to the manufacture of biological drugs. *Biotechnology progress* **2006,** *22* (5), 1294-300.

195.   Sakulkhu, U.; Mahmoudi, M.; Maurizi, L.; Coullerez, G.; Hofmann-Amtenbrink, M.; Vries, M.; Motazacker, M.; Rezaee, F.; Hofmann, H., Significance of surface charge and shell material of superparamagnetic iron oxide nanoparticle (SPION) based core/shell nanoparticles on the composition of the protein corona. *Biomaterials Science* **2015,** *3* (2), 265-278.

VITA

MD. NASIR UDDIN

Education

PhD   University of Kentucky, Department of Chemistry   December 2021(expected)

MS   University of Dhaka, Pharmaceutical Chemistry, M. Pharm   January 2010

BS   University of Dhaka, B. Pharm (Hons.)   January 2009

Professional positions

University of Kentucky, Lexington, KY-40506, USA   August 2016 to Dec 2021
Teaching Assistant, Department of Chemistry

Manarat International University, Dhaka, Bangladesh   July 2015 to July 2016
Assistant Professor, Department of Pharmacy

Manarat International University, Dhaka, Bangladesh   October 2011 to June 2015
Lecturer, Department of Pharmacy

Aristopharma Ltd., Dhaka, Bangladesh   September 2009 to June 2010
Quality control officer

Publications

1. **Uddin, N.**; Warriner, L. W.; Pack, D. W.; DeRouchey, J. E.; Enhanced gene delivery and CRISPR/Cas9 homology-directed repair in serum by minimally succinylated polyethylenimine. *Molecular Pharmaceutics*, **2021**, 18(9), 3452-3463.

2. **Uddin**, **N.;** Hossain, M. K.; Haque, M. R.; Hasan. C. M.; Chemical Investigation of *Paederia foetidae* (Rubiaceae); *AJC,* **2013,** 25(2): 1163-1164.

3. Nayon, A. U.; Nesa, J.; **Uddin, N.**; Amran, S.; Bushra, U.; Development and Validation of UV Spectrometric Method for the Determination of Cefixime trihydrate in Bulk and Pharmaceutical Formulation. *AJBPS* **2013,** *3* (22), 1-5.

4. **Uddin**, **N.;** Hossain, M. K.; Haque, M. R.; Hasan. C. M.; Chemical Investigation of *Paederia foetidae* (Rubiaceae); *AJC,* **2013,** 25(2): 1163-1164.

Awards

University of Kentucky GSC conference award, Cycle 4, (2021)

Education Board scholarship for HSC result, Rajshahi, Bangladesh, (2004-2008)